

國立交通大學

機械工程學系

碩士論文

雙 Ge-Ku 系統, Sprott 4 系統及 Rössler 系統的

渾沌與渾沌同步

Chaos and Chaos Synchronization of Double Ge-Ku  
System, Sprott 4 System and Rössler System



研 究 生：江振賓

指導教授：戈正銘 教授

中華民國九十九年六月

雙 Ge-Ku 系統, Sprott 4 系統及 Rössler 系統的  
渾沌與渾沌同步

Chaos and Chaos Synchronization of Double Ge-Ku System  
,Sprott 4 Systems and Rössler System

研究生：江振賓

Student: Chen- Bin Chiang

指導教授：戈正銘

Advisor: Zheng-Ming Ge



碩士論文

A Thesis

Submitted to Department of Mechanical Engineering

College of Engineering

National Chiao Tung University

In Partial Fulfillment of the Requirement

For the Degree of master of science

In

Mechanical Engineering

June 2010

Hsinchu, Taiwan, Republic of China

中華民國九十九年六月

# 雙 Ge-Ku 系統, Sprott 4 系統及 Rössler 系統的渾沌與渾沌同步

學生：江振賓

指導教授：戈正銘

國立交通大學

機械工程學系

## 摘要

本篇論文以相圖、龐卡萊映射圖、李亞普洛夫指數以及分歧圖等數值方法研究新 Double Ge-Ku 系統的渾沌現象。應用主動控制獲得雙重及多重渾沌交織同步。對此系統應用部分區域穩定性理論和實用漸進穩定理論來達成廣義同步。更進一步使用新模糊模型來研究 Sprott 4 系統以及 Rössler 系統的模糊模型和渾沌同步。此外，將探討新模糊邏輯常數控制器應用在投影同步及含有不確定度的渾沌系統。在以上研究中，皆可由相圖和時間歷程圖得到驗證。

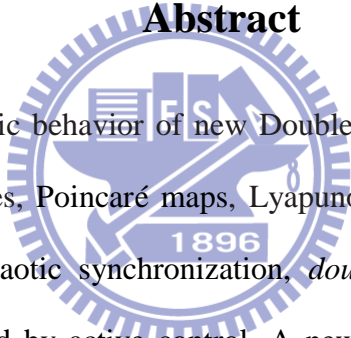
Chaos and Chaos Synchronization of Double Ge-Ku System,  
Sprott 4 System and Rössler System

**Student :** Chen- Bin Chiang

**Advisor :** Zheng-Ming Ge

Department of Mechanical Engineering, National Chiao Tung  
University

**Abstract**



In this thesis, the chaotic behavior of new Double Ge-Ku system is studied by phase portraits, time histories, Poincaré maps, Lyapunov exponents and bifurcation diagrams. New type for chaotic synchronization, *double and multiple symplectic synchronization*, are obtained by active control. A new kind of chaotic generalized synchronization, *different translation pragmatical generalized synchronization*, is obtained by pragmatical asymptotical stability theorem and partial region stability theory. A new method, using new fuzzy model, is studied for fuzzy modeling and synchronization of Sprott 4 system and Rössler system. Moreover, the new fuzzy logic constant controller is studied for projective synchronization and chaotic system with uncertainty. Numerical analyses, such as phase portraits and time histories are provided to verify the effectiveness of all above studies.



## 誌謝

此篇論文及碩士學業之完成，首先必須感謝指導教授 戈正銘老師的耐心指導與教誨。老師在專業領域上的成就以及對於文學和史學上的熱情，都令學生印象深刻且受益匪淺。戈老師在學生的碩士生涯中扮演了很重要的角色。在研究上，戈老師給了許多意見指引學生正確的研究方向，在研究過程中，也讓學生學習到當發現問題時，解決問題的能力。在研究所的後段時間，小宇學長更是不辭辛勞教導我們研究新的題目，並且與老師共同傳授做研究的技巧，著實讓我上了一課。經由這兩年的相處，讓學生發現在學術研究之餘也能體會到古典文學之美，這都使學生開拓了不一樣的視野。

在這段研究的日子當中，承蒙張晉銘、李仕宇、徐瑜韓、張育銘、陳志銘、陳聰文學長的熱心指導，同時也感謝泳厚、尚恩、翔平同學的相互勉勵及幫忙，使得本篇論文能夠順利完成。

最後感謝我的家人，讓我可以不必擔心課業以外的事物，無後顧之憂的完成學業。最後，僅以此論文獻給你們。

# CONTENTS

CHINESE ABSTRACT.....	i
ABSTRACT.....	ii
Acknowledgment.....	iii
CONTENTS.....	iv
LIST OF FIGURES.....	vi
<b>Chapter 1 Introduction.....</b>	<b>1</b>
<b>Chapter 2 Double Symplectic Synchronization for Double Ge-Ku System</b>	
2.1 Preliminary.....	6
2.2 Double Symplectic Synchronization Scheme.....	6
2.3 Synchronization of Two Different New Chaotic Systems.....	8
<b>Chapter 3 Multiple Symplectic Synchronization for Double Ge-Ku System</b>	
3.1 Preliminary.....	22
3.2 Multiple Symplectic Synchronization Scheme.....	22
3.3 Synchronization of Three Different Chaotic Systems.....	23
<b>Chapter 4 Using Partial Region Stability Theory for Different Translation Pragmatical Generalized Synchronization</b>	
4.1 Preliminary.....	37
4.2 The Scheme of Different Translation Pragmatic Generalized by Partial Region Theory.....	37
4.3 Different Translation Pragmatical Synchronization of new DoubleGe-Ku Chaotic System.....	40
<b>Chapter 5 Robust Projective Anti-Synchronization of Non-autonomous and Chaotic Uncertain Stochastic Systems Via Fuzzy Logic Constant Controller</b>	
5.1 Preliminary.....	57
5.2 Projective Anti-Synchronization by FLCC Scheme.....	57
5.3 Simulation Results.....	61
<b>Chapter 6 Fuzzy Modeling and Synchronization of Chaotic Systems by a New Fuzzy Model</b>	
6.1 Preliminary.....	79

6.2 New Fuzzy Model Theory.....	79
6.3 New Fuzzy Model of Chaotic Systems.....	81
6.4 Fuzzy Synchronization Scheme.....	87
6.5 Simulation Results.....	89
 Chapter 7 Conclusions.....	 98
 Appendix A GYC Partial Region Stability Theory.....	 100
Appendix B Pragmatical Asymptotical Stability Theory.....	108
References.....	111



# LIST OF FIGURES

Fig. 2.1 The chaotic attractor of a new Ge-Ku-Duffing system.....	14
Fig. 2.2 The chaotic attractor of uncontrolled new Double Ge-Ku system.....	14
Fig. 2.3 The bifurcation diagram of uncontrolled new Double Ge-Ku system.....	15
Fig. 2.4.The Lyapunov exponents of uncontrolled new Double Ge-Ku system.....	15
Fig. 2.5 The phase portrait of the controlled new Double Ge-Ku system for CASE 1. .....	16
Fig. 2.6 Time histories of the state errors for CASE 1.....	16
Fig. 2.7 Time histories of $\mathbf{x}_i + y_i$ and $\mathbf{x}_i^2 y_i$ for CASE 1.....	17
Fig. 2.8 The chaotic attractor of a new Ge-Ku-van der Pol system.....	17
Fig. 2.9 The phase portrait of the controlled new Double Ge-Ku system for CASE 2 .....	18
Fig. 2.10 Time histories of the state errors for CASE 2.....	18
Fig. 2.11 Time histories of $\mathbf{x}_i + y_i$ and $\mathbf{x}_i^2 y_i$ for CASE 2.....	19
Fig. 2.12 The chaotic attractor of a new Ge-Ku Mathieu system.....	19
Fig. 2.13 The phase portrait of the controlled new Double Ge-Ku system for CASE 3. .....	20
Fig. 2.14 Time histories of the state errors for CASE 3.....	20
Fig. 2.15 Time histories of $\mathbf{x}_i + y_i$ and $\mathbf{x}_i^2 y_i$ for CASE 3.....	21
Fig. 3.1 The chaotic attractor of the Lorenz system.....	30
Fig. 3.2 The chaotic attractor of the Chen system.....	30
Fig. 3.3 The phase portrait of the controlled DGK system.....	31
Fig. 3.4 Time histories of the state errors for Case 1.....	31
Fig. 3.5 Time histories of $G(\mathbf{x}, \mathbf{y}, z, t)$ and $\mathbf{F}(\mathbf{x}, \mathbf{y}, z, t)$ for Case 1.....	32

Fig. 3.6 The chaotic attractor of the <i>Rössler</i> system.....	32
Fig. 3.7 The phase portrait of the controlled DGK system.....	33
Fig. 3.8 Time histories of the state errors for Case 2.....	33
Fig. 3.9 Time histories of $G(\mathbf{x}, \mathbf{y}, z, t)$ and $\mathbf{F}(\mathbf{x}, \mathbf{y}, z, t)$ for Case 2.....	34
Fig. 3.10 The chaotic attractor of a Sprott system.....	34
Fig. 3.11 The phase portrait of the controlled DGK system.....	35
Fig. 3.12 Time histories of the state errors for Case 3.....	35
Fig. 3.13 Time histories of $G(\mathbf{x}, \mathbf{y}, z, t)$ and $\mathbf{F}(\mathbf{x}, \mathbf{y}, z, t)$ for Case 3.....	36
Fig. 4.1 Coordinate translation of state $\mathbf{x}$ .....	49
Fig. 4.2 Coordinate translation of state $\mathbf{y}$ .....	49
Fig. 4.3 Phase portrait of the error dynamics for Case 1.....	50
Fig. 4.4 Time histories of errors for Case 1.....	50
Fig. 4.5 Time histories of $x_i, y_i$ for Case 1.....	51
Fig. 4.6 Time histories of parameter errors for Case 1.....	51
Fig. 4.7 Phase portrait of the error dynamic for Case 2.....	52
Fig. 4.8 Time histories of errors for Case 2.....	52
Fig. 4.9 Time histories of $x_i, y_i$ for Case 2.....	53
Fig. 4.10 Time histories of parameter errors for Case 2.....	53
Fig. 4.11 Phase portrait of the error dynamic for Case 3.....	54
Fig. 4.12 The chaotic attractor of the Ge-Ku-van der Pol system.....	54
Fig. 4.13 Time histories of errors for Case 3.....	55
Fig. 4.14 Time histories of $x_i, y_i$ for Case 3.....	55
Fig. 4.15 Time histories of parameter errors for Case 3.....	56
Fig. 5.1 The configuration of fuzzy logic controller.....	70
Fig. 5.2 Membership function.....	70
Fig. 5.3 The chaotic behavior of Sprott 4 system [50].....	71

Fig. 5.4 Projections of phase portrait of Eq (5.19).....	71
Fig. 5.5 Time histories of error derivatives for master and slave chaotic systems without controllers.....	72
Fig. 5.6 Time histories of states for Example 1 the FLCC is coming into after 30s .....	72
Fig. 5.7 Time histories of errors for Example 1 the FLCC is coming into after 30s .....	73
Fig. 5.8 Time histories of states for the traditional controller is coming into after 30s .....	73
Fig. 5.9 Time histories of states for the traditional controller is coming into after 30s .....	74
Fig. 5.10 The Rayleigh noise used.....	74
Fig. 5.11 Projection of phase portrait of Eq (5.28).....	75
Fig. 5.12 Projections of phase portrait of chaotic DGK systems.....	75
Fig. 5.13 Time histories of error derivatives for master and slave chaotic uncertain stochastic systems without controllers.....	76
Fig. 5.14 Time histories of states for Example 2 the FLCC is coming into after 30s .....	76
Fig. 5.15 Time histories of errors for Example 2 the FLCC is coming into after 30s .....	77
Fig. 5.16 Time histories of states for the traditional controller is coming into after 30s .....	77
Fig. 5.17 Time histories of states for the traditional controller is coming into after 30s .....	78
Fig. 6.1 Chaotic behavior of Sprott 4 system.....	93
Fig. 6.2 Chaotic behavior of Sprott 4 system with uncertainty.....	93

Fig. 6.3 Chaotic behavior of new fuzzy Sprott 4 system with uncertainty.....	94
Fig. 6.4 Chaotic behavior of Rössler system.....	94
Fig. 6.5 Chaotic behavior of Rössler system with uncertainty.....	95
Fig. 6.6 The Rayleigh noise used.....	95
Fig. 6.7 Chaotic behavior of new fuzzy Rössler system with uncertainty.....	96
Fig. 6.8 Time histories of errors for Example 1.....	96
Fig. 6.9 Time histories of errors for Example 2.....	97



# Chapter 1

## Introduction

Chaos is a very interesting nonlinear phenomenon. Chaos as a modern theory is discovered by the age of computer in the middle of the past century, which has an epoch-making significance in exact science.

Generally speaking, designing a system to mimic the behavior of another chaotic system is called synchronization. Synchronization of chaotic systems has received a significant attention, since Pecora and Carroll presented the chaos synchronization method to synchronize two identical chaotic systems with different initial values in 1990 [1].

In recent years, synchronization in chaotic dynamic system is a very interesting problem and has been widely studied. Chaos synchronization has been applied in biological systems [2,3], secure communication [4,5], and many other disciplines. By linear and nonlinear control [6-12] different types of synchronization for interacting chaotic systems, such as complete synchronization [1], phase synchronization [13], lag synchronization [14], generalized synchronization [15-20], anticipating synchronization can be obtained.

Various approaches for achieving chaos synchronization using fuzzy systems have been proposed [21]. Fuzzy set theory was first presented by Zadeh [22], while fuzzy logic control (FLC) schemes have been widely developed and successfully deployed in many applications [23]. Furthermore, adaptive fuzzy controllers have been used to control and synchronize chaotic systems [24,25].

Uncertainties associated with the mathematical characterization of a system can lead to unreliable damage [26]. Probabilistic analysis provides a tool for incorporating randoms in the analysis of frequency response by generally describing the randoms as



random variables. While the studies discussed above addressed measurement noise, some researchers have started looking at the effect of noise present in the model. Collins et al. [27] proposed a statistical identification procedure by treating the initial parameters as normally distributed random variables.

In recent years, some chaos synchronizations based on fuzzy systems have been proposed since the fuzzy set theory was initiated by Zadeh [22], such as fuzzy sliding mode controlling technique [28,29], LMI-based synchronization [30] and extended backstepping sliding mode controlling technique [31]. The fuzzy logic control (FLC) scheme have been widely developed and have been successfully applied to many applications [32]. Recently, Yau and Shieh [33] proposed a new idea in designing fuzzy logic controllers - constructing fuzzy rules subject to a common Lyapunov function such that the master-slave chaotic systems satisfy stability condition in the Lyapunov sense. In [33], there are two main controllers in their slave system. One is used in elimination of nonlinear terms and the other is built by fuzzy rules subject to a common Lyapunov function. Therefore, the resulting controllers are in nonlinear form. In [33], the regular form is necessary. In order to carry out the new method, the original system must to be transformed into their regular form.

In recent years, fuzzy logic proposed [34] has received much attention as a powerful tool for the nonlinear control. Among various kinds of fuzzy methods, Takagi-Sugeno fuzzy (T-S fuzzy) system is widely accepted as a useful tool for design and analysis of fuzzy control system [35-40]. Currently, some chaos control and synchronization based on T-S fuzzy systems have been proposed, such as fuzzy sliding mode controlling technique, LMI-based synchronization [41-43] and robust control [44]. Furthermore, two different nonlinear systems may have different numbers of nonlinear terms. It causes different numbers of linear subsystems. For synchronization of two different nonlinear systems, the traditional method using the

idea of PDC to design the fuzzy control law for stabilization of the error dynamics can not be used here, since the number of subsystems becomes very large.

Ge and Ku [45] gave a chaotic system formed by a simple pendulum with its pivot rotating about an axis as Fig. 1.1. This chaotic system is

$$\begin{cases} \dot{x}_1 = x_2 \\ \dot{x}_2 = -ax_2 - \sin x_1 [b(c + \cos x_1) + d \sin wt] \end{cases} \quad (1.1)$$

where  $a, b, c, d$  are parameters. After simplification,  $\sin x_1 = x_1$ ,  $\cos x_1 = 1 - \frac{x_1^2}{2}$  and addition of coupling terms, we get the Double Ge-Ku system

$$\begin{cases} \dot{x}_1 = x_2 \\ \dot{x}_2 = -fx_2 - x_1 [g(h - x_1^2) + kx_3] \\ \dot{x}_3 = -fx_3 - x_3 [g(h - x_3^2) + lx_1] \end{cases} \quad (1.2)$$

where  $a, b, c, d, g$  are parameters.

In Chapter 2, a new type of synchronization, double symplectic synchronization,  $\mathbf{G}(\mathbf{x}, \mathbf{y}, t) = \mathbf{F}(\mathbf{x}, \mathbf{y}, t)$  is studied. Traditional generalized synchronization and symplectic synchronization are special cases of the double symplectic synchronization. Since the symplectic functions are presented at both the right hand side and the left hand side of the equality. The double symplectic synchronization may be applied to increase the security of secret communication due to the complexity of its synchronization form. By using the Barbalat's lemma[46], the double symplectic synchronization can be achieved. Finally, the effectiveness and feasibility of our proposed scheme are verified by numerical simulations.

In Chapter 3, a new type of synchronization, multiple symplectic synchronization is studied. When the double symplectic functions are extended to a more general form,  $\mathbf{G}(\mathbf{x}, \mathbf{y}, \mathbf{z} \cdots \mathbf{w}, t) = \mathbf{F}(\mathbf{x}, \mathbf{y}, \mathbf{z} \cdots \mathbf{w}, t)$ , “multiple symplectic synchronization” is achieved. The multiple symplectic synchronization may be applied to increase the security of

secret communication more effectively than double symplectic synchronization due to more complexity of its synchronization form.

In Chapter 4, a new chaos generalized synchronization strategy of different translation pragmatism synchronization by stability theory of partial region [47-49] is proposed. By using the stability theory of partial region, the Lyapunov function is a simple linear homogeneous function of error states, the controllers are more simple since they are in lower degree than that of traditional controllers, while the traditional Lyapunov function is a quadratic form of error states.

In Chapter 5, we propose a new strategy which is also constructing fuzzy rules subject to a Lyapunov direct method. Error derivatives are used to be upper bound and lower bound. Through this new approach, a simplest controller, i.e. constant controller, can be obtained and the difficulty in realization of complicated controllers in chaos synchronization by Lyapunov direct method can be also overcome. Unlike conventional approaches, the resulting control law has less maximum magnitude of the instantaneous control command and it can reduce the actuator saturation phenomenon in real physical system. Some computer simulation examples are given in this Chapter.

In Chapter 6, the new fuzzy model is proposed. It gives a new way to linearize complicated nonlinear system and only two subsystems are concluded. In simulation examples, Sprott 4 system [50] and Rössler system are used.

Finally, conclusions are presented in Chapter 7.

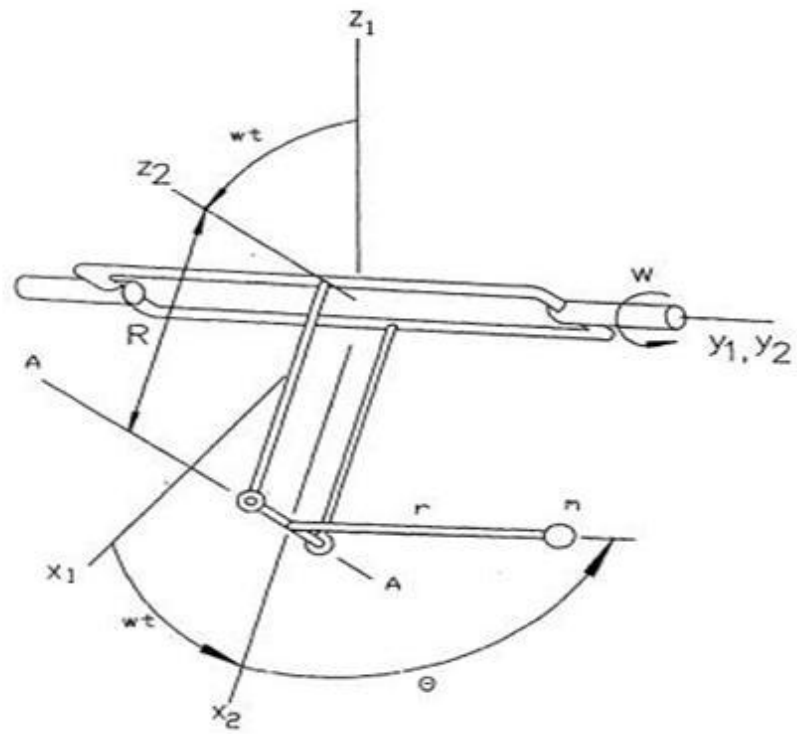
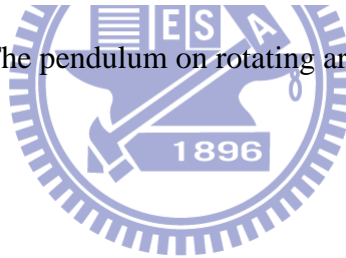


Fig 1.1 The pendulum on rotating arm.

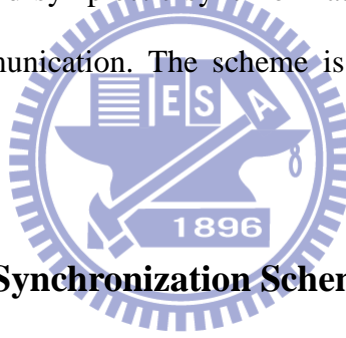


# Chapter 2

## Double Symplectic Synchronization for Double Ge-Ku System

### 2.1 Preliminary

In this Chapter, a new type of synchronization, double symplectic synchronization,  $\mathbf{G}(\mathbf{x}, \mathbf{y}, t) = \mathbf{F}(\mathbf{x}, \mathbf{y}, t)$  is proposed. Double symplectic synchronization is an extension of symplectic synchronization,  $\mathbf{y} = \mathbf{F}(\mathbf{x}, \mathbf{y}, t)$ . Because the symplectic functions are presented at both the right hand side and the left hand side of the equality, it is called “double symplectic synchronization”. Since the synchronization form is more complex than generalized and symplectic synchronizations, so we usually use it on the purpose of secret communication. The scheme is effective as shown by three examples as follows.



### 2.2 Double Symplectic Synchronization Scheme

Consider two different nonlinear chaotic systems, Partner A and Partner B, described by

$$\dot{\mathbf{x}} = \mathbf{f}(\mathbf{x}, t), \quad (2.1)$$

$$\dot{\mathbf{y}} = \mathbf{C}(t)\mathbf{y} + \mathbf{g}(u, t) + \mathbf{u}, \quad (2.2)$$

where  $\mathbf{x} = [x_1, x_2, \dots, x_n]^T \in R^n$  and  $\mathbf{y} = [y_1, y_2, \dots, y_n]^T \in R^n$  are the state vectors of Partner A (2.1) and Partner B (2.2),  $\mathbf{C} \in R^{n \times n}$  is the given matrix,  $\mathbf{f}$  and  $\mathbf{g}$  are continuous nonlinear vector functions, and  $\mathbf{u}$  is the controller. Our goal is to design the controller  $\mathbf{u}$  such that  $\mathbf{G}(\mathbf{x}, \mathbf{y}, t)$  asymptotically approaches  $\mathbf{F}(\mathbf{x}, \mathbf{y}, t)$ . For simplicity take  $\mathbf{G}(\mathbf{x}, \mathbf{y}, t) = \mathbf{x} + \mathbf{y}$  and  $\mathbf{F}(\mathbf{x}, \mathbf{y}, t)$  is a continuous nonlinear vector function.

**Property 1** [5]: An  $m \times n$  matrix  $A$  of real elements defines a linear mapping  $y = Ax$  from  $R^n$  into  $R^m$ , and the induced  $p$ -norm of  $A$  for  $p=1, 2$ , and  $\infty$  is given by

$$\|A\|_1 = \max_j \sum_{i=1}^m |a_{ij}|, \quad \|A\|_2 = [\lambda_{\max}(A^T A)]^{1/2}, \quad \|A\|_\infty = \max_i \sum_{j=1}^n |a_{ij}|. \quad (2.3)$$

The useful property of induced matrix norms for real matrix  $A$  is as follow:

$$\|A\|_2 \leq \sqrt{\|A\|_1 \|A\|_\infty}. \quad (2.4)$$

**Theorem:** For chaotic systems Partner A (2.1) and Partner B (2.2), if the controller  $\mathbf{u}$  is designed as

$$\begin{aligned} \mathbf{u} = & (\mathbf{I} - \mathbf{D}_y \mathbf{F})^{-1} [\mathbf{D}_x \mathbf{F} \mathbf{f}(\mathbf{x}, t) + \mathbf{D}_y \mathbf{F} (\mathbf{C}(t) \mathbf{y} + \mathbf{g}(\mathbf{y}, t)) + \mathbf{D}_t \mathbf{F} - \mathbf{f}(\mathbf{x}, t) - \mathbf{g}(\mathbf{y}, t) \\ & + \mathbf{C}(t)(\mathbf{x} - \mathbf{F}) - \mathbf{K}(\mathbf{x} + \mathbf{y} - \mathbf{F})], \end{aligned} \quad (2.5)$$

where  $\mathbf{D}_x \mathbf{F}$ ,  $\mathbf{D}_y \mathbf{F}$ ,  $\mathbf{D}_t \mathbf{F}$  are the Jacobian matrices of  $\mathbf{F}(\mathbf{x}, \mathbf{y}, t)$ ,

$\mathbf{K} = \text{diag}(k_1, k_2, \dots, k_m)$ , and satisfies

$$\frac{\min(k_i)}{\|C(t)\|} > 1, \quad (2.6)$$

then the double symplectic synchronization will be achieved.

**Proof:** Define the error vectors as

$$\mathbf{e} = \mathbf{x} + \mathbf{y} - \mathbf{F}(\mathbf{x}, \mathbf{y}, t), \quad (2.7)$$

then the following error dynamics can be obtained by introducing the designed controller

$$\begin{aligned} \frac{d\mathbf{e}}{dt} = & \dot{\mathbf{e}} = \dot{\mathbf{x}} + \dot{\mathbf{y}} - \mathbf{D}_x \mathbf{F} \dot{\mathbf{x}} - \mathbf{D}_y \mathbf{F} \dot{\mathbf{y}} - \mathbf{D}_t \mathbf{F} \\ = & \mathbf{f}(\mathbf{x}, t) + \mathbf{C}(t) \mathbf{y} + \mathbf{g}(\mathbf{y}, t) - \mathbf{D}_x \mathbf{F} \mathbf{f}(\mathbf{x}, t) - \mathbf{D}_y \mathbf{F} (\mathbf{C}(t) \mathbf{y} + \mathbf{g}(\mathbf{y}, t)) - \mathbf{D}_t \mathbf{F} \\ & + (\mathbf{I} - \mathbf{D}_y \mathbf{F}) \mathbf{u} \\ = & (\mathbf{C}(t) - \mathbf{K}) \mathbf{e}. \end{aligned} \quad (2.8)$$

Choose a non-negative Lyapunov function of the form

$$V(t) = \frac{1}{2} \mathbf{e}^T \mathbf{e}. \quad (2.9)$$

Taking the time derivative of  $V(t)$  along the trajectory of Eq. (2.8), we have

$$\begin{aligned} \dot{V}(t) &= \mathbf{e}^T \dot{\mathbf{e}} \\ &= \mathbf{e}^T \mathbf{C}(t) \mathbf{e} - \mathbf{e}^T \mathbf{K} \mathbf{e} \\ &\leq \|\mathbf{C}(t)\| \cdot \|\mathbf{e}\|^2 - \min(k_i) \|\mathbf{e}\|^2 \\ &= (\|\mathbf{C}(t)\| - \min(k_i)) \|\mathbf{e}\|^2. \end{aligned} \quad (2.10)$$

Since  $M = \min(k_i) - \|\mathbf{C}(t)\| > 0$ , then  $\dot{V}(t) \leq -M \|\mathbf{e}\|^2 = -2MV(t)$ . Therefore, it can be obtained that

$$V(t) \leq V(0)e^{-2Mt} \quad (2.11)$$

and  $\lim_{t \rightarrow \infty} \int_0^t |V(\xi)| d\xi$  is bounded. Besides,  $V(t)$  is uniformly continuous. According to Barbalat's lemma [46], the conclusion can be drawn that  $\lim_{t \rightarrow \infty} V(t) = 0$ , i.e.  $\lim_{t \rightarrow \infty} \|\mathbf{e}(t)\| = 0$ . Thus, the double symplectic synchronization can be achieved asymptotically.

## 2.3 Synchronization of Two Different New Chaotic Systems

### CASE 1

Consider a new Ge-Ku-Duffing(GKD) system as Partner A described by

$$\begin{cases} \dot{x}_1 = x_2 \\ \dot{x}_2 = -hx_2 - x_1 \left[ l(p - x_1^2) + kx_3 \right] \\ \dot{x}_3 = -x_3 - x_3^3 - fx_2 + gx_1 \end{cases} \quad (2.12)$$

where  $h=0.1$ ;  $l=11$ ;  $p=40$ ;  $k=54$ ;  $f=6$ ;  $g=30$ ; and the initial conditions are  $x_1(0) = 2, x_2(0) = 2.4, x_3(0) = 5$ . Eq. (2.12) can be rewritten in the form of Eq. (2.1),

where  $\mathbf{f}(\mathbf{x}, t) = \begin{bmatrix} x_2 \\ -hx_2 - x_1 \left[ l(p - x_1^2) + kx_3 \right] \\ -x_3 - x_3^3 - fx_2 + gx_1 \end{bmatrix}$ . The chaotic attractor of the new

GKD system is shown in Fig. 2.1.

The controlled new Double Ge-Ku (DGK) system is considered as Partner B described by

$$\begin{cases} \dot{y}_1 = y_2 + u_1 \\ \dot{y}_2 = -ay_2 - y_1 \left[ b(c - y_1^2) + dy_3 \right] + u_2 \\ \dot{y}_3 = -ay_3 - y_3 \left[ b(c - y_3^2) + ey_1 \right] + u_3 \end{cases} \quad (2.13)$$

where  $a=-0.5$ ;  $b=-1.4$ ;  $c=1.9$ ;  $d=-4.5$ ;  $e=6.2$ ; ,  $\mathbf{u} = [u_1, u_2, u_3]^T$  is the controller, and the initial condition is  $y_1(0) = 2$ ,  $y_2(0) = 2.4$ ,  $y_3(0) = 5$ .

The chaotic attractor of uncontrolled new DGK system is shown in Fig. 2.2, Bifurcation diagram in Fig. 2.3 and Lyapunov exponents in Fig. 2.4. Eq. (2.13) can be

rewritten in the form of Eq. (2.2), where  $\mathbf{C}(t) = \begin{bmatrix} 0 & 1 & 0 \\ -bc & -a & 0 \\ 0 & 0 & -a-bc \end{bmatrix}$  and

$$\mathbf{g}(\mathbf{y}, t) = \begin{bmatrix} 0 \\ by_1^3 - dy_1y_3 \\ by_3^3 - ey_1y_3 \end{bmatrix}. \text{ By applying } \textit{Property 1}, \text{ it is derived that } \|\mathbf{C}(t)\|_1 = -a - bc$$

$\|\mathbf{C}(t)\|_\infty = -a - bc$  , and  $\|\mathbf{C}(t)\|_2 \leq \sqrt{(-a - bc)^2} = \sqrt{9.9856}$  . Then  $\|\mathbf{C}(t)\| = 3.1$  is estimated.

$$\text{Define } \mathbf{F}(\mathbf{x}, \mathbf{y}, t) = \begin{bmatrix} x_1^2 y_1 \\ x_2^2 y_2 \\ x_3^2 y_3 \end{bmatrix}, \text{ and our goal is to achieve the double symplectic}$$

synchronization  $\mathbf{x} + \mathbf{y} = \mathbf{F}(\mathbf{x}, \mathbf{y}, t)$ . According to Theorem, the inequality  $\frac{\min(k_i)}{\|\mathbf{C}(t)\|} > 1$

must be satisfied. It can be obtained that  $\min(k_i) > 3.1$  if we choose



$$\mathbf{K} = \begin{bmatrix} k_1 & 0 & 0 \\ 0 & k_2 & 0 \\ 0 & 0 & k_3 \end{bmatrix} = \begin{bmatrix} 4 & 0 & 0 \\ 0 & 5 & 0 \\ 0 & 0 & 6 \end{bmatrix} \text{ and design the controller as}$$

$$u_1 = 2x_1y_1x_2 + x_1^2y_2 - x_2 - y_2 + x_1^2y_1 - x_1 - y_1$$

$$u_2 = 2x_2y_2\{-hx_2 - x_1[l(p - x_1^2) + kx_3]\} + x_2^2\{-ay_2 - y_1[b(c - y_1^2) + dy_3]\} + hx_2 + x_1[l(p - x_1^2) + kx_3] + ay_2 + y_1[b(c - y_1^2) + dy_3] + x_2^2y_2 - x_2 - y_2$$

$$u_3 = 2x_3y_3(-x_3 - x_3^3 - fx_2 + gx_1) + x_3^2\{-ay_3 - y_3[b(c - y_3^2) + ey_1]\} + x_3 + x_3^3 + fx_2 - gx_1 + ay_3 + y_3[b(c - y_3^2) + ey_1] + x_3^2y_3 - x_3 - y_3$$

The Theorem is satisfied and the double symplectic synchronization is achieved.

The phase portrait of the controlled DGK system and the time histories of the state errors are shown in Fig. 2.5 and Fig. 2.6 and Fig. 2.7, respectively.

## CASE 2

Consider a new Ge-Ku-van der Pol(GKv) system as Partner A described by

$$\begin{cases} \dot{x}_1 = x_2 \\ \dot{x}_2 = -fx_2 - x_3[p(k - x_1^2) + mx_3] \\ \dot{x}_3 = -gx_3 - h(1 - x_3^2)x_2 + lx_1 \end{cases} \quad (2.14)$$

where  $f=0.08$ ;  $p=-0.35$ ;  $k=100.56$ ;  $m=-1000.02$ ;  $g=0.61$ ;  $h=0.08$ ;  $l=0.01$ ; and the initial conditions are  $x_1(0) = 0.01$ ,  $x_2(0) = 0.01$ ,  $x_3(0) = 0.01$ . Eq. (2.14) can be

$$\text{rewritten in the form of Eq. (2.1), where } \mathbf{f}(\mathbf{x}, t) = \begin{bmatrix} x_2 \\ -fx_2 - x_3[p(k - x_1^2) + mx_3] \\ -gx_3 - h(1 - x_3^2)x_2 + lx_1 \end{bmatrix}.$$

The chaotic attractor of the GKv system is shown in Fig.2.8.

The controlled DGK system is considered as Partner B described by

$$\begin{cases} \dot{y}_1 = y_2 + u_1 \\ \dot{y}_2 = -ay_2 - y_1[b(c - y_1^2) + dy_3] + u_2 \\ \dot{y}_3 = -ay_3 - y_3[b(c - y_3^2) + ey_1] + u_3^{10} \end{cases} \quad (2.15)$$

where  $a=-0.5$ ;  $b=-1.4$ ;  $c=1.9$ ;  $d=-4.5$ ;  $e=6.2$ ; ,  $\mathbf{u}=[u_1, u_2, u_3]^T$  is the vector controller, and the initial conditions are  $y_1(0)=0.01$ ,  $y_2(0)=0.01$ ,  $y_3(0)=0.01$ .

Eq. (2.15) can be rewritten in the form of Eq. (2.2), where  $\mathbf{C}(t) = \begin{bmatrix} 0 & 1 & 0 \\ -bc & -a & 0 \\ 0 & l & -g \end{bmatrix}$

and  $\mathbf{g}(\mathbf{y}, t) = \begin{bmatrix} 0 \\ by_1^3 - dy_1y_3 \\ by_3^3 - ey_1y_3 \end{bmatrix}$ . By applying **Property 1**, it is derived that

$\|\mathbf{C}(t)\|_1 = -a - bc$ ,  $\|\mathbf{C}(t)\|_\infty = -a - bc$ , and  $\|\mathbf{C}(t)\|_2 \leq \sqrt{(-a - bc)^2} = \sqrt{9.9856}$ . Then  $\|\mathbf{C}(t)\| = 3.1$  is estimated.

Define  $\mathbf{F}(\mathbf{x}, \mathbf{y}, t) = \begin{bmatrix} x_1^2 y_1 \\ x_2^2 y_2 \\ x_3^2 y_3 \end{bmatrix}$ , and our goal is to achieve the double symplectic

synchronization  $\mathbf{x} + \mathbf{y} = \mathbf{F}(\mathbf{x}, \mathbf{y}, t)$ . According to Theorem, the inequality  $\frac{\min(k_i)}{\|\mathbf{C}(t)\|} > 1$  must be satisfied. It can be obtained that  $\min(k_i) > 3.1$ . Thua we

choose  $\mathbf{K} = \begin{bmatrix} k_1 & 0 & 0 \\ 0 & k_2 & 0 \\ 0 & 0 & k_3 \end{bmatrix} = \begin{bmatrix} 4 & 0 & 0 \\ 0 & 5 & 0 \\ 0 & 0 & 6 \end{bmatrix}$  and design the controller as

$$u_1 = 2x_1y_1x_2 + x_1^2y_2 - x_2 - y_2 + x_1^2y_1 - x_1 - y_1$$

$$u_2 = 2x_2y_2\{-fx_2 - x_3[p(k - x_1^2) + mx_3]\} + x_2^2\{-ay_2 - y_1[b(c - y_1^2) + dy_3]\} + fx_2 + x_3[p(k - x_1^2) + mx_3] + ay_2 + y_1[b(c - y_1^2) + dy_3] + x_2^2y_2 - x_2 - y_2$$

$$u_3 = 2x_3y_3[-gx_3 + h(1 - x_3^2)x_2 + lx_1] + x_3^2\{-ay_3 - y_3[b(c - y_3^2) + ey_1]\} + gx_3 - h(1 - x_3^2)x_2 - lx_1 + ay_3 + y_3[b(c - y_3^2) + ey_1] + x_3^2y_3 - x_3 - y_3$$

The Theorem is satisfied and the double symplectic synchronization is achieved.

The phase portrait of the controlled DGK system and the time histories of the errors are shown in Fig.2.9, Fig.2.10 and Fig.2.11, respectively.

### CASE 3

Consider the Ge-Ku Mathieu(GKM) system as Partner A described by

$$\begin{cases} \dot{x}_1 = x_2 \\ \dot{x}_2 = -kx_2 - x_1 \left[ f(m - x_1^2) + nx_2x_3 \right] \\ \dot{x}_3 = -(g + hx_1)x_3 + lx_2 + px_1x_3 \end{cases} \quad (2.16)$$

where  $k=-0.6$ ;  $f=5$ ;  $m=11$ ;  $n=0.3$ ;  $g=8$ ;  $h=10$ ;  $l=0.5$ ;  $p=0.2$ ; and the initial conditions are  $x_1(0)=0.01$ ,  $x_2(0)=0.01$ ,  $x_3(0)=0.01$ . Eq. (2.16) can be rewritten in

the form of Eq. (2.1), where  $\mathbf{f}(\mathbf{x}, t) = \begin{bmatrix} x_2 \\ -kx_2 - x_1 \left[ f(m - x_1^2) + nx_2x_3 \right] \\ -(g + hx_1)x_3 + lx_2 + px_1x_3 \end{bmatrix}$ . The chaotic

attractor of the GKM system is shown in Fig.2.12.

The controlled DGK system is considered as Partner B described by

$$\begin{cases} \dot{y}_1 = y_2 + u_1 \\ \dot{y}_2 = -ay_2 - y_1 \left[ b(c - y_1^2) + dy_3 \right] + u_2 \\ \dot{y}_3 = -ay_3 - y_3 \left[ b(c - y_3^2) + ey_1 \right] + u_3 \end{cases} \quad (2.17)$$

where  $a=-0.5$ ;  $b=-1.4$ ;  $c=1.9$ ;  $d=-4.5$ ;  $e=6.2$ ; ,  $\mathbf{u} = [u_1, u_2, u_3]^T$  is the vector controller, and the initial conditions are  $y_1(0)=0.01$ ,  $y_2(0)=0.01$ ,  $y_3(0)=0.01$ .

Eq. (2.17) can be rewritten in the form of Eq. (2.2), where  $\mathbf{C}(t) = \begin{bmatrix} 0 & 1 & 0 \\ -bc & -a & 0 \\ 0 & l & -g \end{bmatrix}$

and  $\mathbf{g}(\mathbf{y}, t) = \begin{bmatrix} 0 \\ by_1^3 - dy_1y_3 \\ by_3^3 - ey_1y_3 \end{bmatrix}$ . By applying **Property 1**, it is derived that

$\|\mathbf{C}(t)\|_1 = -a - bc$ ,  $\|\mathbf{C}(t)\|_\infty = -a - bc$ , and  $\|\mathbf{C}(t)\|_2 \leq \sqrt{(-a - bc)^2} = \sqrt{9.9856}$ . Then

$\|\mathbf{C}(t)\| = 3.1$  is estimated. Define  $\mathbf{F}(\mathbf{x}, \mathbf{y}, t) = \begin{bmatrix} x_1^2 y_1 \\ x_2^2 y_2 \\ x_3^2 y_3 \end{bmatrix}$ , and our goal is to achieve the

double symplectic synchronization  $\mathbf{x} + \mathbf{y} = \mathbf{F}(\mathbf{x}, \mathbf{y}, t)$ . According to Theorem, the inequality  $\frac{\min(k_i)}{\|\mathbf{C}(t)\|} > 1$  must be satisfied. It can be obtained that  $\min(k_i) > 3.1$ .

Thus we choose  $\mathbf{K} = \begin{bmatrix} k_1 & 0 & 0 \\ 0 & k_2 & 0 \\ 0 & 0 & k_3 \end{bmatrix} = \begin{bmatrix} 4 & 0 & 0 \\ 0 & 5 & 0 \\ 0 & 0 & 6 \end{bmatrix}$  and design the controller as

$$u_1 = 2x_1 y_1 x_2 + x_1^2 y_2 - x_2 - y_2 + x_1^2 y_1 - x_1 - y_1$$

$$u_2 = 2x_2 y_2 \{-kx_2 - x_1[f(m - x_1^2) + nx_2 x_3]\} + x_2^2 \{-ay_2 - y_1[b(c - y_1^2) + dy_3]\} + kx_2 + x_1[f(m - x_1^2) + nx_2 x_3] + ay_2 + y_1[b(c - y_1^2) + dy_3] + x_2^2 y_2 - x_2 - y_2$$

$$u_3 = 2x_3 y_3 [-(g + hx_1)x_3 + lx_2 + px_1 x_3] + x_3^2 \{-ay_3 - y_3[b(c - y_3^2) + ey_1]\} + (g + hx_1)x_3 - lx_2 - px_1 x_3 + ay_3 + y_3[b(c - y_3^2) + ey_1] + x_3^2 y_3 - x_3 - y_3$$

The Theorem is satisfied and the double symplectic synchronization is achieved.

The phase portrait of the controlled DGK system and the time histories of the state errors are shown in Fig2.13, Fig.2.14 and Fig.2.15, respectively.

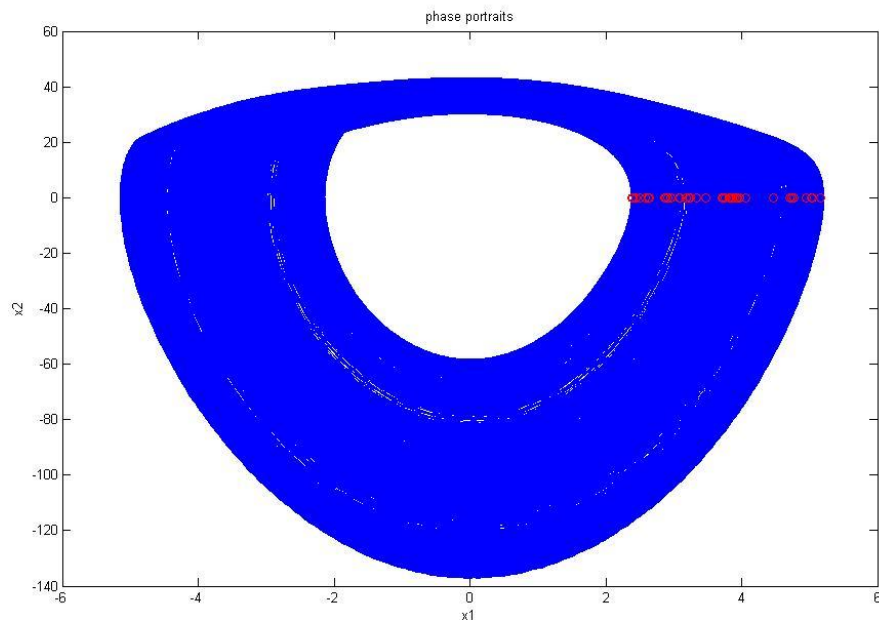


Fig. 2.1 The chaotic attractor of a new Ge-Ku-Duffing system.

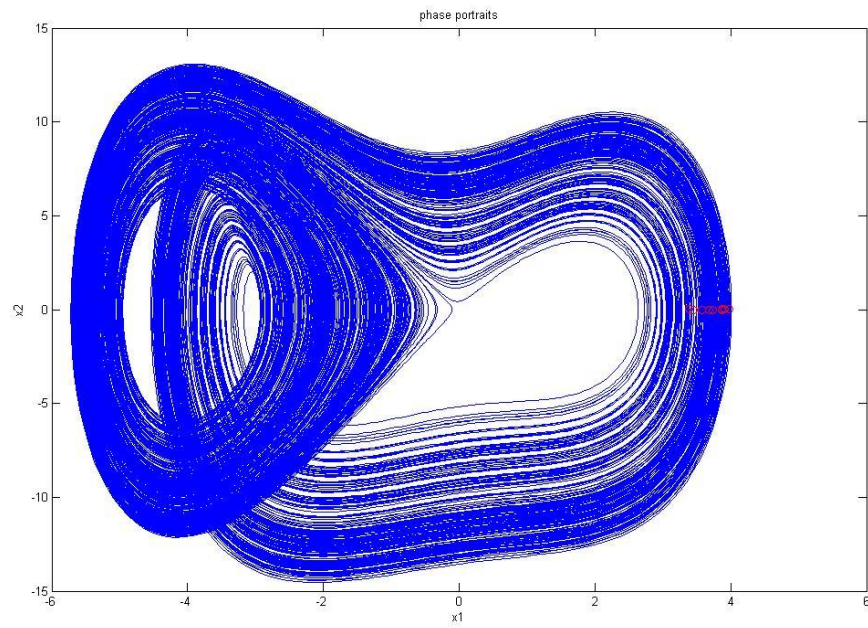


Fig. 2.2 The chaotic attractor of uncontrolled new Double Ge-Ku system.

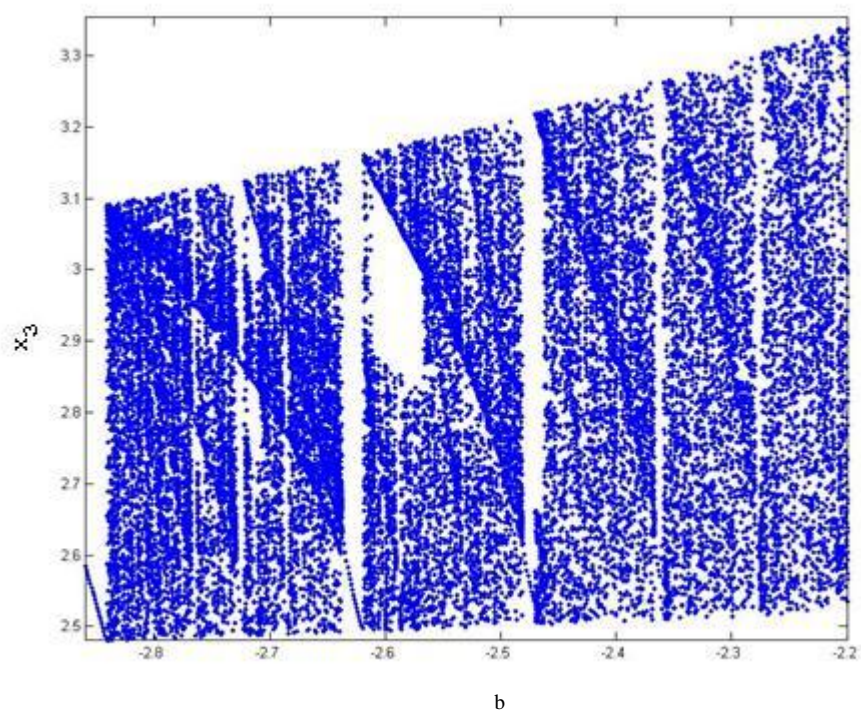


Fig. 2.3 The bifurcation diagram of uncontrolled new Double Ge-Ku system.

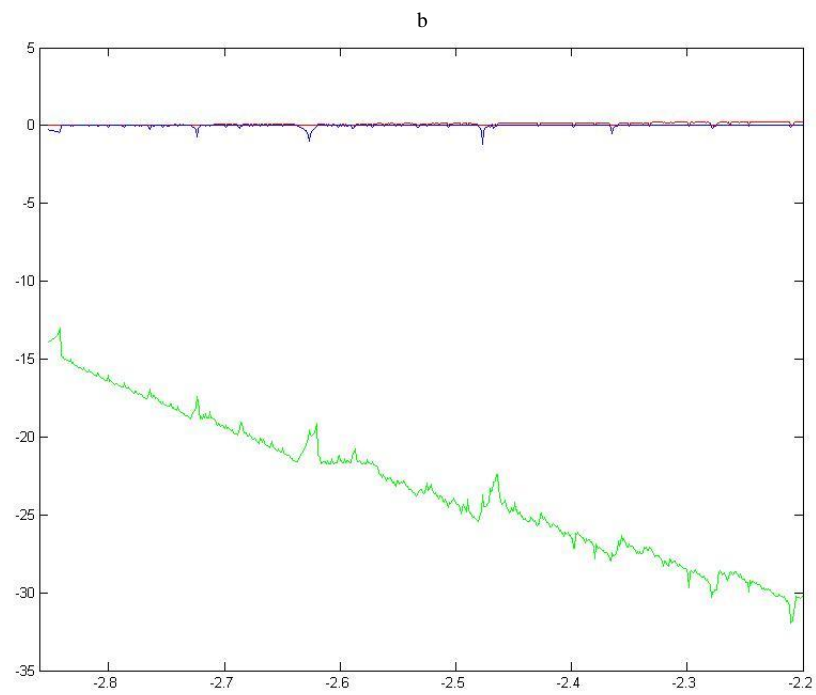


Fig. 2.4. The Lyapunov exponents of uncontrolled new Double Ge-Ku system.

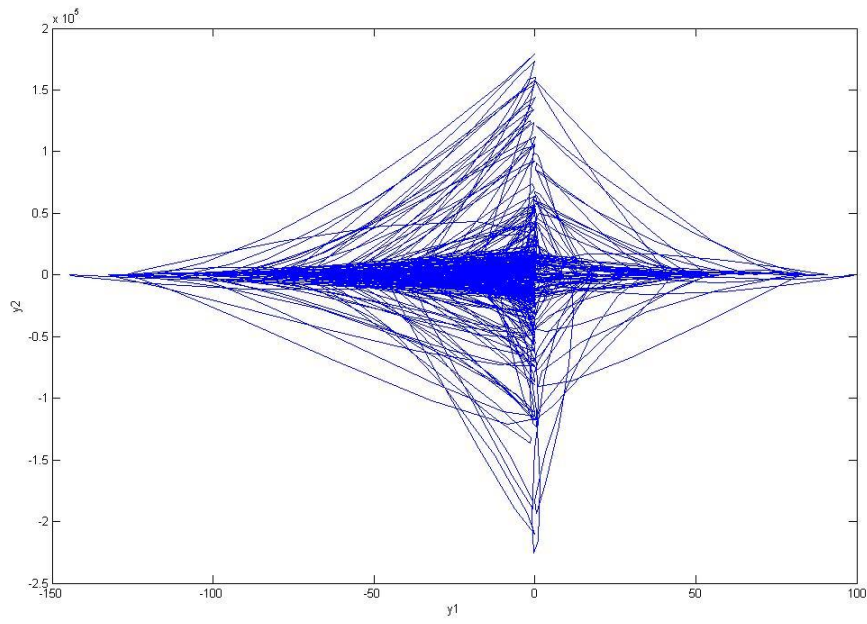


Fig. 2.5 The phase portrait of the controlled new Double Ge-Ku system for CASE 1.

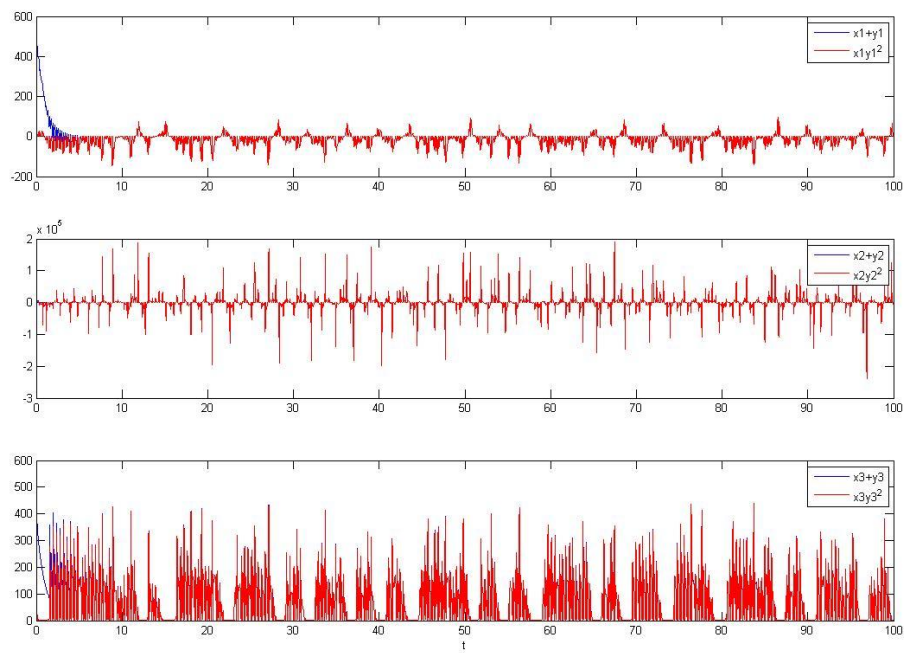


Fig. 2.6 Time histories of  $\mathbf{x}_i + y_i$  and  $\mathbf{x}_i^2 y_i$  for CASE 1.



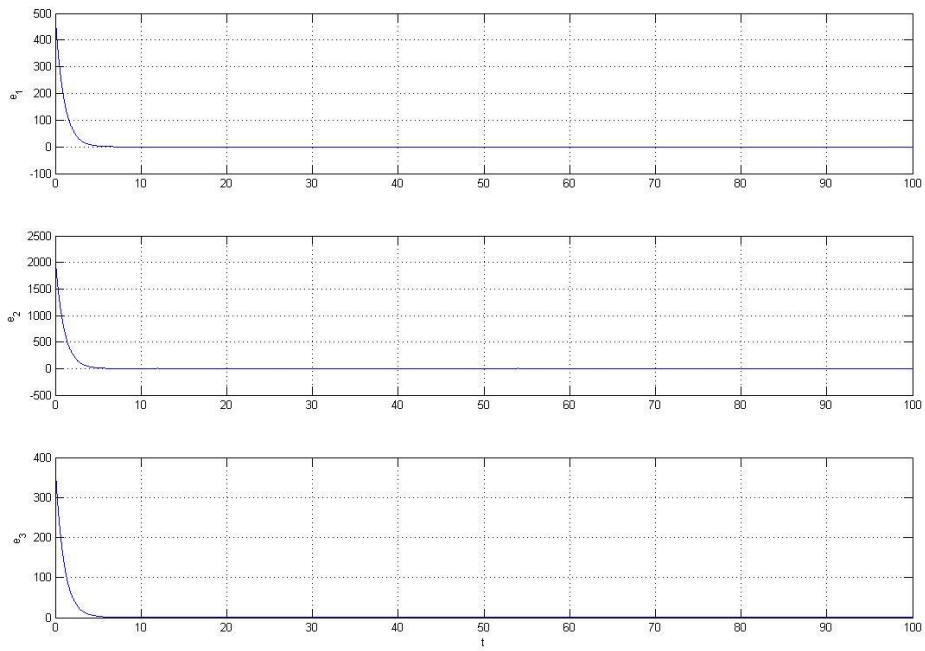


Fig. 2.7 Time histories of the state errors for CASE 1.

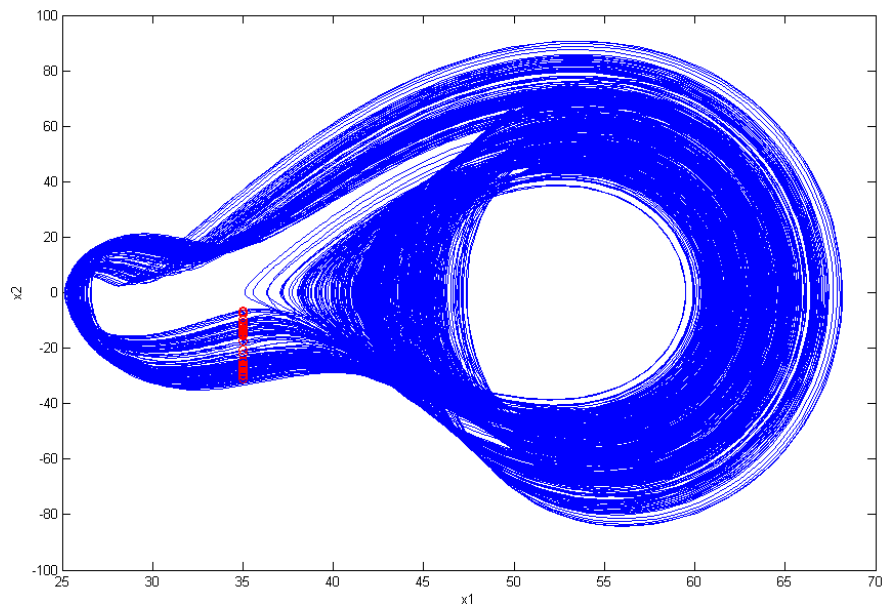


Fig. 2.8 The chaotic attractor of a new Ge-Ku-van der Pol system.



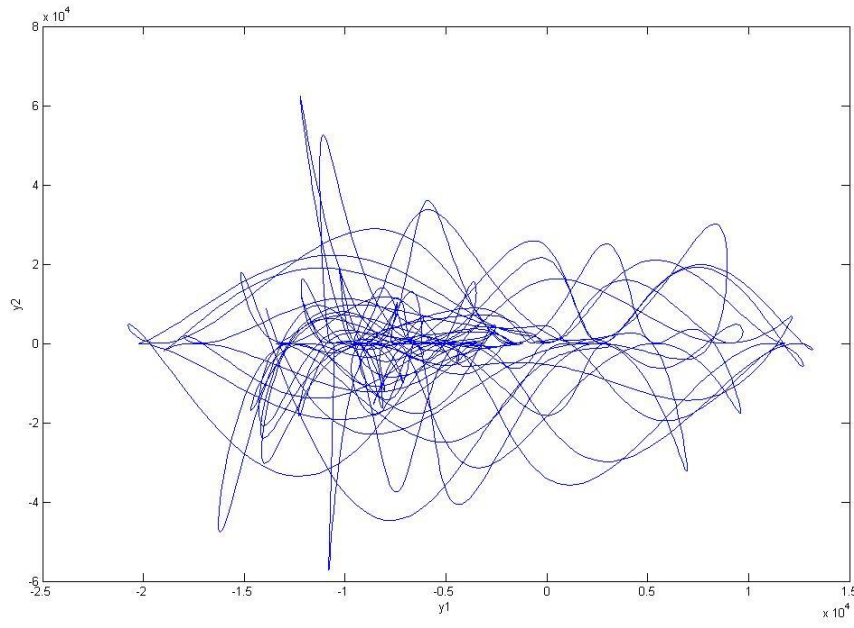


Fig. 2.9 The phase portrait of the controlled new Double Ge-Ku system for CASE 2.

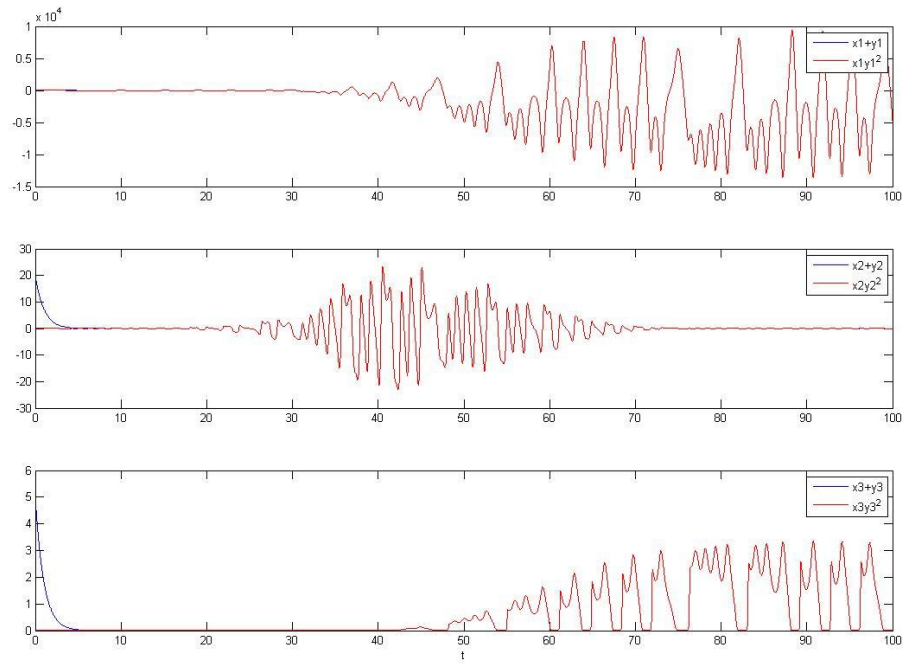


Fig. 2.10 Time histories of  $\mathbf{x}_i + y_i$  and  $\mathbf{x}_i^2 y_i$  for CASE 2.

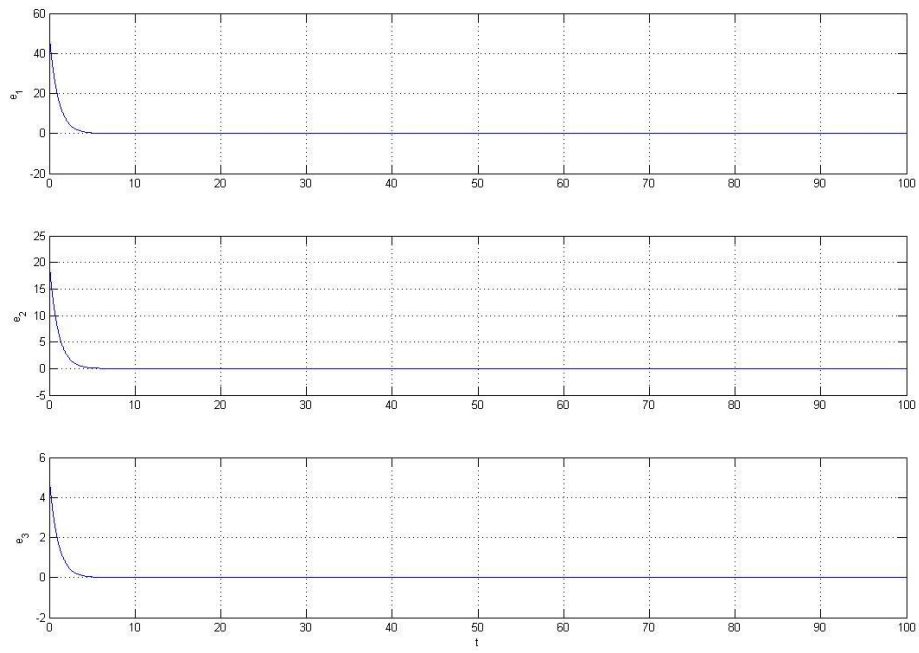


Fig. 2.11 Time histories of the state errors for CASE 2.

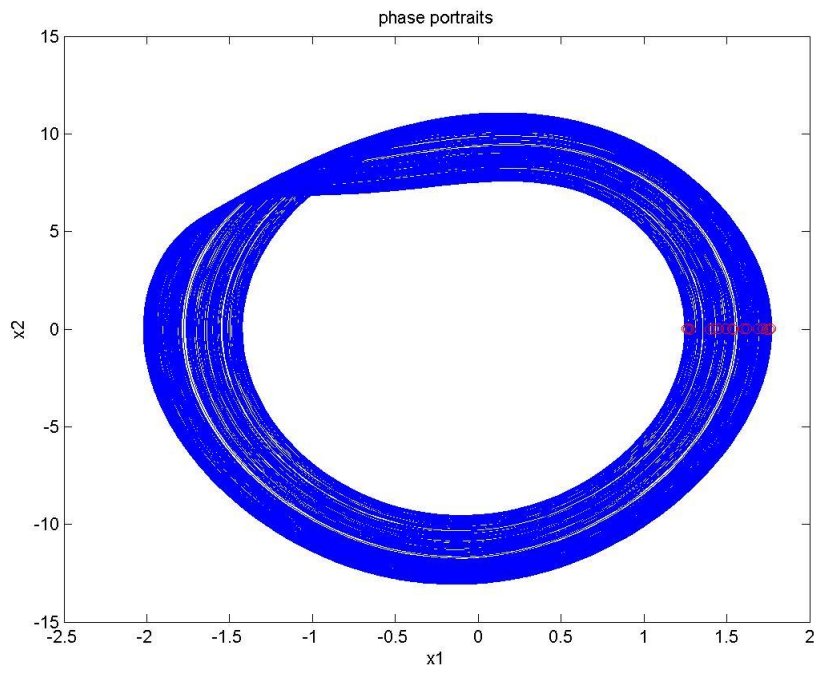


Fig. 2.12 The chaotic attractor of a new Ge-Ku Mathieu system.

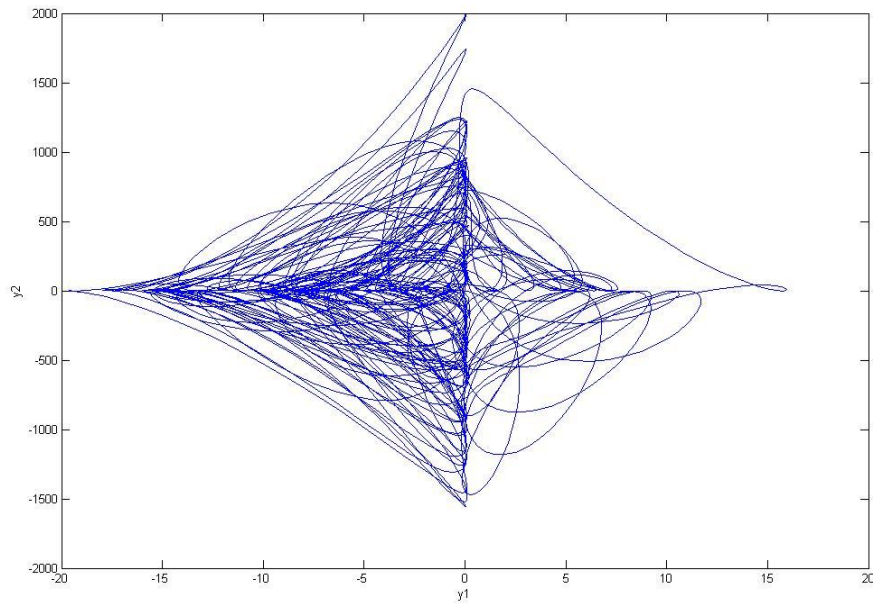


Fig. 2.13 The phase portrait of the controlled new Double Ge-Ku system for CASE 3.

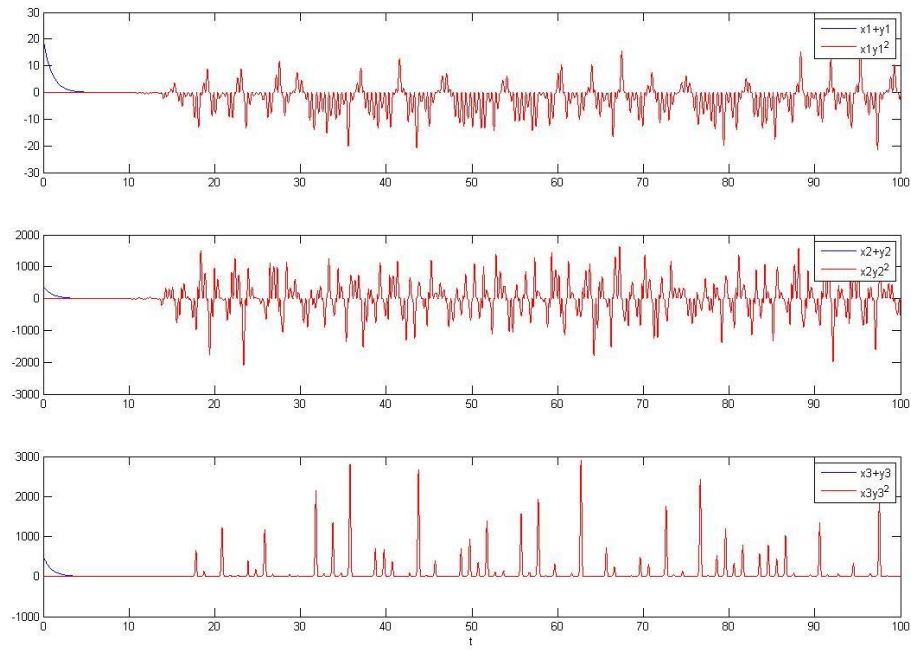


Fig. 2.14 Time histories of  $\mathbf{x}_i + y_i$  and  $\mathbf{x}_i^2 y_i$  for CASE 3.

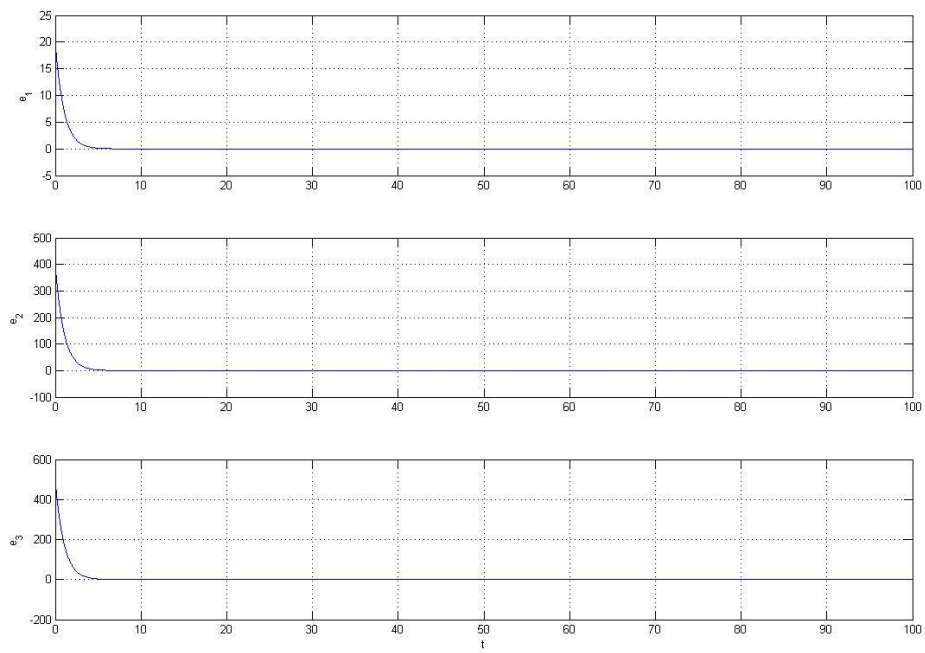
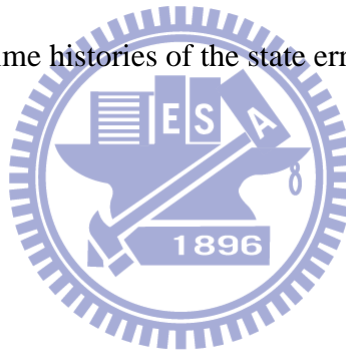


Fig. 2.15 Time histories of the state errors for CASE 3.



# Chapter 3

## Multiple Symplectic Synchronization for Double Ge-Ku System

### 3.1 Preliminary

In this Chapter, a new type of synchronization, multiple symplectic synchronization is studied. Symplectic synchronization and double symplectic synchronization are special cases of the multiple symplectic synchronization. When the double symplectic functions is extended to a more general form,  $G(\mathbf{x}, \mathbf{y}, \mathbf{z} \cdots \mathbf{w}, t) = F(\mathbf{x}, \mathbf{y}, \mathbf{z} \cdots \mathbf{w}, t)$ , it is called “multiple symplectic synchronization”. The multiple symplectic synchronization may be applied to increase the security of secret communication due to the complexity of its synchronization form.

### 3.2 Multiple Symplectic Synchronization Scheme

Chaos synchronization, first proposed by Fujisaka and Yamada in 1983, did not received great attention until 1990. Among many kinds of synchronizations, the generalized synchronization is investigated. It means there exist a functional relationship between the states of the master and those of the slave. Symplectic synchronization is defined as  $\dot{y} = H(x, y, t)$ , where  $x$ ,  $y$  are the state vectors of the “master” and of the “slave”, respectively. The final desired state  $y$  of the “slave” not only depends upon the “master” state  $x$  but also depends upon the “slave” state  $y$  itself. Therefore the “slave” is not a traditional pure slave obeying the “master” completely but plays a role to determine the final desired state of the “slave” system. We call this kind of synchronization, “symplectic synchronization”, and call the “master” system Partner A, the “slave” system Partner B.

Since the symplectic functions are presented at both the right hand side and the

left hand side of the equality, it is called double symplectic synchronization,  $\mathbf{G}(\mathbf{x}, \mathbf{y}, t) = \mathbf{F}(\mathbf{x}, \mathbf{y}, t)$ , where  $\mathbf{x}$ ,  $\mathbf{y}$  are state vectors of Partner A and Partner B, respectively,  $\mathbf{G}(\mathbf{x}, \mathbf{y}, t)$  and  $\mathbf{F}(\mathbf{x}, \mathbf{y}, t)$  are given vector functions of  $\mathbf{x}$ ,  $\mathbf{y}$  and time.

When the double symplectic functions is extended to a more general form,  $\mathbf{G}(\mathbf{x}, \mathbf{y}, \mathbf{z} \cdots \mathbf{w}, t) = \mathbf{F}(\mathbf{x}, \mathbf{y}, \mathbf{z} \cdots \mathbf{w}, t)$ , is called “multiple symplectic synchronization”, where  $\mathbf{x}, \mathbf{y}, \mathbf{z}, \cdots, \mathbf{w}$  are state vectors of Partner A and Partner B, respectively,  $\mathbf{G}(\mathbf{x}, \mathbf{y}, \mathbf{z} \cdots \mathbf{w}, t)$  and  $\mathbf{F}(\mathbf{x}, \mathbf{y}, \mathbf{z} \cdots \mathbf{w}, t)$  are given vector functions of  $\mathbf{x}, \mathbf{y}, \mathbf{z}, \cdots, \mathbf{w}$  and time.

### 3.3 Synchronization of Three Different Chaotic Systems

#### CASE 1.

Define

$$\mathbf{G}(\mathbf{x}, \mathbf{y}, \mathbf{z}, t) = \begin{bmatrix} x_1 + y_1 + z_1 \\ x_2 + y_2 + z_2 \\ x_3 + y_3 + z_3 \end{bmatrix}, \quad \mathbf{F}(\mathbf{x}, \mathbf{y}, \mathbf{z}, t) = \begin{bmatrix} x_1 (\sin y_1) z_1 + x_2 (\sin y_2) z_1 + x_3 (\sin y_3) z_1 \\ x_1 (\sin y_1) z_2 + x_2 (\sin y_2) z_2 + x_3 (\sin y_3) z_2 \\ x_1 (\sin y_1) z_3 + x_2 (\sin y_2) z_3 + x_3 (\sin y_3) z_3 \end{bmatrix},$$

and we wish to achieve the multiple symplectic synchronization  $\mathbf{G}(\mathbf{x}, \mathbf{y}, \mathbf{z}, t) = \mathbf{F}(\mathbf{x}, \mathbf{y}, \mathbf{z}, t)$ .

Let  $\mathbf{e} = \mathbf{G}(\mathbf{x}, \mathbf{y}, \mathbf{z}, t) - \mathbf{F}(\mathbf{x}, \mathbf{y}, \mathbf{z}, t)$

Consider a Lorenz system is described by

$$\begin{cases} \dot{x}_1 = -w_1 x_1 + w_1 x_2 \\ \dot{x}_2 = w_3 x_1 - x_2 - x_1 x_3 \\ \dot{x}_3 = -w_2 x_3 + x_1 x_2 \end{cases} \quad (3.1)$$

where  $w_1 = 10$ ,  $w_2 = \frac{8}{3}$ ,  $w_3 = 28$ , and the initial condition is

$x_1(0) = 0.01$ ,  $x_2(0) = 0.01$ ,  $x_3(0) = 0.01$ . The chaotic attractor of the Lorenz system is shown in Fig. 3.1.

The Chen system is described by

$$\begin{cases} \dot{z}_1 = h_1(z_2 - z_1) \\ \dot{z}_2 = (h_2 - h_1)z_1 - z_1 z_3 + h_2 z_2 \\ \dot{z}_3 = z_1 z_2 - h_3 z_3 \end{cases} \quad 23$$

(3.2)

where  $h_1 = 35, h_2 = 27.2, h_3 = 3$ , and the initial condition is  $z_1(0) = 0.5, z_2(0) = 0.26, z_3(0) = 0.35$ . The chaotic attractor of the Chen system is shown in Fig. 3.2.

The controlled Double Ge-Ku (DGK) system is described by

$$\begin{cases} \dot{y}_1 = y_2 + u_1 \\ \dot{y}_2 = -ay_2 - y_1 \left[ b(c - y_1^2) + dy_3 \right] + u_2 \\ \dot{y}_3 = -ay_3 - y_3 \left[ b(c - y_3^2) + ey_1 \right] + u_3 \end{cases} \quad (3.3)$$

where  $a=-0.5; b=-1.4; c=1.9; d=-4.5; e=6.2$ , is the controller parameters, and the initial condition is  $y_1(0) = 0.01, y_2(0) = 0.01, y_3(0) = 0.01, .$

Thus we design the controller as

$$\begin{aligned} u_1 = & -(-w_1x_1 + w_1x_2) - y_2 - \left[ h_1(z_2 - z_1) \right] + (-w_1x_1 + w_1x_2)(\sin y_1)z_1 \\ & + x_1y_2(\cos y_1)z_1 + x_1(\sin y_1) \left[ h_1(z_2 - z_1) \right] + (w_3x_1 - x_2 - x_1x_3)(\sin y_2)z_1 \\ & + x_2 \left\{ -ay_2 - y_1 \left[ b(c - y_1^2) + dy_3 \right] \right\} (\cos y_2)z_1 + x_2(\sin y_2) \left[ h_1(z_2 - z_1) \right] \\ & + (-w_2x_3 + x_1x_2)(\sin y_3)z_1 + x_3 \left\{ -ay_3 - y_3 \left[ b(c - y_3^2) + ey_1 \right] \right\} (\cos y_3)z_1 \\ & + x_3(\sin y_3) \left[ h_1(z_2 - z_1) \right] \\ u_2 = & -(w_3x_1 - x_2 - x_1x_3) - \left\{ -ay_2 - y_1 \left[ b(c - y_1^2) + dy_3 \right] \right\} \\ & - \left[ (h_2 - h_1)z_1 - z_1z_3 + h_2z_2 \right] + (-w_1x_1 + w_1x_2)(\sin y_1)z_2 + x_1y_2(\cos y_1)z_2 \\ & + x_1(\sin y_1) \left[ (h_2 - h_1)z_1 - z_1z_3 + h_2z_2 \right] + (w_3x_1 - x_2 - x_1x_3)(\sin y_2)z_2 \\ & + x_2 \left\{ -ay_2 - y_1 \left[ b(c - y_1^2) + dy_3 \right] \right\} (\cos y_2)z_2 + x_2(\sin y_2) \left[ (h_2 - h_1)z_1 - z_1z_3 + h_2z_2 \right] \\ & + (-w_2x_3 + x_1x_2)(\sin y_3)z_2 + x_3 \left\{ -ay_3 - y_3 \left[ b(c - y_3^2) + ey_1 \right] \right\} (\cos y_3)z_2 \\ & + x_3(\sin y_3) \left[ (h_2 - h_1)z_1 - z_1z_3 + h_2z_2 \right] \end{aligned}$$

$$\begin{aligned}
u_3 = & -(-w_2x_3 + x_1x_2) - \left\{ -ay_3 - y_3 \left[ b(c - y_3^2) + ey_1 \right] \right\} \\
& - (z_1z_2 - h_3z_3) + (-w_1x_1 + w_1x_2)(\sin y_1)z_3 + x_1y_2(\cos y_1)z_3 \\
& + x_1(\sin y_1)(z_1z_2 - h_3z_3) + (w_3x_1 - x_2 - x_1x_3)(\sin y_2)z_3 \\
& + x_2 \left\{ -ay_2 - y_1 \left[ b(c - y_1^2) + dy_3 \right] \right\} (\cos y_2)z_3 + x_2(\sin y_2)(z_1z_2 - h_3z_3) \\
& + (-w_2x_3 + x_1x_2)(\sin y_3)z_3 + x_3 \left\{ -ay_3 - y_3 \left[ b(c - y_3^2) + ey_1 \right] \right\} (\cos y_3)z_3 \\
& + x_3(\sin y_3)(z_1z_2 - h_3z_3)
\end{aligned}$$

The Theorem in Chapter 2 is satisfied and the multiple symplectic synchronization is achieved. The phase portrait of the controlled DGK system and the time histories of the state errors and the time histories of  $G(\mathbf{x}, \mathbf{y}, \mathbf{z}, t)$  and  $F(\mathbf{x}, \mathbf{y}, \mathbf{z}, t)$  are shown in Fig. 3.3 and Fig. 3.4 and Fig. 3.5, respectively.

## CASE 2.

Define

$$\mathbf{G}(\mathbf{x}, \mathbf{y}, \mathbf{z}, t) = \begin{bmatrix} x_1 + y_1 + z_1 \\ x_2 + y_2 + z_2 \\ x_3 + y_3 + z_3 \end{bmatrix}, \quad \mathbf{F}(\mathbf{x}, \mathbf{y}, \mathbf{z}, t) = \begin{bmatrix} (\cos x_1)y_1z_1 + (\cos x_2)y_2z_1 + (\cos x_3)y_3z_1 \\ (\cos x_1)y_1z_2 + (\cos x_2)y_2z_2 + (\cos x_3)y_3z_2 \\ (\cos x_1)y_1z_3 + (\cos x_2)y_2z_3 + (\cos x_3)y_3z_3 \end{bmatrix},$$

and we wish to achieve the multiple symplectic synchronization

$$\mathbf{G}(\mathbf{x}, \mathbf{y}, \mathbf{z}, t) = \mathbf{F}(\mathbf{x}, \mathbf{y}, \mathbf{z}, t).$$

Let  $\mathbf{e} = \mathbf{G}(\mathbf{x}, \mathbf{y}, \mathbf{z}, t) - \mathbf{F}(\mathbf{x}, \mathbf{y}, \mathbf{z}, t)$

Consider a Rössler system is described by

$$\begin{cases} \dot{x}_1 = -x_2 - x_3 \\ \dot{x}_2 = x_1 + w_1x_2 \\ \dot{x}_3 = w_2 + x_1x_3 - w_3x_3 \end{cases} \quad (3.4)$$

where  $w_1 = 0.15$ ,  $w_2 = 0.2$ ,  $w_3 = 10$ , and the initial condition is

$x_1(0) = 2$ ,  $x_2(0) = 2.4$ ,  $x_3(0) = 5$ , . The chaotic attractor of the Rössler system is

shown in Fig. 3.6.



The Chen system is described

$$\begin{cases} \dot{z}_1 = h_1(z_2 - z_1) \\ \dot{z}_2 = (h_2 - h_1)z_1 - z_1z_3 + h_2z_2 \\ \dot{z}_3 = z_1z_2 - h_3z_3 \end{cases} \quad (3.5)$$

where  $h_1 = 35, h_2 = 27.2, h_3 = 3$ , and the initial condition is  $z_1(0) = 0.5, z_2(0) = 0.26, z_3(0) = 0.35$ .

The controlled DGK system is described by

$$\begin{cases} \dot{y}_1 = y_2 + u_1 \\ \dot{y}_2 = -ay_2 - y_1[b(c - y_1^2) + dy_3] + u_2 \\ \dot{y}_3 = -ay_3 - y_3[b(c - y_3^2) + ey_1] + u_3 \end{cases} \quad (3.6)$$

where  $a=-0.5; b=-1.4; c=1.9; d=-4.5; e=6.2$ , is the controller parameters, and the initial condition is  $y_1(0) = 0.01, y_2(0) = 0.01, y_3(0) = 0.01, .$

Thus we design the controller as

$$\begin{aligned} u_1 = & -(-x_2 - x_3) - y_2 - [h_1(z_2 - z_1)] - (-x_2 - x_3)(\sin x_1)y_1z_1 \\ & + (\cos x_1)y_2z_1 + (\cos x_1)y_1[h_1(z_2 - z_1)] - (x_1 + w_1x_2)(\sin x_2)y_2z_1 \\ & + (\cos x_2)\{-ay_2 - y_1[b(c - y_1^2) + dy_3]\}z_1 + (\cos x_2)y_2[h_1(z_2 - z_1)] \\ & - (w_2 + x_1x_3 - w_3x_3)(\sin x_3)y_3z_1 + (\cos x_3)\{-ay_3 - y_3[b(c - y_3^2) + ey_1]\}z_1 \\ & + (\cos x_3)y_3[h_1(z_2 - z_1)] \\ u_2 = & -(x_1 + w_1x_2) - \{-ay_2 - y_1[b(c - y_1^2) + dy_3]\} - [(h_2 - h_1)z_1 - z_1z_3 + h_2z_2] \\ & - (-x_2 - x_3)(\sin x_1)y_1z_2 + (\cos x_1)y_2z_2 + (\cos x_1)y_1[(h_2 - h_1)z_1 - z_1z_3 + h_2z_2] \\ & - (x_1 + w_1x_2)(\sin x_2)y_2z_2 + (\cos x_2)\{-ay_2 - y_1[b(c - y_1^2) + dy_3]\}z_2 \\ & + (\cos x_2)y_2[(h_2 - h_1)z_1 - z_1z_3 + h_2z_2] - (w_2 + x_1x_3 - w_3x_3)(\sin x_3)y_3z_2 \\ & + (\cos x_3)\{-ay_3 - y_3[b(c - y_3^2) + ey_1]\}z_2 + (\cos x_3)y_3[(h_2 - h_1)z_1 - z_1z_3 + h_2z_2] \end{aligned}$$

$$\begin{aligned}
u_3 = & -(w_2 + x_1x_3 - w_3x_3) - \left\{ -ay_3 - y_3 \left[ b(c - y_3^2) + ey_3 \right] \right\} - (z_1z_2 - h_3z_3) \\
& - (-x_2 - x_3)(\sin x_1)y_1z_3 + (\cos x_1)y_2z_3 + (\cos x_1)y_1(z_1z_2 - h_3z_3) \\
& - (x_1 + w_1x_2)(\sin x_2)y_2z_3 + (\cos x_2) \left\{ -ay_2 - y_1 \left[ b(c - y_1^2) + dy_3 \right] \right\} z_3 \\
& + (\cos x_2)y_2(z_1z_2 - h_3z_3) - (w_2 + x_1x_3 - w_3x_3)(\sin x_3)y_3z_3 \\
& + (\cos x_3) \left\{ -ay_3 - y_3 \left[ b(c - y_3^2) + ey_1 \right] \right\} z_3 + (\cos x_3)y_3(z_1z_2 - h_3z_3)
\end{aligned}$$

The Theorem in Chapter 2 is satisfied and the multiple symplectic synchronization is achieved. The phase portrait of the controlled DGK system and the time histories of the state errors and the time histories of  $G(\mathbf{x}, \mathbf{y}, \mathbf{z}, t)$  and  $\mathbf{F}(\mathbf{x}, \mathbf{y}, \mathbf{z}, t)$  are shown in Fig. 3.7 and Fig. 3.8 and Fig. 3.9, respectively.

### CASE 3.

Define

$$\mathbf{G}(\mathbf{x}, \mathbf{y}, \mathbf{z}, t) = \begin{bmatrix} x_1 + y_1 + z_1 \\ x_2 + y_2 + z_2 \\ x_3 + y_3 + z_3 \end{bmatrix}, \quad \mathbf{F}(\mathbf{x}, \mathbf{y}, \mathbf{z}, t) = \begin{bmatrix} x_1y_1z_1 + x_2y_2z_1 + x_3y_3z_1 \\ x_1y_1z_2 + x_2y_2z_2 + x_3y_3z_2 \\ x_1y_1z_3 + x_2y_2z_3 + x_3y_3z_3 \end{bmatrix},$$

and we wish to achieve the multiple symplectic synchronization.

$$\mathbf{G}(\mathbf{x}, \mathbf{y}, \mathbf{z}, t) = \mathbf{F}(\mathbf{x}, \mathbf{y}, \mathbf{z}, t).$$

$$\text{Let } \mathbf{e} = \mathbf{G}(\mathbf{x}, \mathbf{y}, \mathbf{z}, t) - \mathbf{F}(\mathbf{x}, \mathbf{y}, \mathbf{z}, t)$$

Consider a Sprott E system is described by

$$\begin{cases} \dot{x}_1 = x_2x_3 \\ \dot{x}_2 = x_1^2 - x_2 \\ \dot{x}_3 = 1 - w_1x_1 \end{cases} \quad (3.7)$$

where  $w_1 = 4$ , and the initial condition is  $x_1(0) = -1, x_2(0) = -1, x_3(0) = -1$ . The chaotic attractor of the Sprott E system is shown in Fig. 3.10.

The Chen system is described

$$\begin{cases} \dot{z}_1 = h_1(z_2 - z_1) \\ \dot{z}_2 = (h_2 - h_1)z_1 - z_1z_3 + h_2z_2 \\ \dot{z}_3 = z_1z_2 - h_3z_3 \end{cases} \quad (3.8)$$

where  $h_1 = 35$ ,  $h_2 = 27.2$ ,  $h_3 = 3$ , and the initial condition is

$$z_1(0) = 0.5, z_2(0) = 0.26, z_3(0) = 0.35.$$

The controlled DGK system is described by

$$\begin{cases} \dot{y}_1 = y_2 + u_1 \\ \dot{y}_2 = -ay_2 - y_1 \left[ b(c - y_1^2) + dy_3 \right] + u_2 \\ \dot{y}_3 = -ay_3 - y_3 \left[ b(c - y_3^2) + ey_1 \right] + u_3 \end{cases} \quad (3.9)$$

where  $a=-0.5$ ;  $b=-1.4$ ;  $c=1.9$ ;  $d=-4.5$ ;  $e=6.2$ , are the controller parameters, and the initial condition is  $y_1(0) = 0.01$ ,  $y_2(0) = 0.01$ ,  $y_3(0) = 0.01$ .

Thus we design the controller as

$$\begin{aligned} u_1 &= -x_2x_3 - y_2 - \left[ h_1(z_2 - z_1) \right] + x_2x_3y_1z_1 + x_1y_2z_1 + x_1y_1 \left[ h_1(z_2 - z_1) \right] \\ &\quad + (x_1^2 - x_2)y_2z_1 + x_2 \left\{ -ay_2 - y_1 \left[ b(c - y_1^2) + dy_3 \right] \right\} z_1 \\ &\quad + x_2y_2 \left[ h_1(z_2 - z_1) \right] + (1 - w_1x_1)y_3z_1 + x_3 \left\{ -ay_3 - y_3 \left[ b(c - y_3^2) + ey_1 \right] \right\} z_1 \\ &\quad + x_3y_3 \left[ h_1(z_2 - z_1) \right] \\ u_2 &= -(x_1^2 - x_2) - \left\{ -ay_2 - y_1 \left[ b(c - y_1^2) + dy_3 \right] \right\} - \left[ (h_2 - h_1)z_1 - z_1z_3 + h_2z_2 \right] \\ &\quad + x_2x_3y_1z_2 + x_1y_2z_2 + x_1y_1 \left[ (h_2 - h_1)z_1 - z_1z_3 + h_2z_2 \right] + (x_1^2 - x_2)y_2z_2 \\ &\quad + x_2 \left\{ -ay_2 - y_1 \left[ b(c - y_1^2) + dy_3 \right] \right\} z_2 + x_2y_2 \left[ (h_2 - h_1)z_1 - z_1z_3 + h_2z_2 \right] \\ &\quad + (1 - w_1x_1)y_3z_2 + x_3 \left\{ -ay_3 - y_3 \left[ b(c - y_3^2) + ey_1 \right] \right\} z_2 + x_3y_3 \left[ (h_2 - h_1)z_1 - z_1z_3 + h_2z_2 \right] \\ u_3 &= -(1 - w_1x_1) - \left\{ -ay_3 - y_3 \left[ b(c - y_3^2) + ey_1 \right] \right\} - (z_1z_2 - h_3z_3) \\ &\quad + x_2x_3y_1z_3 + x_1y_2z_3 + x_1y_1(z_1z_2 - h_3z_3) + (x_1^2 - x_2)y_2z_3 \\ &\quad + x_2 \left\{ -ay_2 - y_1 \left[ b(c - y_1^2) + dy_3 \right] \right\} z_3 + x_2y_2(z_1z_2 - h_3z_3) \\ &\quad + (1 - w_1x_1)y_3z_3 + x_3 \left\{ -ay_3 - y_3 \left[ b(c - y_3^2) + ey_1 \right] \right\} z_3 + x_3y_3(z_1z_2 - h_3z_3) \end{aligned}$$

The Theorem in Chapter 2 is satisfied and the multiple symplectic synchronization

is achieved. The phase portrait of the controlled DGK system and the time histories of the state errors and the time histories of  $G(\mathbf{x}, \mathbf{y}, z, t)$  and  $\mathbf{F}(\mathbf{x}, \mathbf{y}, z, t)$  are shown in Fig. 3.11 and Fig. 3.12 and Fig. 3.13, respectively.



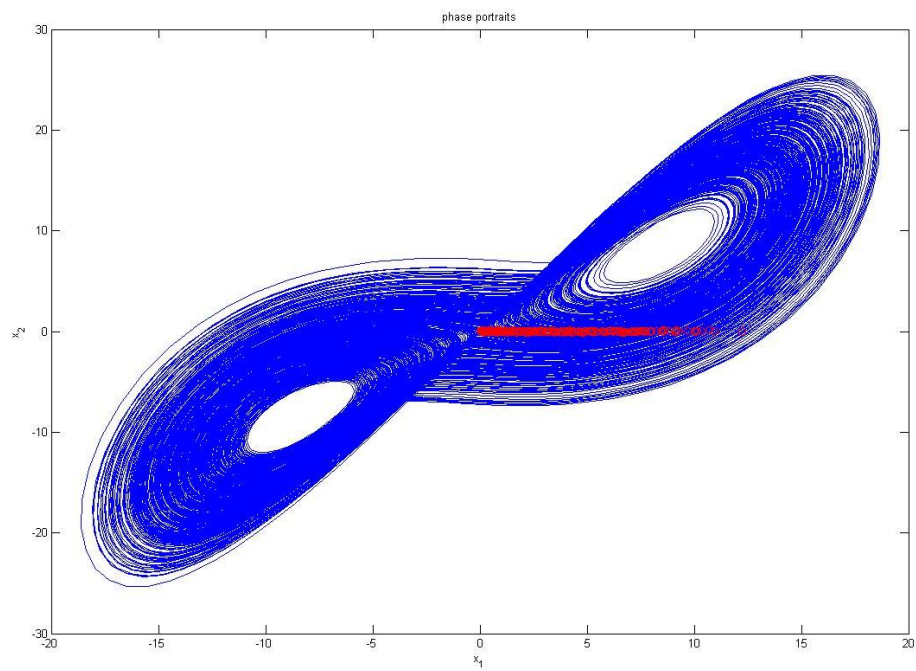


Fig. 3.1 The chaotic attractor of the Lorenz system.

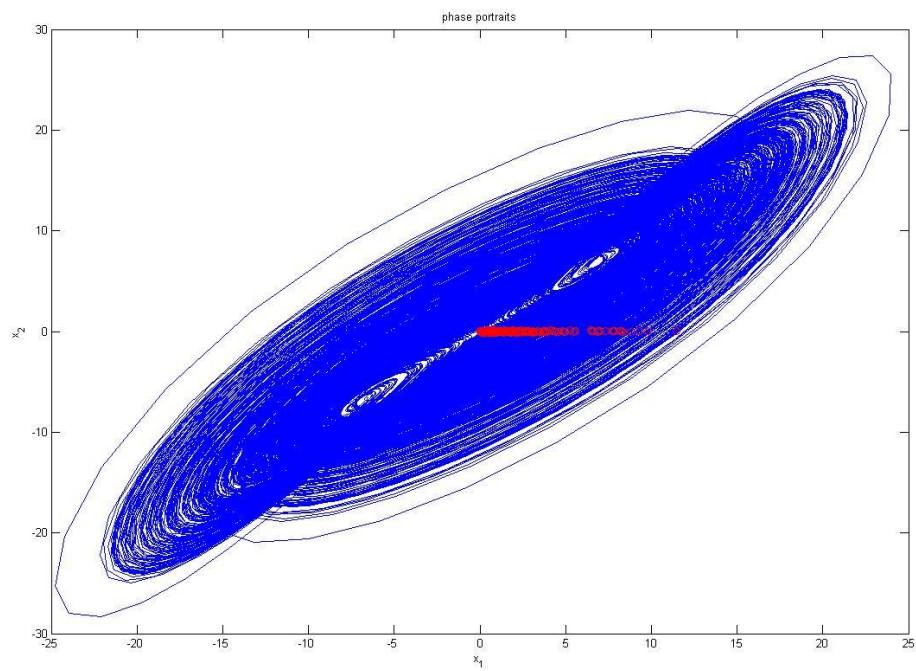


Fig. 3.2 The chaotic attractor of the Chen system.

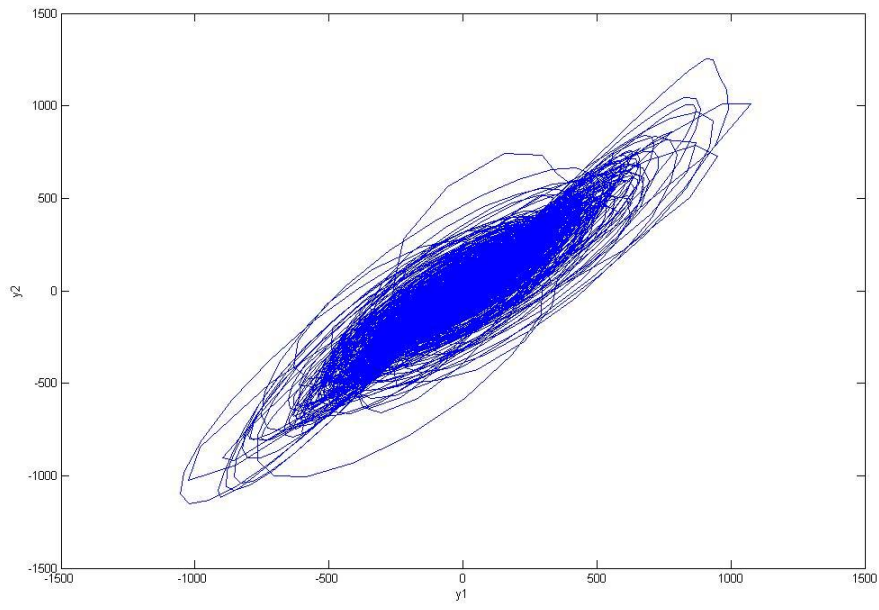


Fig. 3.3 The phase portrait of the controlled DGK system.

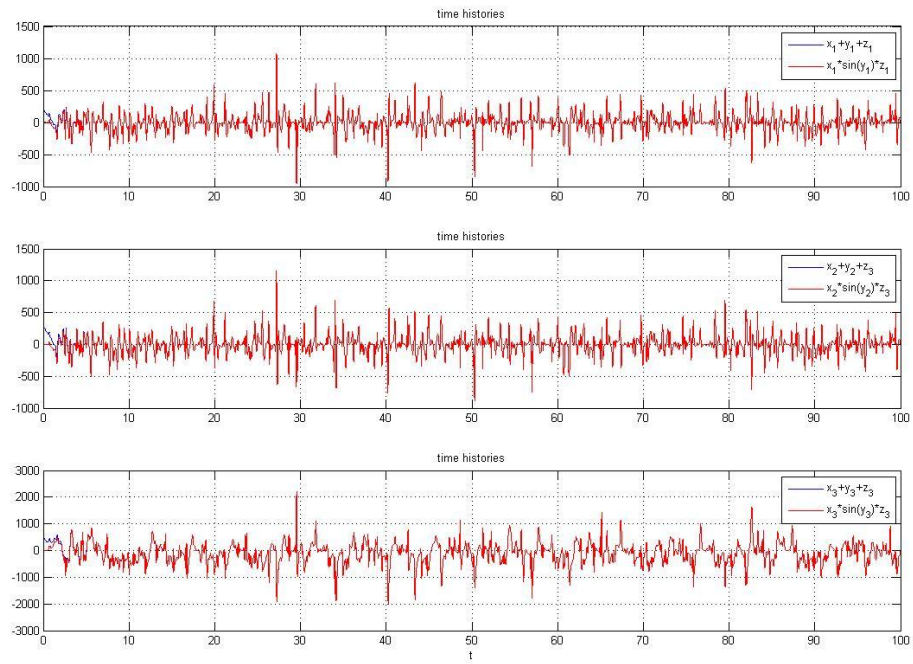


Fig. 3.4 Time histories of  $G(\mathbf{x}, \mathbf{y}, \mathbf{z}, t)$  and  $\mathbf{F}(\mathbf{x}, \mathbf{y}, \mathbf{z}, t)$  for Case 1.

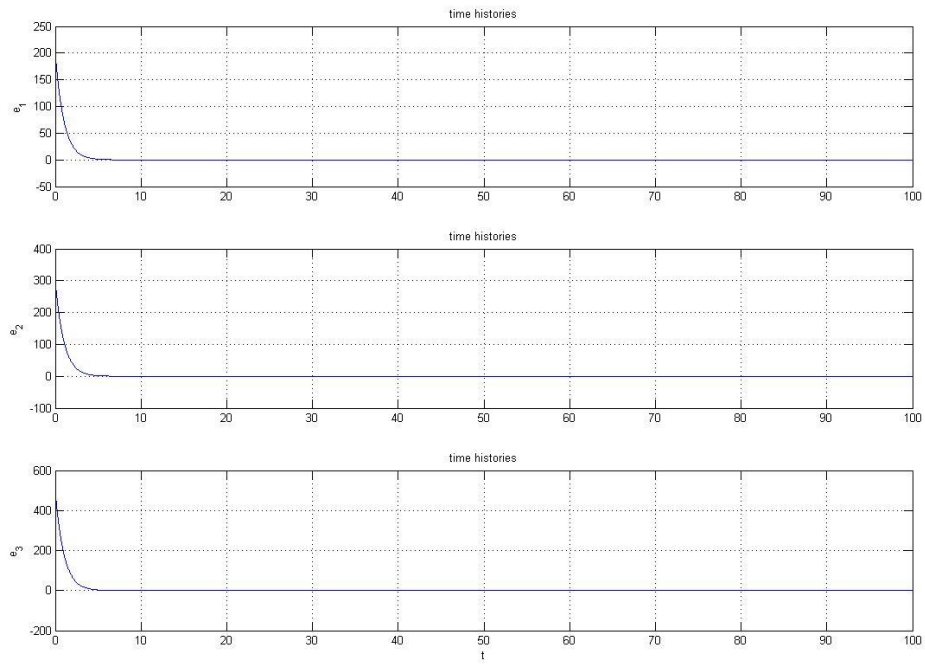


Fig. 3.5 Time histories of the errors for Case 1.

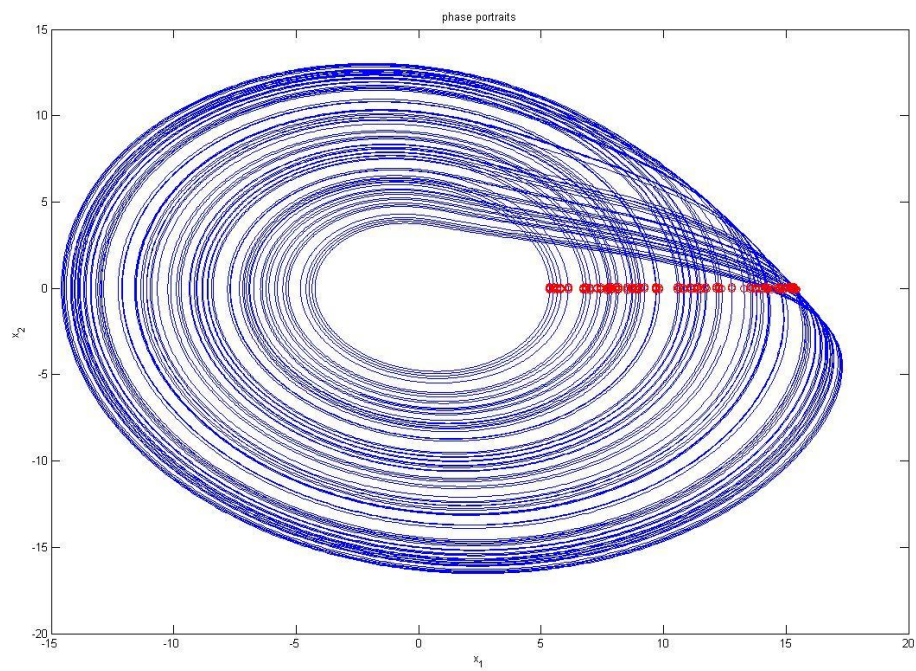


Fig. 3.6 The chaotic attractor of the Rössler system.



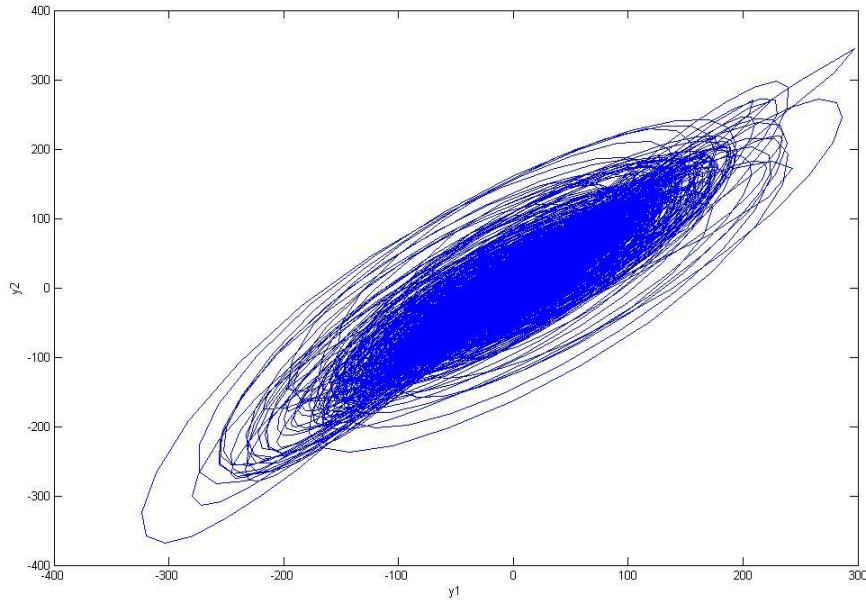


Fig. 3.7 The phase portrait of the controlled DGK system.

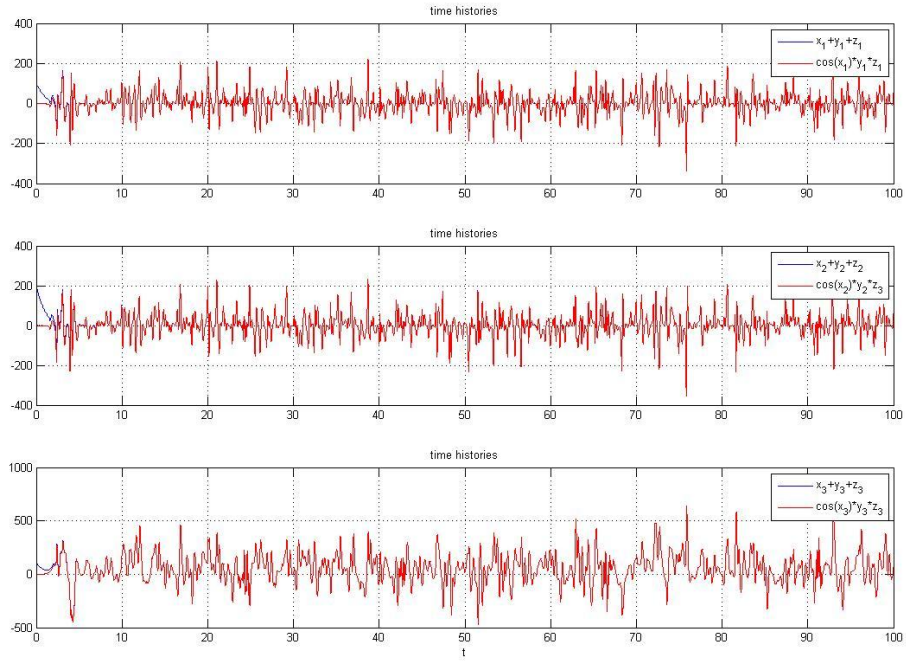


Fig. 3.8 Time histories of  $G(\mathbf{x}, \mathbf{y}, \mathbf{z}, t)$  and  $\mathbf{F}(\mathbf{x}, \mathbf{y}, \mathbf{z}, t)$  for Case 2.



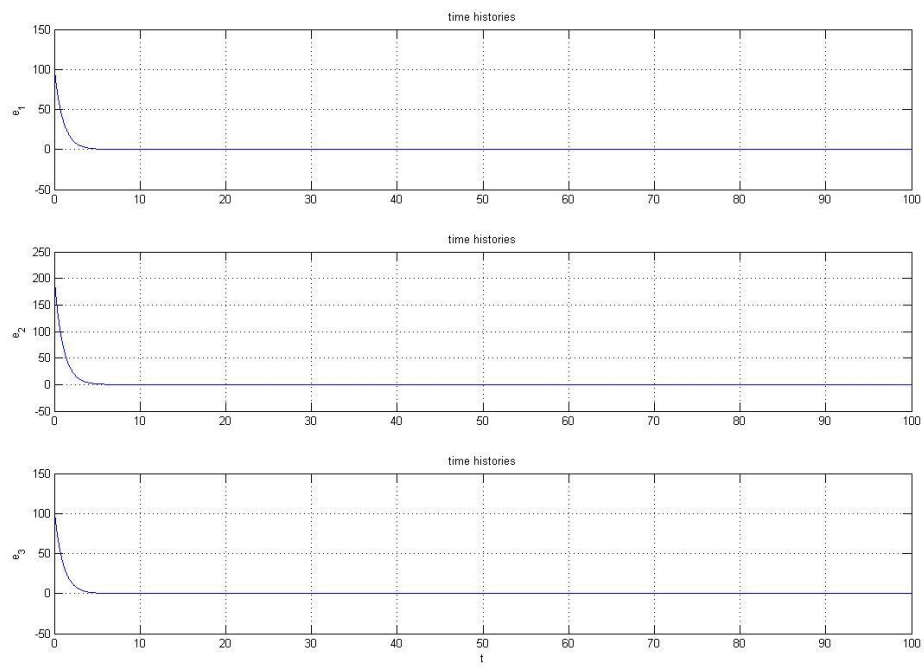


Fig. 3.9 Time histories of the errors for Case 2.

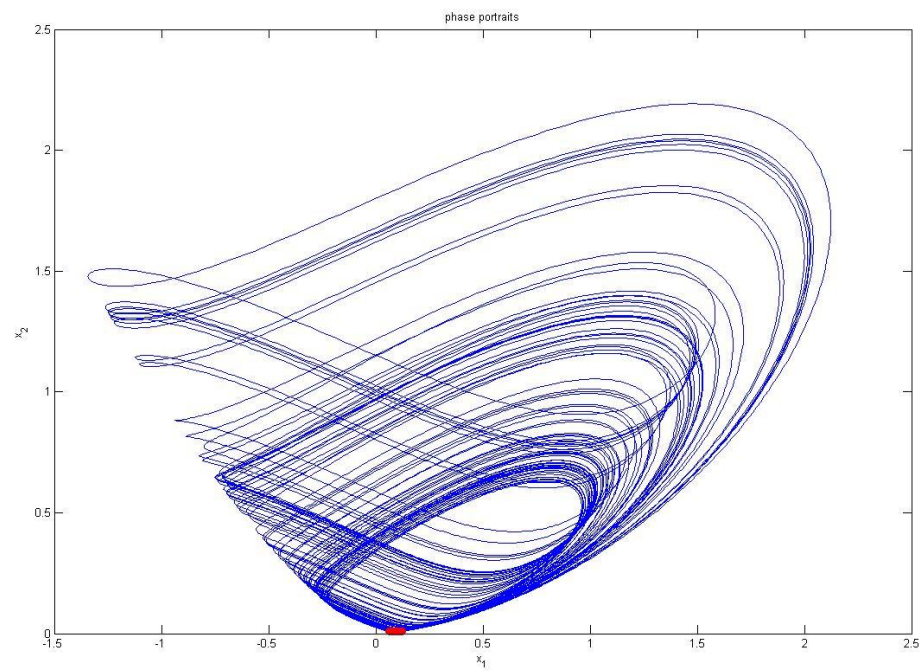


Fig. 3.10 The chaotic attractor of a Sprott E system.

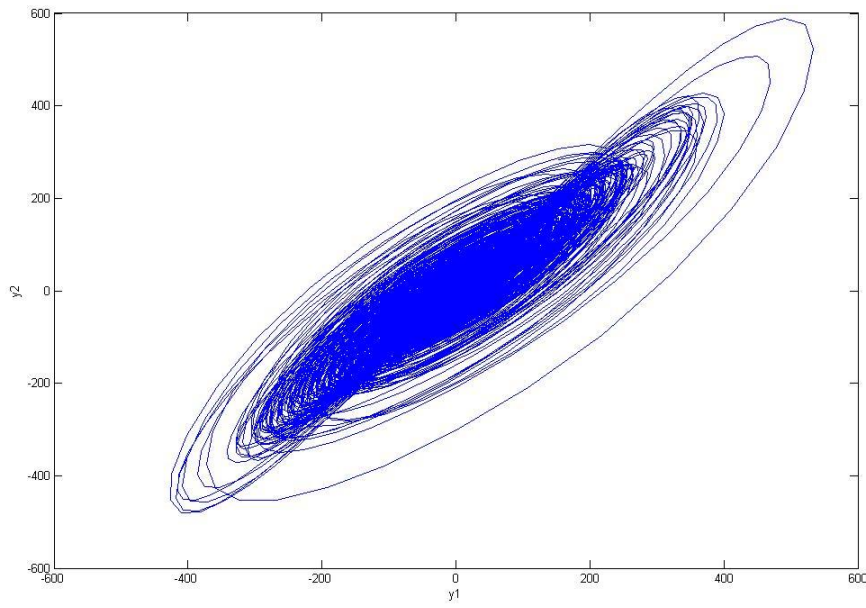


Fig. 3.11 The phase portrait of the controlled DGK system.

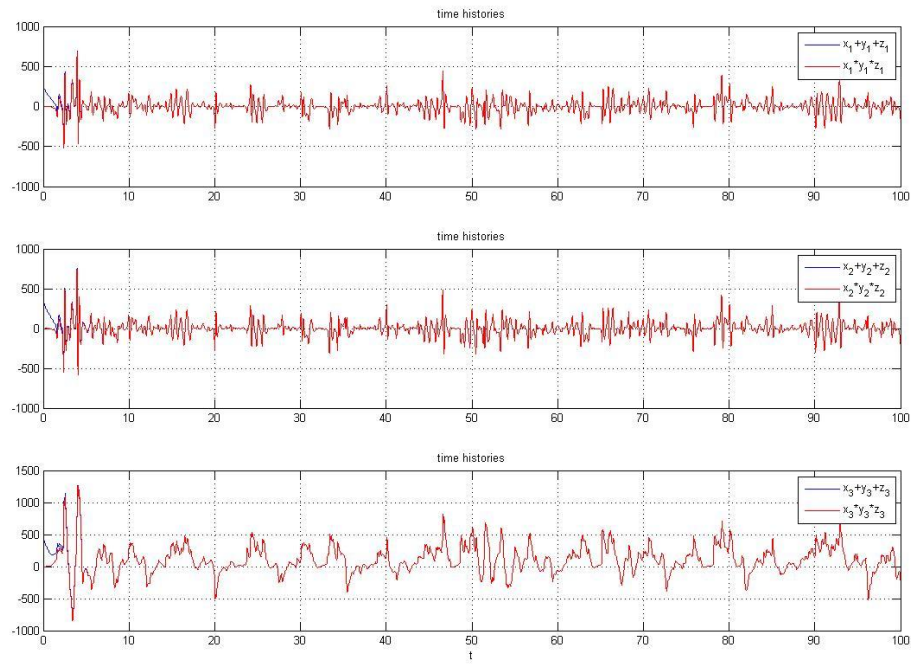


Fig. 3.12 Time histories of  $G(\mathbf{x},\mathbf{y},\mathbf{z},t)$  and  $\mathbf{F}(\mathbf{x},\mathbf{y},\mathbf{z},t)$  for Case 3.

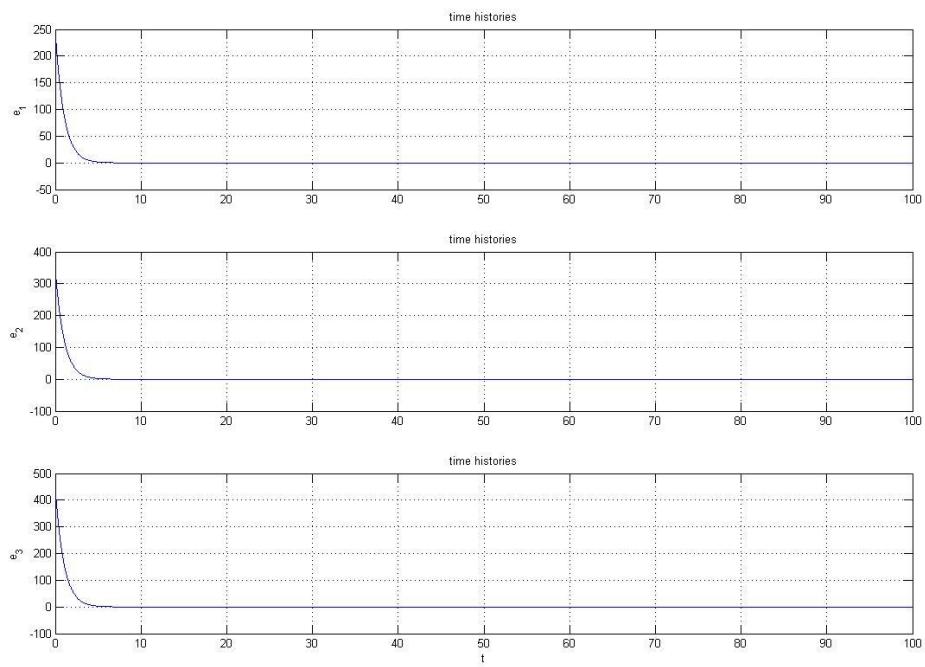
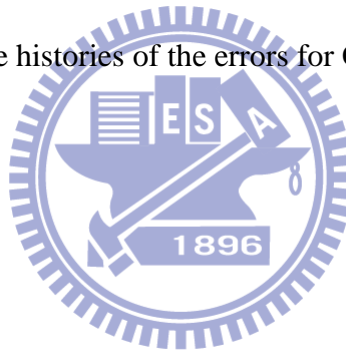


Fig. 3.13 Time histories of the errors for Case 3.



# Chapter 4

## Different Translation Pragmatical Generalized Synchronization by Stability Theory of Partial Region for Double Ge-Ku System

### 4.1 Preliminary

In this Chapter, a new strategy to achieve different translation generalized synchronization by stability theory of partial region by which the Lyapunov function is simple linear homogeneous function of error states, the controllers are more simple since they are in lower degree than that of traditional controllers.

By a pragmatical theorem of asymptotical stability based on an assumption of equal probability of initial point, an adaptive control law is derived such that it can be proved strictly that the common zero solution of error dynamics and of parameter dynamics is asymptotically stable. Numerical simulations of a new Double Ge-Ku(DGK) system are given to show the effectiveness of the proposed scheme.

### 4.2 The Scheme of Different Translation Pragmatical Generalized Synchronization by Stability Theory of Partial Region

There are two identical nonlinear dynamical systems, and the master system synchronizes the slave system. The master system is given by

$$\dot{x} = A x + f(x) \quad (4.1)$$

The master system after the origin of x-coordinate system is translated to  $(k_1, k_1, \dots, k_1)$  is

$$\dot{x}' = A x' + f(x') \quad (4.1)$$

where  $x' = [x'_1, x'_2, \dots, x'_n]^T = x - k_1 = [x_1 - k_1, x_2 - k_1, \dots, x_n - k_1] \in R^n$  denotes a state

vector where  $k_1 = [k_1, k_1, \dots, k_1]$  is a constant vector with positive coefficient  $k_1$  as shown in Fig.4.1.  $A$  is an  $n \times n$  uncertain constant coefficients matrix,  $f$  is a nonlinear vector function, and  $B$  is a vector of uncertain constant coefficients in  $f$ .

The slave system is given by

$$\dot{y} = Ay + (f(y) - B) + \xi \quad (4.2)$$

The slave system after the origin of  $y$ -coordinate system is translated to  $(k_2, k_2, \dots, k_2)$  is

$$\dot{y}' = Ay' + (f(y') - B) + \xi \quad (4.2)$$

where  $y' = [y'_1, y'_2, \dots, y'_n]^T = y - k_2 = [y_1 - k_2, y_2 - k_2, \dots, y_n - k_2] \in R^n$  denotes a state vector where  $k_2$  is a constant vector with positive coefficient  $k_2$  as shown in Fig.4.2.  $A$  is an  $n \times n$  estimated coefficient matrix,  $B$  is a vector of estimated coefficients in  $f$ , and  $u(t) = [u_1(t), u_2(t), \dots, u_n(t)]^T \in R^n$  is a control input vector.

Our goal is to design a controller  $u(t)$  so that the state vector of the translated slave system (4.2)' asymptotically approaches the state vector of the translated master system (4.1)' plus a given nonchaotic or chaotic vector function

$$F(t) = [F_1(t), F_2(t), \dots, F_n(t)]^T :$$

$$y' = G(x) = \dot{x} + K. \quad (4.3)$$

This generalized synchronization can be accomplished when  $t \rightarrow \infty$ , the limit of the error vector  $e(t) = [e_1, e_2, \dots, e_n]^T$  approaches zero:

$$\lim_{t \rightarrow \infty} e = 0 \quad (4.4)$$

where

$$e = \dot{x} + K - \dot{y} = \dot{x} - \dot{y} + K. \quad (4.5)$$

From Eq. (4.5) we have

$$\dot{e} = \dot{x}' - \dot{y}' + \dot{F}(t) \quad (4.6)$$

$$\dot{e} = A'x - A'y + (f', x)B - (f', y)B - \dot{F}(t) \quad (4.7)$$

where  $k_1$  and  $k_2$  are chosen to guarantee that the error dynamics always occurs in the first quadrant of  $e$  coordinate system.

A Lyapunov function  $V(e, A_c, B_c)$  is chosen as a positive definite function in first quadrant of  $e$  coordinate system by stability theory in partial region as shown in Appendix A :

$$V(e, A_c, B_c) = e^T A_c + \quad (4.8)$$

where  $A_c = A - A$ ,  $B_c = B - B$ ,  $A_c$  and  $B_c$  are two column matrices whose elements are all the elements of matrix  $A_c$  and of matrix  $B_c$ , respectively.

Its derivative along any solution of the differential equation system consisting of Eq. (4.7) and update parameter differential equations for  $A_c$  and  $B_c$  is

$$\dot{V}(e, A_c, B_c) = Ax' - Ay' + f'(x)B - f'(y)B + \dot{F}(t) - u(t) + \dot{\tilde{A}}_c + \dot{\tilde{B}}_c \quad (4.9)$$

where  $u(t)$ ,  $\dot{\tilde{A}}_c$ , and  $\dot{\tilde{B}}_c$  are chosen so that  $\dot{V} = Ce$ ,  $C$  is a diagonal negative definite matrix, and  $\dot{V}$  is a negative semi-definite function of  $e$  and parameter differences  $\tilde{A}_c$  and  $\tilde{B}_c$ . By pragmatical asymptotically stability theorem in Appendix B, the Lyapunov function used is a simple linear homogeneous function of states and the controllers are simpler because they in lower order than that of traditional controllers. In many papers [51-55], traditional Lyapunov stability theorem and Babalat lemma are used to prove the error vector approaches zero, as time approaches infinity. But the question, why the estimated parameters also approach to the uncertain parameters, remains no answer. By pragmatical asymptotical stability theorem, the question can be answered strictly.

### 4.3 Different Translation Pragmatical Generalized Synchronization of New Double Ge-Ku Chaotic System

#### Case 1

The following chaotic systems are two translated DGK systems of which the old origin is translated to  $(x_1, x_2, x_3) = (150, 150, 150)$ ,  $(y_1, y_2, y_3) = (50, 50, 50)$  to guarantee the error dynamics always happens in the first quadrant of  $e$  coordinate system.

$$\begin{cases} \dot{x}_1 = x_2 - 150 \\ \dot{x}_2 = -a(x_2 - 150) - (x_1 - 150)\{b[c - (x_1 - 150)^2] + d(x_3 - 150)\} \\ \dot{x}_3 = -a(x_3 - 150) - (x_3 - 150)\{b[c - (x_3 - 150)^2] + g(x_1 - 150)\} \end{cases} \quad (4.10)$$

$$\begin{cases} \dot{y}_1 = y_2 - 50 + u_1 \\ \dot{y}_2 = -a(y_2 - 50) - (y_1 - 50)\{\hat{b}[\hat{c} - (y_1 - 50)^2] + d(y_3 - 50)\} + u_2 \\ \dot{y}_3 = -a(y_3 - 50) - (y_3 - 50)\{\hat{b}[\hat{c} - (y_3 - 50)^2] + g(y_1 - 50)\} + u_3 \end{cases} \quad (4.11)$$

Let initial states be  $(x_1, x_2, x_3) = (150.01, 150.01, 150.01)$ ,  $(y_1, y_2, y_3) = (50.01, 50.01, 50.01)$  and system parameters  $a = -0.5, b = -1.4, c = 1.9, d = -4.5, g = 6.2$ .

The state error is

$$e = x - y + F(t) = x - y + e^{-c \cos t}$$

where  $F(t) = e^{-c \cos t}$  is a nonchaotic given function of time. We find that the error dynamic without controller always exists in first quadrant as shown in Fig.4.3.

$$\lim_{t \rightarrow \infty} e_i = \lim_{t \rightarrow \infty} (y_i + e^{-c \cos t}), i = 1, 2, 3 \quad (4.12)$$

Our aim is  $\lim_{t \rightarrow \infty} e = 0$ . We obtain the error dynamics:

$$\begin{cases} \dot{e}_1 = x_2 - 150 - y_2 + 50 - u_1 + (\sin t)e^{-\cos t} \\ \dot{e}_2 = -a(x_2 - 150) - (x_1 - 150)\{b[c - (x_1 - 150)^2] + d(x_3 - 150)\} \\ \quad + a(y_2 - 50) + (y_1 - 50)\{\hat{b}[\hat{c} - (y_1 - 50)^2] + d(y_3 - 50)\} - u_2 + (\sin t)e^{-\cos t} \\ \dot{e}_3 = -a(x_3 - 150) - (x_3 - 150)\{b[c - (x_3 - 150)^2] + g(x_3 - 150)\} \\ \quad + a(y_3 - 50) + (y_3 - 50)\{\hat{b}[\hat{c} - (y_3 - 50)^2] + \widehat{g}(\widehat{y_1} - 50)\} - u_3 + (\sin t)e^{-\cos t} \end{cases} \quad (4.13)$$

where  $\tilde{a} = a - \hat{a}$ ,  $\tilde{b} = b - \hat{b}$ ,  $\tilde{c} = c - \hat{c}$ ,  $\tilde{d} = d - \hat{d}$ ,  $\tilde{g} = g - \hat{g}$ , and  $a, \hat{b}, \hat{c}, d, g$  are estimates of uncertain parameters  $a, b, c, d$  and  $g$  respectively.

Using different translation pragmatical synchronization by stability theory of partial region, we can choose a Lyapunov function in the form of a positive definite function in first quadrant:

$$V = e_1 + e_2 + e_3 + \tilde{a} + \tilde{b} + \tilde{c} + \tilde{d} \quad (4.14)$$

Its time derivative is

$$\begin{aligned} \dot{V} &= \dot{e}_1 + \dot{e}_2 + \dot{e}_3 + \dot{\tilde{a}} + \dot{\tilde{b}} + \dot{\tilde{c}} + \dot{\tilde{d}} + \dot{\tilde{g}} \\ &= (x_2 - 150 - y_2 + 50 - u_1 + (\sin t)e^{\cos t}) \\ &\quad - a(x_2 - 150) - (x_1 - 150)\{b[c - (x_1 - 150)^2] + d(x_3 - 150)\} \\ &\quad + a(y_2 - 50) + (y_1 - 50)\{\hat{b}[\hat{c} - (y_1 - 50)^2] + d(y_3 - 50)\} - u_2 + (\sin t)e^{\cos t} \\ &\quad - a(x_3 - 150) - (x_3 - 150)\{b[c - (x_3 - 150)^2] + g(x_3 - 150)\} \\ &\quad + \widehat{a}(\widehat{y_3} - 50) + (y_3 - 50)\{\hat{b}[\hat{c} - (y_3 - 50)^2] + \widehat{g}(\widehat{y_1} - 50)\} - u_3 + (\sin t)e^{\cos t} \\ &\quad + w_{z_1} + \dot{\tilde{a}} + \dot{\tilde{b}} + \dot{\tilde{c}} + \dot{\tilde{d}} + \dot{\tilde{g}} \end{aligned} \quad (4.15)$$

Choose

$$\begin{cases} \dot{\tilde{a}} = -\dot{\hat{a}} = -\tilde{a}e_2 \\ \dot{\tilde{b}} = -\dot{\hat{b}} = -\tilde{b}e_2 \\ \dot{\tilde{c}} = -\dot{\hat{c}} = -\tilde{c}e_2 \\ \dot{\tilde{d}} = -\dot{\hat{d}} = -\tilde{d}e_3 \\ \dot{\tilde{g}} = -\dot{\hat{g}} = -\tilde{g}e_3 \end{cases} \quad (4.16)$$



$$\begin{cases} u_1 = x_2 - 150 - y_2 + 50 + (\sin t)e^{-\cos t} + e_1 \\ u_2 = -a(x_2 - 150) - (x_1 - 150)\{b[c - (x_1 - 150)^2] + d(x_3 - 150)\} \\ \quad + a(y_2 - 50) + (y_1 - 50)\{\hat{b}[\hat{c} - (y_1 - 50)^2] + d(y_3 - 50)\} + (\sin t)e^{-\cos t} \\ \quad + e_2 - ae_2 - \tilde{b}e_2 - \tilde{c}e_2 \\ u_3 = -a(x_3 - 150) - (x_3 - 150)\{b[c - (x_3 - 150)^2] + g(x_3 - 150)\} \\ \quad + \widehat{a}(y_3 - 50) + (y_3 - 50)\{\hat{b}[\hat{c} - (y_3 - 50)^2] + \widehat{g}(y_1 - 50)\} + (\sin t)e^{-\cos t} \\ \quad + e_3 - \tilde{d}e_3 - \widetilde{ge}_3 \end{cases} \quad (4.17)$$

We obtain

$$\dot{V} = -e_1 - e_2 - e_3 < 0 \quad (4.18)$$

which is a negative semi-definite function of  $e_1, e_2, e_3, \tilde{a}, \tilde{b}, \tilde{c}, \tilde{d}, \tilde{g}$ , in the first quadrant. The Lyapunov asymptotical stability theorem is not satisfied. We can not obtain that common origin of error dynamics (13) and parameter dynamics (16) is asymptotically stable. By pragmatical asymptotically stability theorem, D is a 8-manifold,  $n=8$  and the number of error state variables  $p=3$ . When  $e_1 = e_2 = e_3 = 0$  and  $\tilde{a}, \tilde{b}, \tilde{c}, \tilde{d}, \tilde{g}$  take arbitrary values,  $\dot{V}=0$ , so X is of 3 dimensions,  $m=n-p=8-3=5$ ,  $m+1<n$  is satisfied. According to the pragmatical asymptotically stability theorem, error vector  $e$  approaches zero and the estimated parameters also approach the uncertain parameters. The equilibrium point is pragmatically asymptotically stable. Under the assumption of equal probability, it is actually asymptotically stable. The simulation results are shown in Figs.4.4-4.6.

## Case 2

The following chaotic systems are two translated DGK systems of which the old origin is translated to  $(x_1, x_2, x_3) = (150, 150, 150)$ ,  $(y_1, y_2, y_3) = (50, 50, 50)$  to guarantee that the error dynamics always happens in the first quadrant of  $e$  coordinate system.

$$\begin{cases} \dot{x}_1 = x_2 - 150 \\ \dot{x}_2 = -a(x_2 - 150) - (x_1 - 150)\{b[c - (x_1 - 150)^2] + d(x_3 - 150)\} \\ \dot{x}_3 = -a(x_3 - 150) - (x_3 - 150)\{b[c - (x_3 - 150)^2] + g(x_1 - 150)\} \end{cases} \quad (4.19)$$

$$\begin{cases} \dot{y}_1 = y_2 - 50 + u_1 \\ \dot{y}_2 = -a(y_2 - 50) - (y_1 - 50)\{\hat{b}[\hat{c} - (y_1 - 50)^2] + d(y_3 - 50)\} + u_2 \\ \dot{y}_3 = -a(y_3 - 50) - (y_3 - 50)\{\hat{b}[\hat{c} - (y_3 - 50)^2] + g(y_1 - 50)\} + u_3 \end{cases} \quad (4.20)$$

Let initial states be  $(x_1, x_2, x_3) = (150.01, 150.01, 150.01)$ ,  $(y_1, y_2, y_3) = (50.01, 50.01, 50.01)$  and system parameters  $a = -0.5, b = -1.4, c = 1.9, d = -4.5, g = 6.2$ .

The state error is  $e = x - y + F(t)$ , where  $F(t) = \mathbf{z} = [z_1, z_2, z_3]$  is the state vector of Chen system :

$$\begin{cases} \dot{z}_1 = h(z_2 - z_1) \\ \dot{z}_2 = (w - h)z_1 - z_1 z_3 + wz_3 \\ \dot{z}_3 = z_1 z_2 - lz_3 \end{cases} \quad (4.21)$$

Let initial states be  $\mathbf{z} = [z_1, z_2, z_3] = [0.5, 0.26, 0.35]$  and system parameters  $h = 35, l = 3, w = 27.2$ . The Chen system is chaotic,  $F(t) = \mathbf{z} = [z_1, z_2, z_3]$  is a given chaotic vector function of time.

Define

$$e = x_i - y_i + \mathbf{z}_i$$

We find that the error dynamics without controller always exists in first quadrant as shown in Fig.4.7.

$$\lim_{t \rightarrow \infty} e_i = \lim_{t \rightarrow \infty} [x_i - y_i + \mathbf{z}_i], \quad i = 1, 2, 3 \quad (4.22)$$

Our aim is  $\lim_{t \rightarrow \infty} e = 0$ .

We obtain the error dynamics:

$$\begin{cases} \dot{e}_1 = x_2 - 150 - y_2 + 50 - u_1 + h(z_2 - z_1) \\ \dot{e}_2 = -a(x_2 - 150) - (x_1 - 150)\{b[c - (x_1 - 150)^2] + d(x_3 - 150)\} \\ \quad + a(y_2 - 50) + (y_1 - 50)\{\hat{b}[\hat{c} - (y_1 - 50)^2] + d(y_3 - 50)\} - u_2 \\ \quad + (w - h)z_1 - z_1 z_3 + wz_2 \\ \dot{e}_3 = -a(x_3 - 150) - (x_3 - 150)\{b[c - (x_3 - 150)^2] + g(x_3 - 150)\} \\ \quad + \widehat{a}(\widehat{y}_3 - 50) + (y_3 - 50)\{\hat{b}[\hat{c} - (y_3 - 50)^2] + \widehat{g}(\widehat{y}_1 - 50)\} - u_3 + z_1 z_2 - lz_3 \end{cases} \quad (4.23)$$

where  $\tilde{a} = a - \hat{a}$ ,  $\tilde{b} = b - \hat{b}$ ,  $\tilde{c} = c - \hat{c}$ ,  $\tilde{d} = d - \hat{d}$ ,  $\tilde{g} = g - \hat{g}$ , and  $a$ ,  $\hat{b}$ ,  $\hat{c}$ ,  $d$ ,

$g$ , are estimates of uncertain parameters  $a$ ,  $b$ ,  $c$ ,  $d$  and  $g$  respectively.

Using different translation pragmatistical synchronization by stability theory of partial region, we can choose a Lyapunov function in the form of a positive definite function in first quadrant:

$$V = \varphi + \varrho + \varrho + \tilde{a} + \tilde{b} + \tilde{c} + \tilde{d} \quad (4.24)$$

Its time derivative is

$$\begin{aligned} \dot{V} &= \dot{e}_1 + \dot{e}_2 + \dot{e}_3 + \dot{\tilde{a}} + \dot{\tilde{b}} + \dot{\tilde{c}} + \dot{\tilde{d}} + \dot{\tilde{g}} \\ &= (x_2 - 150 - y_2 + 50 - u_1 + h(z_2 - z_1)) \\ &\quad - a(x_2 - 150) - (x_1 - 150)\{b[c - (x_1 - 150)^2] + d(x_3 - 150)\} \\ &\quad + a(y_2 - 50) + (y_1 - 50)\{\hat{b}[\hat{c} - (y_1 - 50)^2] + d(y_3 - 50)\} - u_2 \\ &\quad + (w - h)z_1 - z_1 z_3 + wz_2 \\ &\quad - a(x_3 - 150) - (x_3 - 150)\{b[c - (x_3 - 150)^2] + g(x_3 - 150)\} \\ &\quad + \widehat{a}(\widehat{y}_3 - 50) + (y_3 - 50)\{\hat{b}[\hat{c} - (y_3 - 50)^2] + \widehat{g}(\widehat{y}_1 - 50)\} - u_3 + z_1 z_2 - lz_3 \\ &\quad + \dot{\tilde{a}} + \dot{\tilde{b}} + \dot{\tilde{c}} + \dot{\tilde{d}} + \dot{\tilde{g}} \end{aligned} \quad (4.25)$$

Choose

$$\begin{cases} \dot{\tilde{a}} = -\dot{\hat{a}} = -\tilde{a}e_2 \\ \dot{\tilde{b}} = -\dot{\hat{b}} = -\tilde{b}e_2 \\ \dot{\tilde{c}} = -\dot{\hat{c}} = -\tilde{c}e_2 \\ \dot{\tilde{d}} = -\dot{\hat{d}} = -\tilde{d}e_3 \\ \dot{\tilde{g}} = -\dot{\hat{g}} = -\tilde{g}e_3 \end{cases} \quad (4.26)$$

$$\left\{ \begin{array}{l} u_1 = x_2 - 150 - y_2 + 50 + h(z_2 - z_1) + e_1 \\ u_2 = -a(x_2 - 150) - (x_1 - 150)\{b[c - (x_1 - 150)^2] + d(x_3 - 150)\} \\ \quad + a(y_2 - 50) + (y_1 - 50)\{\hat{b}[\hat{c} - (y_1 - 50)^2] + d(y_3 - 50)\} \\ \quad + (w - h)z_1 - z_1 z_3 + wz_2 \\ \quad + e_2 - ae_2 - \tilde{b}e_2 - \tilde{c}e_2 \\ u_3 = -a(x_3 - 150) - (x_3 - 150)\{b[c - (x_3 - 150)^2] + g(x_3 - 150)\} \\ \quad + \widehat{a}(y_3 - 50) + (y_3 - 50)\{\hat{b}[\hat{c} - (y_3 - 50)^2] + \widehat{g}(y_1 - 50)\} + z_1 z_2 - lz_3 \\ \quad + e_3 - \tilde{d}e_3 - \tilde{g}e_3 \end{array} \right. \quad (4.27)$$

We obtain

$$\dot{V} = -e_1 - e_2 - e_3 \quad (4.28)$$

which is a negative semi-definite function of  $e_1, e_2, e_3, \tilde{a}, \tilde{b}, \tilde{c}, \tilde{d}, \tilde{g}$  in the first quadrant. The Lyapunov asymptotical stability theorem is not satisfied. We can not obtain that common origin of error dynamics (23) and parameter dynamics (26) is asymptotically stable. By pragmatical asymptotically stability theorem, D is a 8-manifold,  $n=8$  and the number of error state variables  $p=3$ . When  $e_1 = e_2 = e_3 = 0$  and  $\tilde{a}, \tilde{b}, \tilde{c}, \tilde{d}, \tilde{g}$ , take arbitrary values,  $\dot{V}=0$ , so X is of 3 dimensions,  $m=n-p=8-3=5$ ,  $m+1 < n$  is satisfied. According to the pragmatical asymptotically stability theorem, error vector  $e$  approaches zero and the estimated parameters also approach the uncertain parameters. The equilibrium point is pragmatically asymptotically stable. Under the assumption of equal probability, it is actually asymptotically stable. The simulation results are shown in Figs.4.8-4.10.

### Case 3

The following chaotic systems are the two translated DGK systems of which the old origin is translated to  $(x_1, x_2, x_3) = (150, 150, 150)$ ,  $(y_1, y_2, y_3) = (50, 50, 50)$  to guarantee error dynamics always happens in the first quadrant of  $e$  coordinate system.

$$\begin{cases} \dot{x}_1 = x_2 - 150 \\ \dot{x}_2 = -a(x_2 - 150) - (x_1 - 150)\{b[c - (x_1 - 150)^2] + d(x_3 - 150)\} \\ \dot{x}_3 = -a(x_3 - 150) - (x_3 - 150)\{b[c - (x_3 - 150)^2] + g(x_1 - 150)\} \end{cases} \quad (4.29)$$

$$\begin{cases} \dot{y}_1 = y_2 - 50 + u_1 \\ \dot{y}_2 = -a(y_2 - 50) - (y_1 - 50)\{\hat{b}[\hat{c} - (y_1 - 50)^2] + d(y_3 - 50)\} + u_2 \\ \dot{y}_3 = -a(y_3 - 50) - (y_3 - 50)\{\hat{b}[\hat{c} - (y_3 - 50)^2] + g(y_1 - 50)\} + u_3 \end{cases} \quad (4.30)$$

Let initial states be  $(x_1, x_2, x_3) = (150.01, 150.01, 150.01)$ ,  $(y_1, y_2, y_3) = (50.01, 50.01, 50.01)$  and system parameters  $a = -0.5, b = -1.4, c = 1.9, d = -4.5, g = 6.2$ .

The state error is  $e = x - y + F(t)$ , where  $F(t) = \mathbf{z} = [z_1, z_2, z_3]$  is state vector the new Ge-Ku-van der Pol(GKv) system :

$$\begin{cases} \dot{z}_1 = z_2 \\ \dot{z}_2 = -f_1 z_2 - z_3[f_2(f_3 - z_1^2) + f_4 z_3] \\ \dot{z}_3 = -g z_3 + h(1 - z_3^2)z_2 + l z_1 \end{cases} \quad (4.31)$$

Let initial states be  $(z_1, z_2, z_3) = (0.01, 0.01, 0.01)$  and system parameters  $f_1 = 0.08, f_2 = -0.35, f_3 = 100.56, f_4 = -1000.02, h = 0.61, l = 0.08, w = 0.01$ , the Ge-Ku-van der Pol system [56] is chaotic in Fig.4.11,  $F(t) = \mathbf{z} = [z_1, z_2, z_3]$  is a given chaotic vector function of time.

Define

$$e = x_i - y_i + \mathbf{z}_i$$

We find that the error dynamic without controller always exists in first quadrant as shown in Fig. 4.12.

$$\lim_{t \rightarrow \infty} e_i = \lim_{t \rightarrow \infty} [x_i - y_i + \mathbf{z}_i], \quad i = 1, 2, 3 \quad (4.32)$$

Our aim is  $\lim_{t \rightarrow \infty} e = 0$ .

We obtain the error dynamics:

$$\left\{ \begin{array}{l} \dot{e}_1 = x_2 - 150 - y_2 + 50 - u_1 + z_1 \\ \dot{e}_2 = -a(x_2 - 150) - (x_1 - 150)\{b[c - (x_1 - 150)^2] + d(x_3 - 150)\} \\ \quad + a(y_2 - 50) + (y_1 - 50)\{\hat{b}[\hat{c} - (y_1 - 50)^2] + d(y_3 - 50)\} - u_2 \\ \quad - f_1 z_2 - z_3[f_2(f_3 - z_1^2) + f_4 z_3] \\ \dot{e}_3 = -a(x_3 - 150) - (x_3 - 150)\{b[c - (x_3 - 150)^2] + g(x_3 - 150)\} \\ \quad + \widehat{a}(\widehat{y}_3 - 50) + (y_3 - 50)\{\hat{b}[\hat{c} - (y_3 - 50)^2] + \widehat{g}(\widehat{y}_1 - 50)\} - u_3 \\ \quad - h z_3 + l(1 - z_3^2)z_2 + w z_1 \end{array} \right. \quad (4.33)$$

where  $\tilde{a} = a - \hat{a}$ ,  $\tilde{b} = b - \hat{b}$ ,  $\tilde{c} = c - \hat{c}$ ,  $\tilde{d} = d - \hat{d}$ ,  $\tilde{g} = g - \hat{g}$ , and  $a$ ,  $\hat{b}$ ,  $\hat{c}$ ,  $d$ ,  $g$ , are estimates of uncertain parameters  $a$ ,  $b$ ,  $c$ ,  $d$  and  $g$  respectively.

Using different translation pragmatical synchronization by stability theory of partial region, we can choose a Lyapunov function in the form of a positive definite function in first quadrant:

$$V = \varphi + \varrho + \vartheta + \tilde{a} + \tilde{b} + \tilde{c} + \tilde{d} \quad (4.34)$$

Its time derivative is

$$\begin{aligned} \dot{V} &= \dot{e}_1 + \dot{e}_2 + \dot{e}_3 + \dot{\tilde{a}} + \dot{\tilde{b}} + \dot{\tilde{c}} + \dot{\tilde{d}} + \dot{\tilde{g}} \\ &= (x_2 - 150 - y_2 + 50 - u_1 + z_1) \\ &\quad - a(x_2 - 150) - (x_1 - 150)\{b[c - (x_1 - 150)^2] + d(x_3 - 150)\} \\ &\quad + a(y_2 - 50) + (y_1 - 50)\{\hat{b}[\hat{c} - (y_1 - 50)^2] + d(y_3 - 50)\} - u_2 \\ &\quad - f_1 z_2 - z_3[f_2(f_3 - z_1^2) + f_4 z_3] \\ &\quad - a(x_3 - 150) - (x_3 - 150)\{b[c - (x_3 - 150)^2] + g(x_3 - 150)\} \\ &\quad + \widehat{a}(\widehat{y}_3 - 50) + (y_3 - 50)\{\hat{b}[\hat{c} - (y_3 - 50)^2] + \widehat{g}(\widehat{y}_1 - 50)\} - u_3 \\ &\quad - h z_3 + l(1 - z_3^2)z_2 + w z_1 + \dot{\tilde{a}} + \dot{\tilde{b}} + \dot{\tilde{c}} + \dot{\tilde{d}} + \dot{\tilde{g}} \end{aligned} \quad (4.35)$$

Choose

$$\begin{cases} \dot{\tilde{a}} = -\dot{\hat{a}} = -\tilde{a}e_2 \\ \dot{\tilde{b}} = -\dot{\hat{b}} = -\tilde{b}e_2 \\ \dot{\tilde{c}} = -\dot{\hat{c}} = -\tilde{c}e_2 \\ \dot{\tilde{d}} = -\dot{\hat{d}} = -\tilde{d}e_3 \\ \dot{\tilde{g}} = -\dot{\hat{g}} = -\tilde{g}e_3 \end{cases} \quad (4.36)$$

$$\begin{cases} u_1 = x_2 - 150 - y_2 + 50 + z_1 + e_1 \\ u_2 = -a(x_2 - 150) - (x_1 - 150)\{b[c - (x_1 - 150)^2] + d(x_3 - 150)\} \\ \quad + a(y_2 - 50) + (y_1 - 50)\{\hat{b}[\hat{c} - (y_1 - 50)^2] + d(y_3 - 50)\} \\ \quad - f_1 z_2 - z_3[f_2(f_3 - z_1^2) + f_4 z_3] + e_2 - \tilde{a}e_2 - \tilde{b}e_2 - \tilde{c}e_2 \\ u_3 = -a(x_3 - 150) - (x_3 - 150)\{b[c - (x_3 - 150)^2] + g(x_3 - 150)\} \\ \quad + \widehat{a}(y_3 - 50) + (y_3 - 50)\{\hat{b}[\hat{c} - (y_3 - 50)^2] + \widehat{g}(y_1 - 50)\} \\ \quad - h z_3 + l(1 - z_3^2)z_2 + w z_1 + e_3 - \tilde{d}e_3 - \tilde{g}e_3 \end{cases} \quad (4.37)$$

We obtain

$$\dot{V} = -e_1 - e_2 - e_3 \leq 0 \quad (4.38)$$

which is a negative semi-definite function of  $e_1, e_2, e_3, \tilde{a}, \tilde{b}, \tilde{c}, \tilde{d}, \tilde{g}$ , in the first quadrant. The Lyapunov asymptotical stability theorem is not satisfied. We can not obtain that common origin of error dynamics (33) and parameter dynamics (36) is asymptotically stable. By pragmatical asymptotically stability theorem, D is a 8-manifold,  $n=8$  and the number of error state variables  $p=3$ . When  $e_1 = e_2 = e_3 = 0$  and  $\tilde{a}, \tilde{b}, \tilde{c}, \tilde{d}, \tilde{g}$ , take arbitrary values,  $\dot{V} = 0$ , so X is of 3 dimensions,  $m=n-p=8-3=5$ ,  $m+1 < n$  is satisfied. According to the pragmatical asymptotically stability theorem, error vector  $e$  approaches zero and the estimated parameters also approach the uncertain parameters. The equilibrium point is pragmatically asymptotically stable. Under the assumption of equal probability, it is actually asymptotically stable. The simulation results are shown in Figs.4.13-4.15.

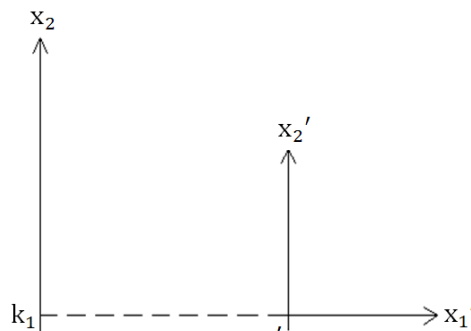


Fig. 4.1 Coordinate translation of state x.

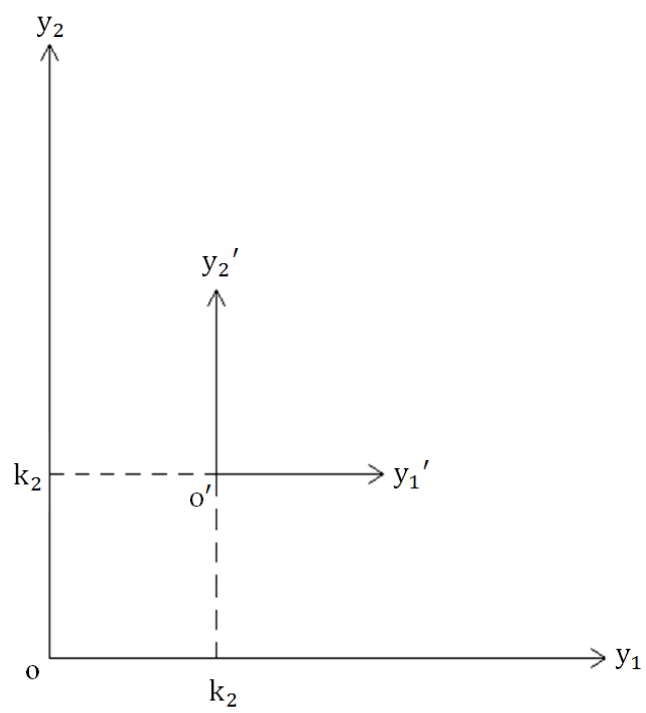


Fig. 4.2 Coordinate translation of state y.

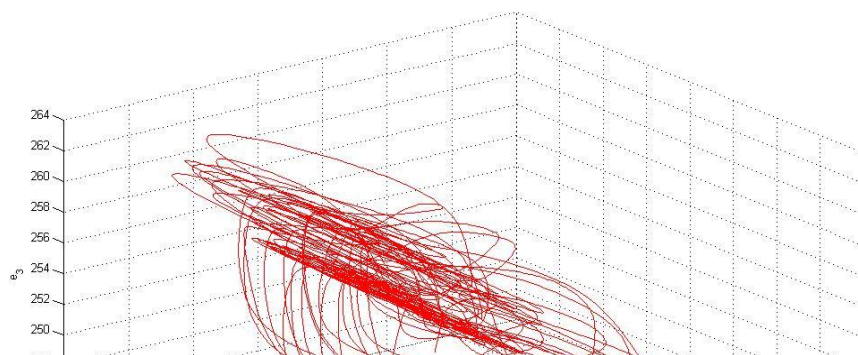




Fig. 4.3 Phase portrait of the error dynamics for Case 1.

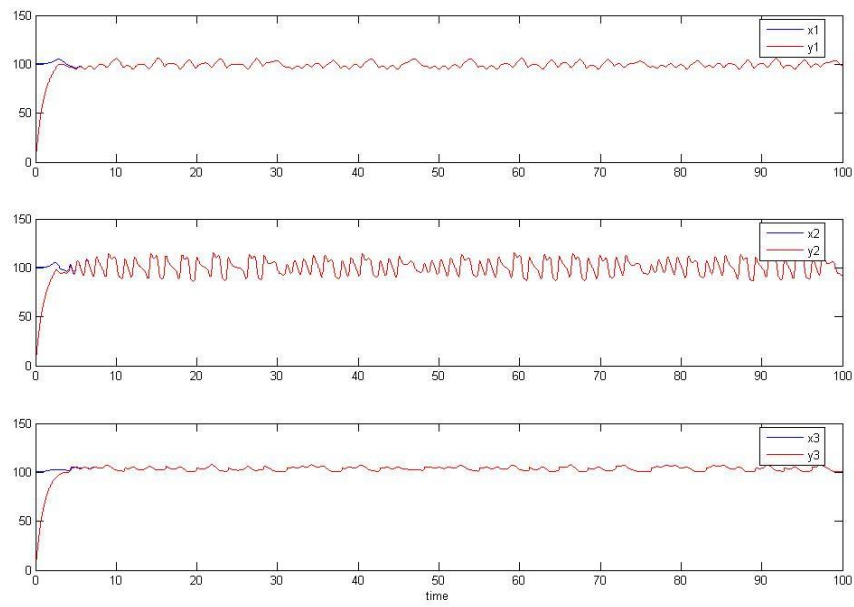


Fig. 4.4 Time histories of  $x_i$ ,  $y_i$  for Case 1.

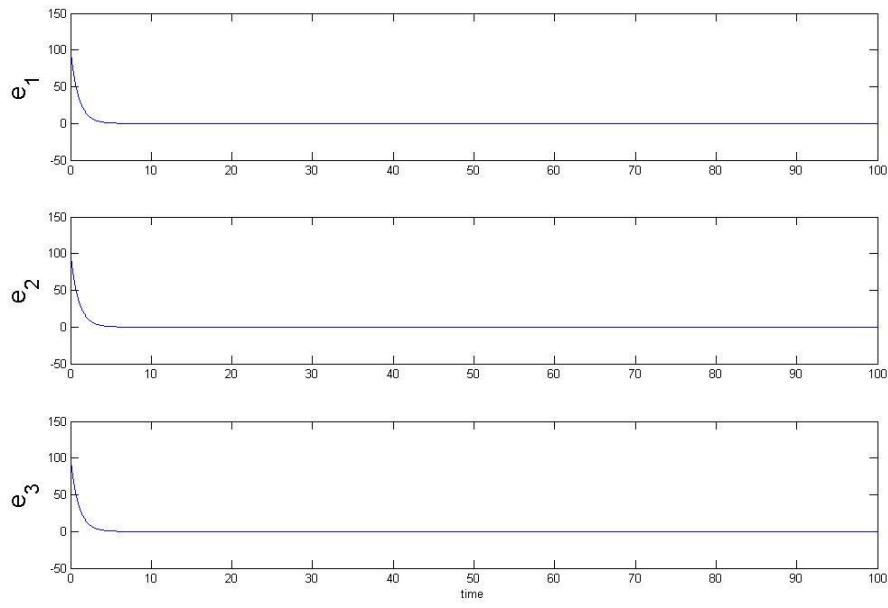


Fig. 4.5 Time histories of errors for Case 1.

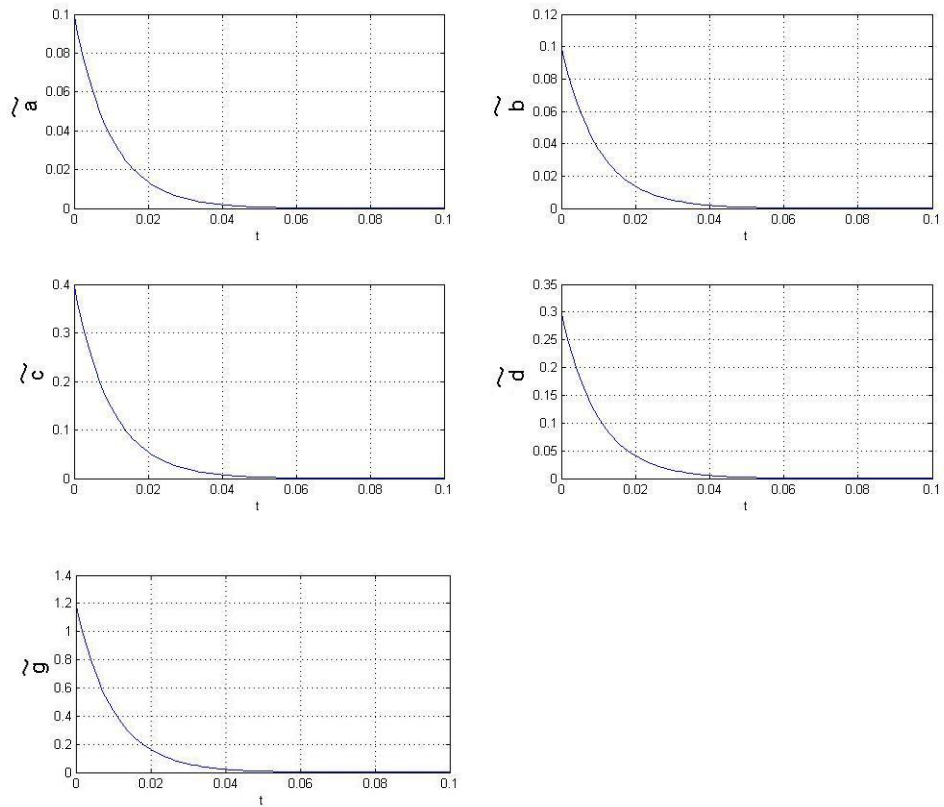


Fig. 4.6 Time histories of parameter errors for Case 1.

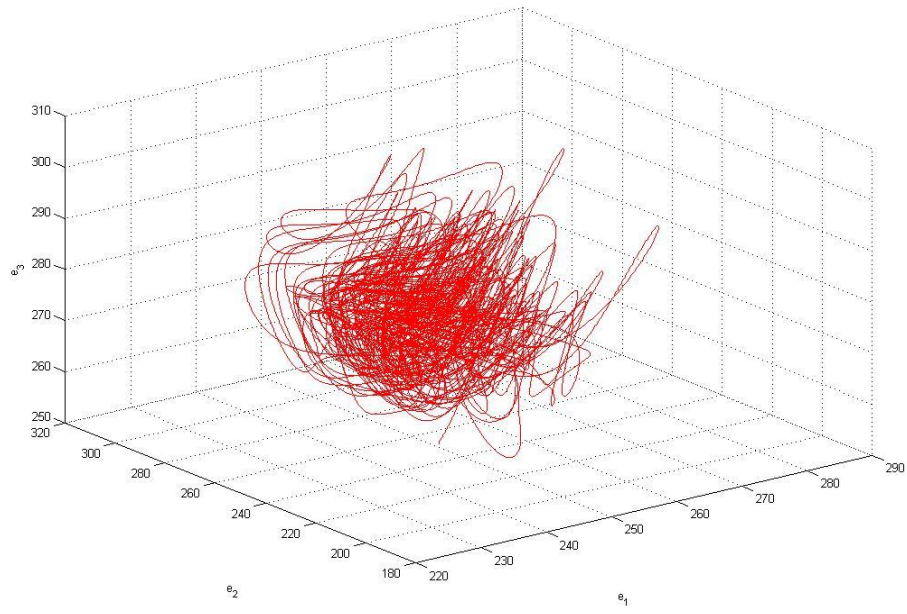


Fig. 4.7 Phase portrait of the error dynamic for Case 2.

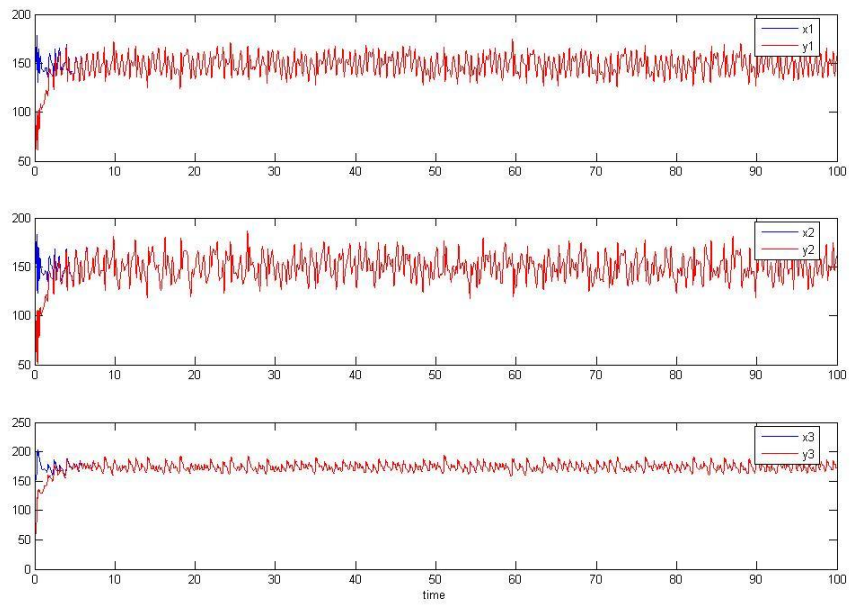


Fig. 4.8 Time histories of  $x_i$ ,  $y_i$  for Case 2.

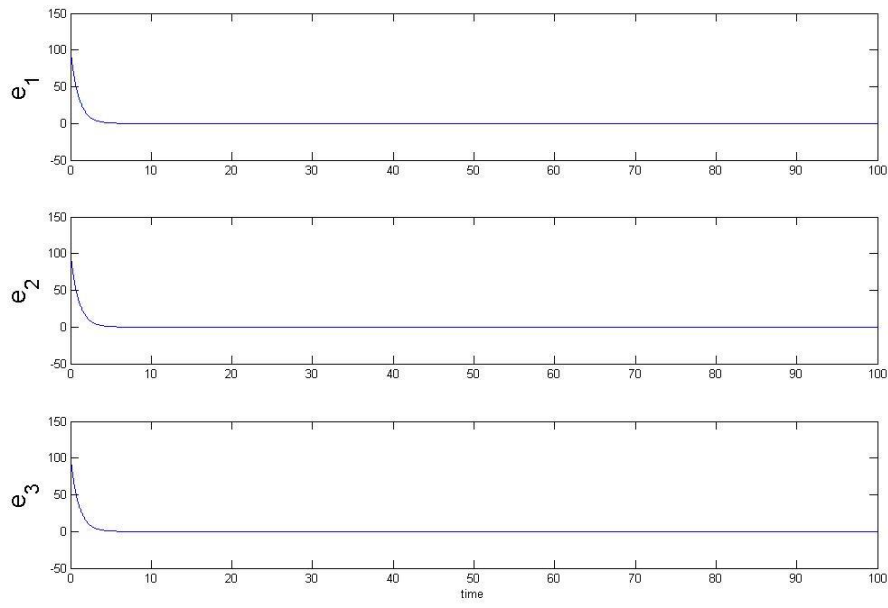


Fig. 4.9 Time histories of errors for Case 2.

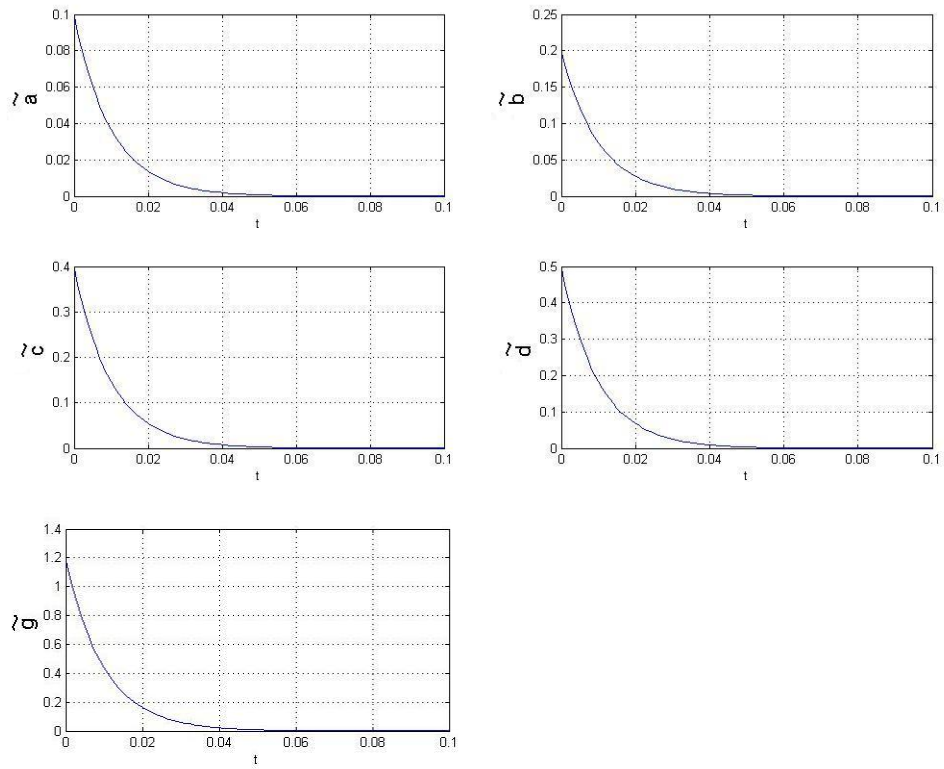


Fig. 4.10 Time histories of parameter errors for Case 2.

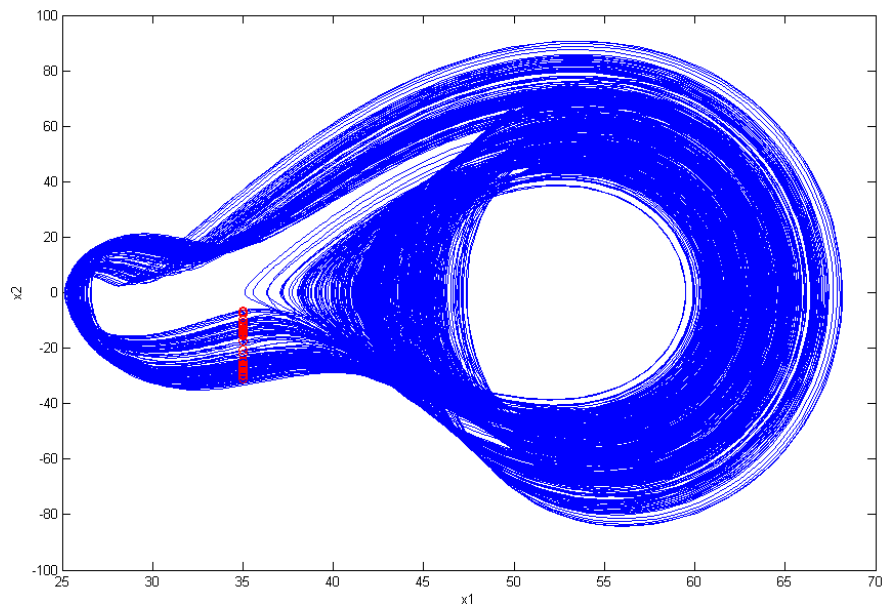


Fig. 4.11 The chaotic attractor of the Ge-Ku-van der Pol system.

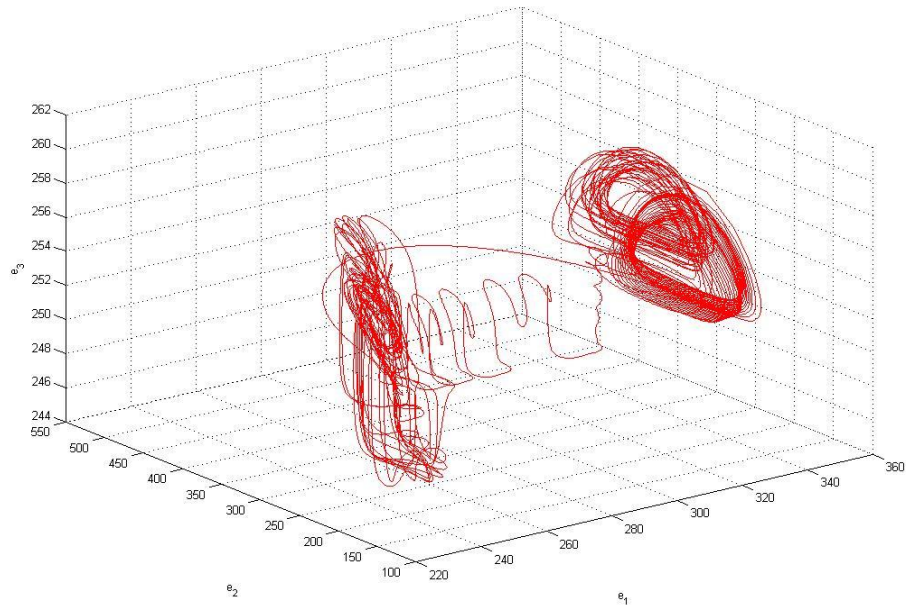


Fig. 4.12 Phase portrait of the error dynamic for Case 3.

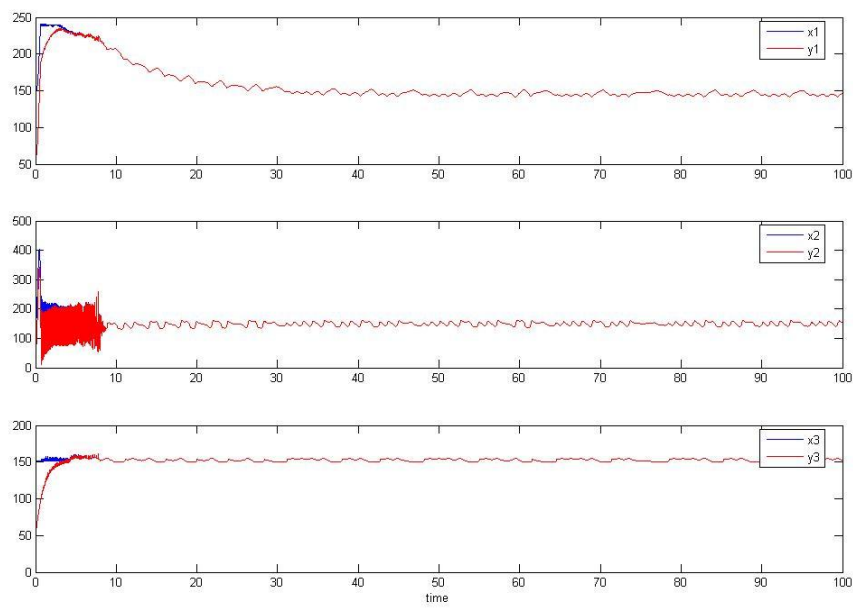


Fig. 4.13 Time histories of  $x_i$ ,  $y_i$  for Case 3.

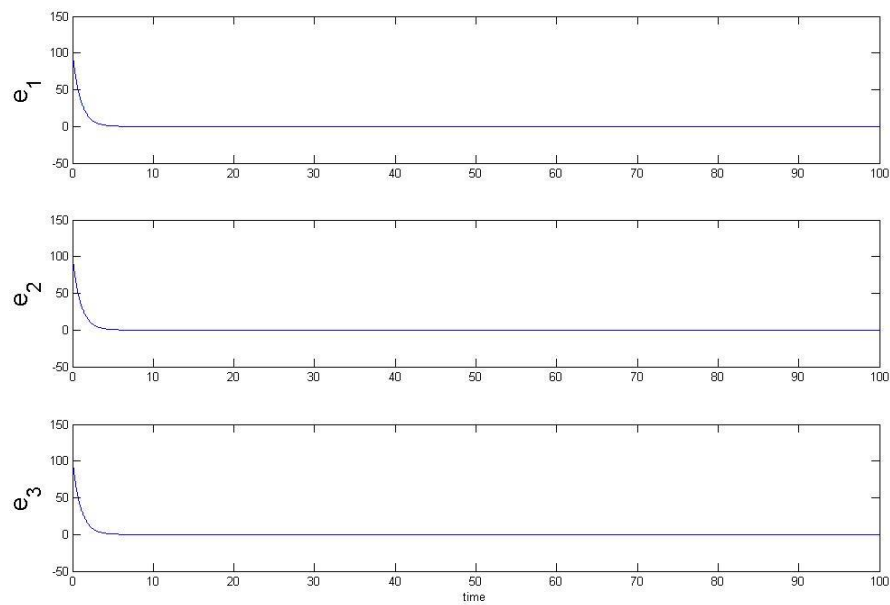
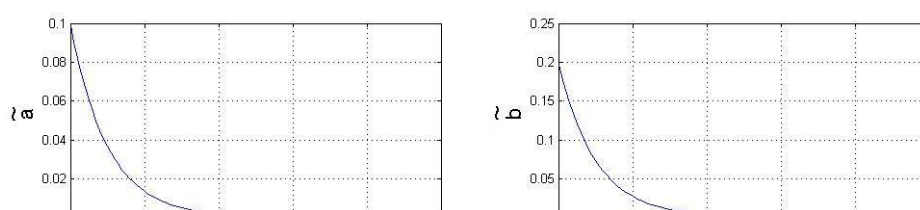


Fig. 4.14 Time histories of errors for Case 3.



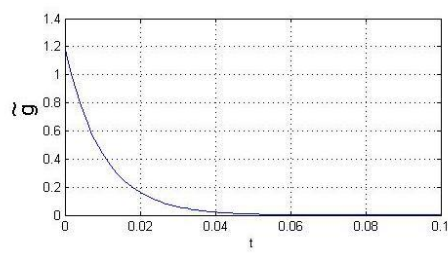
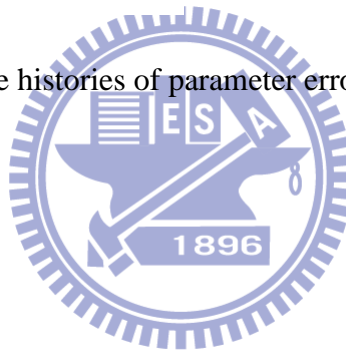


Fig. 4.15 Time histories of parameter errors for Case 3.



# Chapter 5

## Robust Projective Anti-Synchronization of Non-autonomous and Chaotic Uncertain Stochastic Systems Via Fuzzy Logic Constant Controller

### 5.1 Preliminary

In this Chapter, the simplest controller – fuzzy logic constant controller (FLCC) which is derived by fuzzy logic design and Lyapunov direct method is introduced. Controllers in traditional method are always complicated or nonlinear. FLCC proposed are such simple controllers which are constructed by constant number decided by the values of the upper and lower bound of the error derivatives. Therefore this tool is further used in projective anti-synchronization of chaotic uncertain and stochastic systems with to show the robustness and effectiveness of FLCC. There are two cases illustrated in simulation results to show the feasibility of the FLCC – Sprott 4 system and Double Ge-Ku (DGK) system. Comparison of the efficiency and complexity for the FLCC for traditional nonlinear controllers are given in tables and figures.

### 5.2 Projective Anti-Synchronization by FLCC Scheme

Consider the following non-autonomous or uncertain chaotic system

$$\dot{x} = Ax + f(x) + \zeta \quad (5.1)$$

where  $x = [x_1, x_2, \dots, x_n]^T \in R^n$  denotes a state vector,  $A$  is an  $n \times n$  constant coefficient matrix and  $f$  is a nonlinear vector function,  $\zeta$  is uncertain term.

The goal system which can be either chaotic or regular, is

$$\dot{y} = By + g(y) + u \quad (5.2)$$



where  $y = [y_1, y_2, \dots, y_n]^T \in R^n$  denotes a state vector,  $B$  is an  $n \times n$  constant coefficient matrix,  $g$  is a nonlinear vector function, and  $u = [u_1, u_2, \dots, u_n]^T \in R^n$  is the fuzzy logic controller needed to be designed.

In order to make the chaotic state  $x$  approaching the goal state  $y$ , define  $e = \alpha x + y$  as the state error, here  $\alpha$  is projective constant. The projective chaos anti-synchronization is accomplished in the sense that [57]:

$$\lim_{t \rightarrow \infty} e = \lim_{t \rightarrow \infty} (\alpha x + y) = 0 \quad (5.3)$$

where

$$e = \alpha x + y \quad (5.4)$$

From Eq. (2-4) we have the following error dynamics:

$$\dot{e} = \alpha \dot{x} + \dot{y} = \alpha[Ax + f(x)] + B[y - g(y)] \quad (5.5)$$

According to Lyapunov direct method, we have the following Lyapunov function to derive the fuzzy logic controller for anti-synchronization:

$$V = f(e_1, \dots, e_m, \dots, e_n) = \frac{1}{2}(e_1^2 + \dots + e_m^2 + \dots + e_n^2) > 0 \quad (5.6)$$

The derivative of the Lyapunov function in Eq. (5.5) is:

$$\dot{V} = e_1 \dot{e}_1 + \dots + e_m \dot{e}_m + \dots + e_n \dot{e}_n \quad (5.7)$$

If the controllers included in  $\dot{e}_1 \dots \dot{e}_m \dots \dot{e}_n$  can be suitably designed to achieve the target:  $\dot{V} < 0$ , then the two chaotic systems are asymptotically stable. The design process of FLCC is introduced in the following section.

We use one signal, error derivatives  $\dot{e}(t) = [\dot{e}_1, \dot{e}_2 \dots \dot{e}_m, \dots \dot{e}_n]^T$ , as the antecedent part of the proposed FLCC to design the control input  $u$  that will be used in the consequent part of the proposed FLCC as follows:

$$u = [u_1, u_2 \dots u_m, \dots u_n]^T \quad (5.8)$$

where  $u$  is a constant column vector and the FLCC accomplishes the objective to stabilize the error dynamics (5.5).

The strategy of the FLCC designing is proposed as follow and the configuration of the strategy is shown in Fig. 5.1.

Assume the upper bound and lower bound of  $\dot{e}_m$  are  $Z_m$  and  $-Z_m$ , then the FLCC can be design step by step as follow:

(1) If  $e_m$  is detected as positive ( $e_m > 0$ ), we have to design a controller for  $\dot{e}_m < 0$ , then  $\dot{V} = e_m \dot{e}_m < 0$  can be achieved. Therefore we have the following if-then fuzzy rule as:

$$\text{Rule 1 : IF } \dot{e}_m \text{ is } M_1 \text{ THEN } u_{m1} = -Z_m \quad (5.9)$$

$$\text{Rule 2 : IF } \dot{e}_m \text{ is } M_2 \text{ THEN } u_{m2} = -Z_m \quad (5.10)$$

$$\text{Rule 3 : IF } \dot{e}_m \text{ is } M_3 \text{ THEN } u_{m3} = e_m \quad (5.11)$$

(2) If  $e_m$  is detected as negative ( $e_m < 0$ ), we have to design a controller for  $\dot{e}_m > 0$ , then  $\dot{V} = e_m \dot{e}_m < 0$  can be achieved. Therefore we have the following if-then fuzzy rule as:

$$\text{Rule 1 : IF } \dot{e}_m \text{ is } M_1 \text{ THEN } u_{m1} = Z_m \quad (5.12)$$

$$\text{Rule 2 : IF } \dot{e}_m \text{ is } M_2 \text{ THEN } u_{m2} = Z_m \quad (5.13)$$

$$\text{Rule 3 : IF } \dot{e}_m \text{ is } M_3 \text{ THEN } u_{m3} = e_m \quad (5.14)$$

(3) If  $e_m$  approaches to zero, then the anti-synchronization is nearly achieved.

Therefore we have the following if-then fuzzy rule as:

$$\text{Rule 1 : IF } \dot{e}_m \text{ is } M_1 \text{ THEN } u_{m1} = e_m \approx 0 \quad (5.15)$$

$$\text{Rule 2 : IF } \dot{e}_m \text{ is } M_2 \text{ THEN } u_{m2} = e_m \approx 0 \quad (5.16)$$

$$\text{Rule 3 : IF } \dot{e}_m \text{ is } M_3 \text{ THEN } u_{m3} = e_m \approx 0 \quad (5.17)$$

where  $M_1 = \frac{|\dot{e}_m|}{Z_m}$ ,  $M_2 = \frac{|\dot{e}_m|}{Z_m}$  and  $M_3 = \text{sgn}(\frac{Z_m - \dot{e}_m}{Z_m}) + \text{sgn}(\frac{\dot{e}_m - Z_m}{Z_m})$ ,  $M_1, M_2$  and  $M_3$

refer to the membership functions of positive (P), negative (N) and zero (Z) separately

which are presented in Fig. 5.2 For each case,  $u_{mi}$ ,  $i=1\sim3$  is the  $i$ -rd output of  $\dot{e}_m$  which is a constant controller. The centriod defuzzifier evaluates the output of all rules as follows:

$$u_m = \frac{\sum_{i=1}^3 M_i \times u_{mi}}{\sum_{i=1}^3 M_i} \quad (5.18)$$

The fuzzy rule base is listed in Table 5.1, in which the input variables in the antecedent part of the rules are  $\dot{e}_m$  and the output variable in the consequent part is  $u_{mi}$ .

Table 5.1 Rule-table of FLCC

Rule	Antecedent	Consequent Part
	$\dot{e}_m$	$u_{mi}$
1	Negative (N)	$u_{m1}$
2	Positive (P)	$u_{m2}$
3	Zero (Z)	$u_{m3}$

After designing appropriate fuzzy logic constant controllers and being substituted into Eq. (5.7), a negative definite of derivatives of Lyapunov function  $\dot{V}$  can be obtained and the asymptotically stability of Lyapunov theorem can be achieved.

Consequently, the processes of FLCC designing to control a system following the trajectory of a goal system is — getting the upper bound and lower bound of the error derivatives of the goal and control systems without any controller, i.e.  $-Z_m \leq \dot{e}_m \leq Z_m$ . Through the fuzzy logic system which follows the rules of Eq. (5.9) ~ Eq. (5.17), a negative definite of derivatives of Lyapunov function  $\dot{V}$  can be obtained and the asymptotically stability of Lyapunov theorem can be achieved.

### 5.3 Simulation Results

There are two cases in this section. Each example is divided into two parts projection anti-synchronization by FLCC and traditional method. In the end of each example, we further conclude the simulation results of the two controllers and list tables and figures to show the effectiveness and robustness of our method.

### 5.3.1 Example 1. Projective Anti-synchronization of Non-autonomous Chaotic Systems by FLCC

The master Sprott 4 system [50] with uncertainty is :

$$\begin{cases} \frac{dx_1(t)}{dt} = x_2 + \Delta_1 \\ \frac{dx_2(t)}{dt} = x_3 + \Delta_1 \\ \frac{dx_3(t)}{dt} = a_1 x_3 - x_2 + x_1 - x_1^2 + \delta \end{cases} \quad (5.19)$$

For initial condition  $(x_{10}, x_{20}, x_{30}) = (0, 1, 1)$ ,  $\Delta_1$  is  $B\sin(wt)$ ,  $\delta = C\sin(wt)$  and parameters  $a=-0.5$ ,  $B=0.01$ ,  $C=1.01$ ,  $w=10.01$ , chaos of the Sprott 4 system [50] appears. The chaotic behavior of Sprott 4 system [50] is shown in Fig 5.3. And Eq. (5.19) is shown in Fig 5.4.

The identical slave DGK system is:

$$\begin{cases} \frac{dy_1(t)}{dt} = y_2 + u_1 \\ \frac{dy_2(t)}{dt} = -b_1 y_2 - y_1 [b_2 (b_3 - y_1^2) + b_4 y_3] + u_2 \\ \frac{dy_3(t)}{dt} = -b_1 y_3 - y_3 [b_2 (b_3 - y_3^2) + b_5 y_1] + u_3 \end{cases} \quad (5.20)$$

For initial condition  $(y_{10}, y_{20}, y_{30}) = (0.01, 0.01, 0.01)$  and parameters  $b_1 = -0.5$ ,  $b_2 = -1.4$ ,  $b_3 = 1.9$ ,  $b_4 = -4.5$ ,  $b_5 = 6.2$ , chaos of the slave DGK system appears as well.  $u_1$ ,  $u_2$  and  $u_3$  are FLCC to anti-synchronize the slave DGK system to master one, i.e., the projection of phase portraits of system (5.20) with chaotic behaviors is shown

in Fig. 5.12.

$$\lim_{t \rightarrow \infty} \mathbf{e} = 0 \quad (5.21)$$

where the error vector

$$\begin{bmatrix} e \\ \mathbf{e} \end{bmatrix} = \begin{bmatrix} e_1(t) \\ e_2(t) \\ e_3(t) \end{bmatrix} = A \begin{bmatrix} x_1(t) \\ x_2(t) \\ x_3(t) \end{bmatrix} + \begin{bmatrix} y_1(t) \\ y_2(t) \\ y_3(t) \end{bmatrix} \quad (5.22)$$

Let  $A = 2$ .

From Eq. (5.22), we have the following error dynamics:

$$\begin{cases} \dot{e}_1 = A[x_2 + \Delta_1] + (y_2 + u_1) \\ \dot{e}_2 = A[x_3 + \Delta_1] + (-b_1 y_2 - y_1[b_2(b_3 - y_1^2) + b_4 y_3] + u_2) \\ \dot{e}_3 = A[a_1 x_3 - x_2 + x_1 - x_1^2 + \delta] + (-b_1 y_3 - y_3[b_2(b_3 - y_3^2) + b_5 y_1] + u_3) \end{cases} \quad (5.23)$$

Choosing Lyapunov function as:

$$V = \frac{1}{2}(e_1^2 + e_2^2 + e_3^2) \quad (5.24)$$

Its time derivative is:

$$\begin{aligned} \dot{V} &= e_1 \dot{e}_1 + e_2 \dot{e}_2 + e_3 \dot{e}_3 \\ &= e_1 \{A[x_2 + \Delta_1] + (y_2 + u_1)\} \\ &\quad + e_2 \{A[x_3 + \Delta_1] + (-b_1 y_2 - y_1[b_2(b_3 - y_1^2) + b_4 y_3] + u_2)\} \\ &\quad + e_3 \{A[a_1 x_3 - x_2 + x_1 - x_1^2 + \delta] + (-b_1 y_3 - y_3[b_2(b_3 - y_3^2) + b_5 y_1] + u_3)\} \end{aligned} \quad (5.25)$$

In order to design FLCC, we divide Eq. (5.25) into three parts as follows:

$$\text{Assume } V = \frac{1}{2}(e_1^2 + e_2^2 + e_3^2) = V_1 + V_2 + V_3,$$

$$\text{then } \dot{V} = e_1 \dot{e}_1 + e_2 \dot{e}_2 + e_3 \dot{e}_3 = \dot{V}_1 + \dot{V}_2 + \dot{V}_3, \quad \text{where } V_1 = \frac{1}{2}e_1^2, \quad V_2 = \frac{1}{2}e_2^2 \quad \text{and}$$

$$V_3 = \frac{1}{2}e_3^2.$$

$$\text{Part 1: } \dot{V}_1 = e_1 \dot{e}_1 = e_1 \{A[x_2 + \Delta_1] + (y_2 + u_1)\}$$

$$\text{Part 2: } \dot{V}_2 = e_2 \dot{e}_2 = e_2 \{A[x_3 + \Delta_1] + (-b_1 y_2 - y_1[b_2(b_3 - y_1^2) + b_4 y_3] + u_2)\}$$

$$\begin{aligned} \text{Part 3: } \dot{V}_3 = e_3 \dot{e}_3 = e_3 \{ & A(a_1 x_3 - x_2 + x_1 - x_1^2 + \delta) \\ & + (-b_1 y_3 - y_3 [b_2 (b_3 - y_3^2) + b_5 y_1] + u_3) \} \end{aligned}$$

FLCC in *Part 1*, *2* and *3* can be obtained via the fuzzy rules in Table 1. The maximum value and minimum value without any controller can be observed in time histories of error derivatives shown in Fig 5.5:  $Z_1 = 3$ ,  $Z_2 = 2$ ,  $Z_3 = 6$ .

The anti-synchronization scheme is proposed in *Part 1*, *2* and *3* and let  $\dot{V}_1 = e_1 \dot{e}_1 < 0$ ,  $\dot{V}_2 = e_2 \dot{e}_2 < 0$  and  $\dot{V}_3 = e_3 \dot{e}_3 < 0$ . Hence we have  $\dot{V} = \dot{V}_1 + \dot{V}_2 + \dot{V}_3 < 0$ . It is clear that all of the rules in FLCC can lead the Lyapunov function satisfies the asymptotically stable theorem. The simulation results are shown in Fig. 5.6 and Fig. 5.7.

### 5.3.2 Projective Anti-synchronization of Sprott 4 System [50] and DGK System by Traditional Method

In order to lead the derivative of Lyapunov function in Eq. (5.25) to negative definite, we choose traditional nonlinear controller as:

$$\begin{cases} u_1 = -[A(x_2 + \Delta_1) + y_2 + e_1] \\ u_2 = -\{A(x_3 + \Delta_1) - b_1 y_2 - y_1 [b_2 (b_3 - y_1^2) + b_4 y_3] + e_2\} \\ u_3 = -\{A(-0.5x_3 - x_2 + x_1 - x_1^2 + \delta) - b_1 y_3 - y_3 [b_2 (b_3 - y_3^2) + b_5 y_1] + e_3\} \end{cases} \quad (5.26)$$

then we can obtain

$$\dot{V} = -\dot{e}_1 e_1 - \dot{e}_2 e_2 - \dot{e}_3 e_3 \quad (5.27)$$

The derivative of Lyapunov function is negative definite and the error dynamics in Eq. (5.23) are going to achieve asymptotically stable. The simulation results are shown in Fig. 5.8 and Fig. 5.9.

### 5.3.3 Robust FLCC Compared with Traditional Method

In this section, we compare the numerical simulation results in 5.3.1 and 5.3.2

which are listed in Tables 5.2 and 5.3. Comparing the two simulation results in Tables 5.2 and 5.3, it is clear to find out that: (1) The performance of the error convergence of states by FLCC is much better than by traditional method; (2) The controller in FLCC designing are much simpler than traditional ones.

Consequently, even the system contains parameter uncertainty, the FLCC can still remain the high performance to anti-synchronize the two chaotic systems with uncertainty and exactly and efficiently.



Table 5.2. Controllers are compared between the traditional method and FLCC method.

Controller	FLCC	Traditional
$u_1$	$Z_1 = 3, e_1 \rightarrow 0$ $Z_2 = 2, e_2 \rightarrow 0$ $Z_3 = 6, e_3 \rightarrow 0$	$-[A(x_2 + \Delta_1) + y_2 + e_1]$
$u_2$		$-\{A(x_3 + \Delta_1) - b_1 y_2$
$u_3$		$-y_1[b_2(b_3 - y_1^2) + b_4 y_3] + e_2\}$
		$-\{A[a(1 + \delta)x_3 + bx_2 - x_2^3 - x_1 + \Delta_1]$
		$+cy_3 - y_2 - \sin y_1 + e_3\}$

Table 5.3. FLCC is compared to traditional method between errors data.

Time(s)	FLCC	Traditional
---------	------	-------------

	$e_1$	$e_1$
30.64	0.0000000000057509	1.9626864386128202
30.65	0.0000000000056967	1.9431573822503669
30.66	0.0000000000056488	1.9238226432454417
30.67	-0.0000000000014122	1.9046802881080391
30.68	-0.0000000000014015	1.8857284025866791
	$e_2$	$e_2$
31.50	0.0000000000030644	-1.9992357790530976
31.51	0.0000000000030987	-1.9793430506769120
31.52	0.0000000000031366	-1.9596482582552452
31.53	0.0000000000031786	-1.9401494322924568
31.54	0.0000000000032247	-1.9208446228896871
	$e_3$	$e_3$
30.30	0.0000000000009261	0.4342688430600326
30.31	0.0000000000009192	0.4299477958740284
30.32	0.0000000000009124	0.4256697438259025
30.33	0.0000000000009056	0.4214342591068866
30.34	0.0000000000008988	0.4172409181649763

#### 5.3.4 Example 2. Chaos Projective Anti-synchronization of Uncertain Stochastic Sprott 4 System [50] and DGK System

The uncertain stochastic Sprott 4 system [50] with noise is:

$$\begin{cases} \frac{dx_1(t)}{dt} = x_2 + \Delta_3 \\ \frac{dx_2(t)}{dt} = x_3 \\ \frac{dx_3(t)}{dt} = a_1 x_3 - (1 + \varsigma)x_2 + x_1 - x_1^2 \end{cases} \quad (5.28)$$

For initial condition  $(x_{10}, x_{20}, x_{30}) = (0, 1, 1)$ , the uncertain term  $\Delta_3$  is  $D\sin(wt)$ , the stochastic term  $\varsigma$  is Rayleigh noise and parameters  $a=-0.5$ ,  $D=0.2$ ,  $w=0.5$ , chaos of the uncertain stochastic Sprott 4 system appears. Rayleigh noise is shown in Fig



5.10. The chaotic behavior of Eq. (5.28) is shown in Fig 5.11.

The identical slave DGK system is:

$$\begin{cases} \frac{dy_1(t)}{dt} = y_2 + u_1 \\ \frac{dy_2(t)}{dt} = -b_1 y_2 - y_1 [b_2 (b_3 - y_1^2) + b_4 y_3] + u_2 \\ \frac{dy_3(t)}{dt} = -b_1 y_3 - y_3 [b_2 (b_3 - y_3^2) + b_5 y_1] + u_3 \end{cases} \quad (5.29)$$

When initial condition  $(y_{10}, y_{20}, y_{30}) = (0.01, 0.01, 0.01)$  and parameters  $b_1 = -0.5$ ,

$b_2 = -1.4$ ,  $b_3 = 1.9$ ,  $b_4 = -4.5$ ,  $b_5 = 6.2$ , chaos of the slave DGK system appears as well.

$u_1$ ,  $u_2$  and  $u_3$  are FLCC to anti-synchronize the slave DGK system to the master one, i.e., the projection of phase portraits of system (3-11) with chaotic behaviors is shown in Fig. 5.12.

$$\lim_{t \rightarrow \infty} \mathbf{e} = 0 \quad (5.30)$$

where the error vector

$$[e] = \begin{bmatrix} e_1(t) \\ e_2(t) \\ e_3(t) \end{bmatrix} = A \begin{bmatrix} x_1(t) \\ x_2(t) \\ x_3(t) \end{bmatrix} + \begin{bmatrix} y_1(t) \\ y_2(t) \\ y_3(t) \end{bmatrix} \quad (5.31)$$

Let  $A = 2$ .

From Eq. (5.31), we have the following error dynamics:

$$\begin{cases} \dot{e}_1 = A[x_2 + \Delta_3 + (y_2 + u_1)] \\ \dot{e}_2 = A[x_3 + (-b_1 y_2 - y_1 [b_2 (b_3 - y_1^2) + b_4 y_3] + u_2)] \\ \dot{e}_3 = A[a_1 x_3 - (1 + \varsigma)x_2 + x_1 - x_1^2 + (-b_1 y_3 - y_3 [b_2 (b_3 - y_3^2) + b_5 y_1] + u_3)] \end{cases} \quad (5.32)$$

Choosing Lyapunov function as:

$$V = \frac{1}{2}(e_1^2 + e_2^2 + e_3^2) \quad (5.33)$$

Its time derivative is:

$$\begin{aligned}
\dot{V} &= e_1 \dot{e}_1 + e_2 \dot{e}_2 + e_3 \dot{e}_3 \\
&= e_1 \{A[x_2 + \Delta_3 + (y_2 + u_1)]\} \\
&+ e_2 \{A[x_3 + (-b_1 y_2 - y_1[b_2(b_3 - y_1^2) + b_4 y_3] + u_2)]\} \\
&+ e_3 \{A[a_1 x_3 - (1 + \varsigma)x_2 + x_1 - x_1^2 + (-b_1 y_3 - y_3[b_2(b_3 - y_3^2) + b_5 y_1] + u_3)]\}
\end{aligned} \tag{5.34}$$

In order to design FLCC, we divide Eq. (5.34) into three parts as follows:

Assume  $V = \frac{1}{2}(e_1^2 + e_2^2 + e_3^2) = V_1 + V_2 + V_3$ , then

$$\dot{V} = e_1 \dot{e}_1 + e_2 \dot{e}_2 + e_3 \dot{e}_3 = \dot{V}_1 + \dot{V}_2 + \dot{V}_3, \text{ where } V_1 = \frac{1}{2}e_1^2, V_2 = \frac{1}{2}e_2^2 \text{ and } V_3 = \frac{1}{2}e_3^2.$$

$$\text{Part 1: } \dot{V}_1 = e_1 \dot{e}_1 = e_1 A[x_2 + \Delta_3 + (y_2 + u_1)]$$

$$\text{Part 2: } \dot{V}_2 = e_2 \dot{e}_2 = e_2 A[x_3 + (-b_1 y_2 - y_1[b_2(b_3 - y_1^2) + b_4 y_3] + u_2)]$$

$$\begin{aligned} \text{Part 3: } \dot{V}_3 &= e_3 \dot{e}_3 = e_3 A[a_1 x_3 - (1 + \varsigma)x_2 + x_1 - x_1^2 \\ &+ (-b_1 y_3 - y_3[b_2(b_3 - y_3^2) + b_5 y_1] + u_3)] \end{aligned}$$

FLCC in *Part 1*, *2* and *3* can be obtained via the fuzzy rules in Table 5.1. The maximum value and minimum value without any controller can be observed in time histories of error derivatives shown in Fig 5.13:  $Z_1 = 3$ ,  $Z_2 = 2$ ,  $Z_3 = 5$ .

FLCC are proposed in *Part 1, 2* and *3* and make  $\dot{V}_1 = e_1 \dot{e}_1 < 0$ ,  $\dot{V}_2 = e_2 \dot{e}_2 < 0$  and  $\dot{V}_3 = e_3 \dot{e}_3 < 0$ . Hence, we have  $\dot{V} = \dot{V}_1 + \dot{V}_2 + \dot{V}_3 < 0$ . It is clear that all of the rules in our FLCC can lead the Lyapunov function satisfies the asymptotically stable theorem. The simulation results are shown in Fig. 5.14 and 5.15.

### 5.3.5 Chaos Projective Anti-synchronization of Uncertainty Stochastic Sprott 4 System [50] and DGK System by Traditional Method

According to Eq. (5.34), we design complicated controllers to anti-synchronize chaotic system with uncertainty by traditional method.

We choose the controllers as follows

$$\begin{cases} u_1 = -[A(x_2 + \Delta_3) + y_2 + e_1] \\ u_2 = -\{Ax_3 - b_1y_2 - y_1[b_2(b_3 - y_1^2) + b_4y_3] + e_2\} \\ u_3 = -\{A(-0.5x_3 - (1 + \varsigma)x_2 + x_1 - x_1^2) - b_1y_3 - y_3[b_2(b_3 - y_3^2) + b_5y_1] + e_3\} \end{cases} \quad (5.35)$$

then we can obtain

$$\dot{V} = -\dot{e}_1 e_1 - \dot{e}_2 e_2 - \dot{e}_3 e_3 \quad (5.36)$$

The derivative of Lyapunov function is negative definite and the error dynamics in Eq. (5.32) are going to achieve asymptotically stable. The simulation results are shown in Fig. 5.16 and Fig. 5.17.

### 5.3.6 Robust FLCC Compared to Traditional Method

In this case, we compare the numerical simulation results in 5.3.4 and 5.3.5 which are listed in Table 5.4 and 5.5. The two main superiorities are still existed – (1) The performance of the error convergence of states by FLCC are much better than by traditional method; (2) The controllers in FLCC designing are much simpler than traditional ones

Table 5.4. Controllers are compared between the traditional method and FLCC method.

Controller	FLCC	Traditional
$u_1$	$Z_1 = 4, e_1 \rightarrow 0$	$-[A(x_2 + \Delta_3) + y_2 + e_1]$
$u_2$		$-\{Ax_3 - b_1y_3 - y_3[b_2(b_3 - y_3^2) + b_4y_1] + e_2\}$
$u_3$	$Z_2 = 3, e_2 \rightarrow 0$	$-\{A(-0.5x_3 - (1 + \varsigma)x_2 + x_1 - x_1^2) - b_1y_3 - y_3[b_2(b_3 - y_3^2) + b_5y_1] + e_3\}$
	$Z_3 = 5, e_3 \rightarrow 0$	

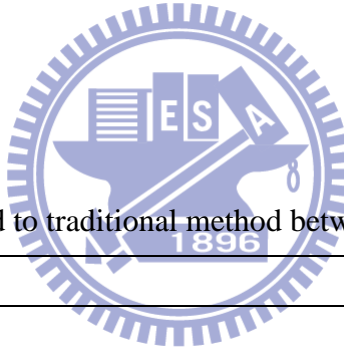


Table 5.5. FLCC is compared to traditional method between errors data.

Time(s)	FLCC	Traditional
	$e_1$	$e_1$
30.89	0.0000000000000932	2.1740747303217302
30.90	0.0000000000000923	2.1524423253132938
30.91	0.0000000000000914	2.1310251663310966
30.92	0.0000000000000905	2.1098211116414002
30.93	0.0000000000000897	2.0888280408210504
	$e_2$	$e_2$

30.95	0.0000000000000463	-3.0273284266466253
30.96	0.0000000000000480	-2.9972060055056282
30.97	0.0000000000000498	-2.9673833074628515
30.98	0.0000000000000516	-2.9378573502236489
30.99	0.0000000000000535	-2.9086251811677015

$e_3$

$e_3$

30.40	-0.0000000000000200	-0.1715451013099150
30.41	-0.0000000000000198	-0.1698381990323653
30.42	-0.0000000000000196	-0.1681482807162518
30.43	-0.0000000000000194	-0.1664751773683333
30.44	-0.0000000000000192	-0.1648187216768820



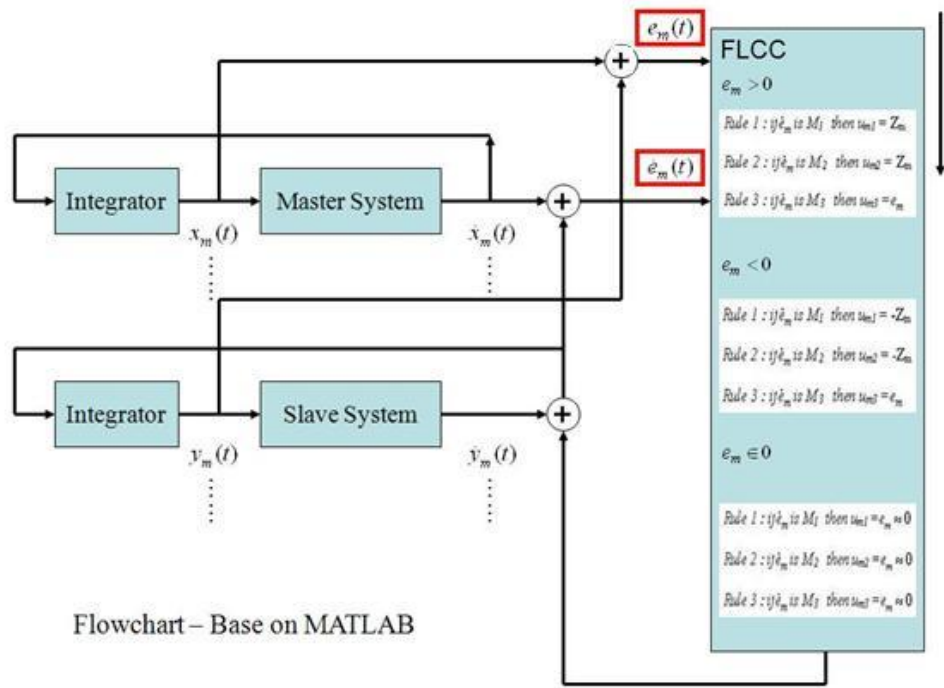


Fig. 5.1 The configuration of fuzzy logic controller.

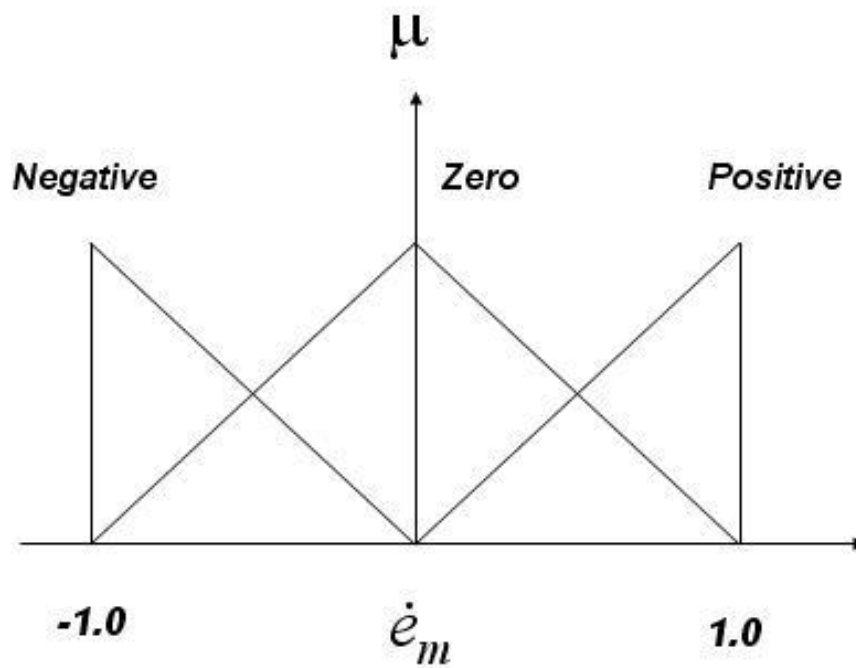


Fig. 5.2 Membership function.

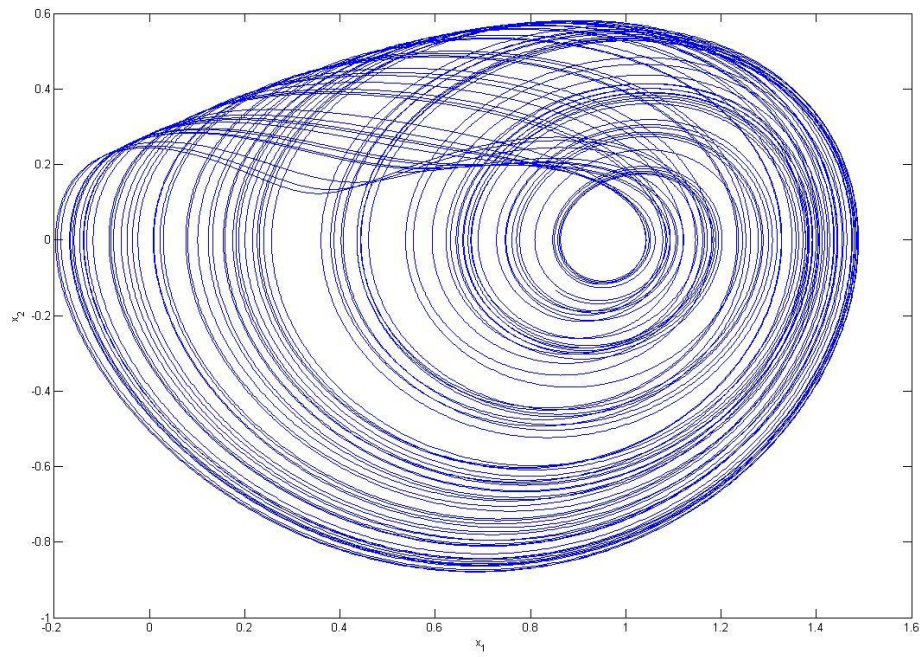


Fig. 5.3 The chaotic behavior of Sprott 4 system [50]

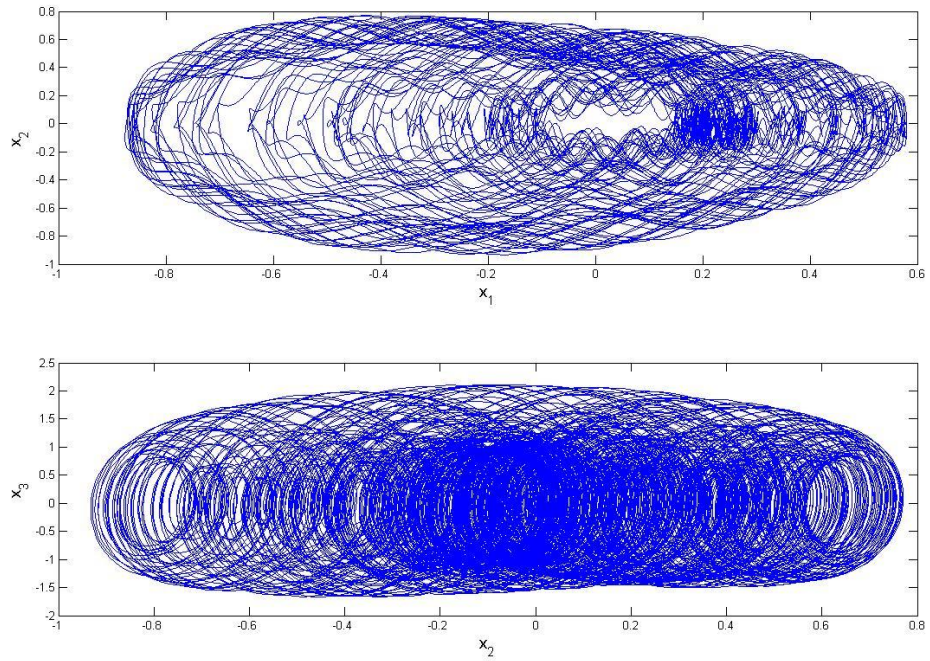


Fig. 5.4 Projections of phase portrait of Eq (5.19).



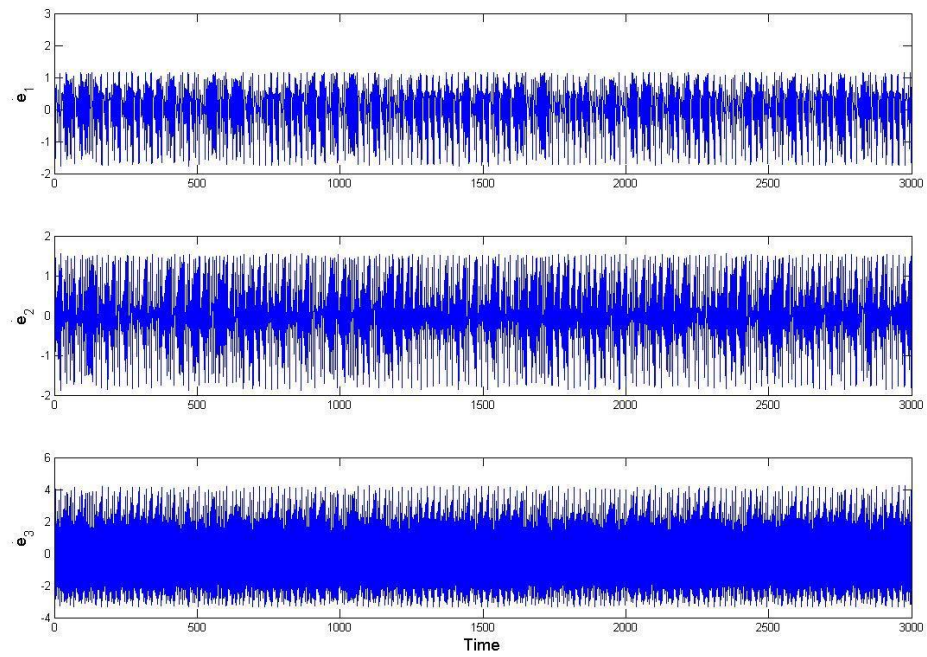


Fig. 5.5 Time histories of error derivatives for master and slave chaotic systems without controllers.

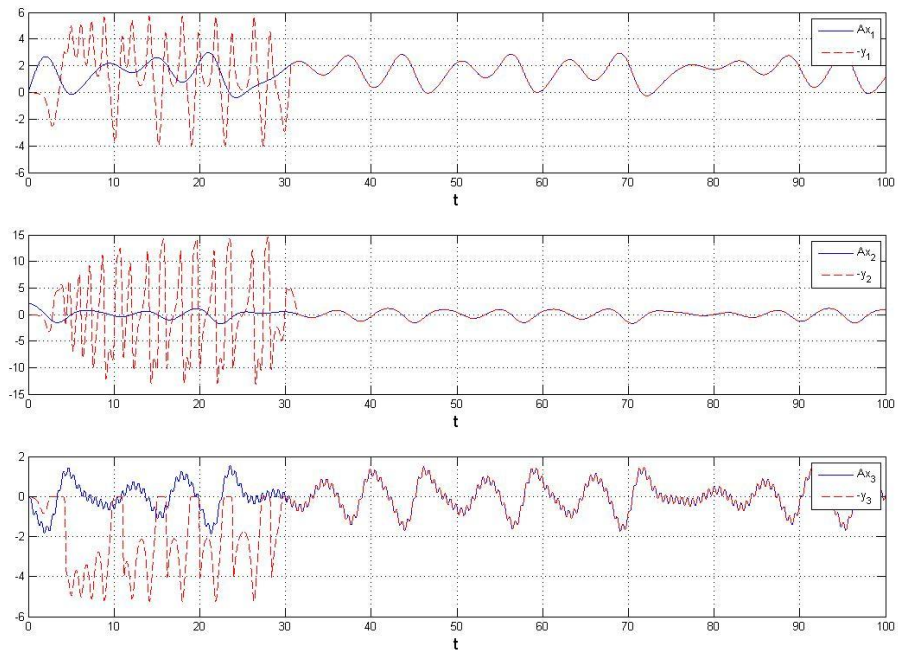


Fig. 5.6 Time histories of states for Example 1 the FLCC is coming into after 30s.



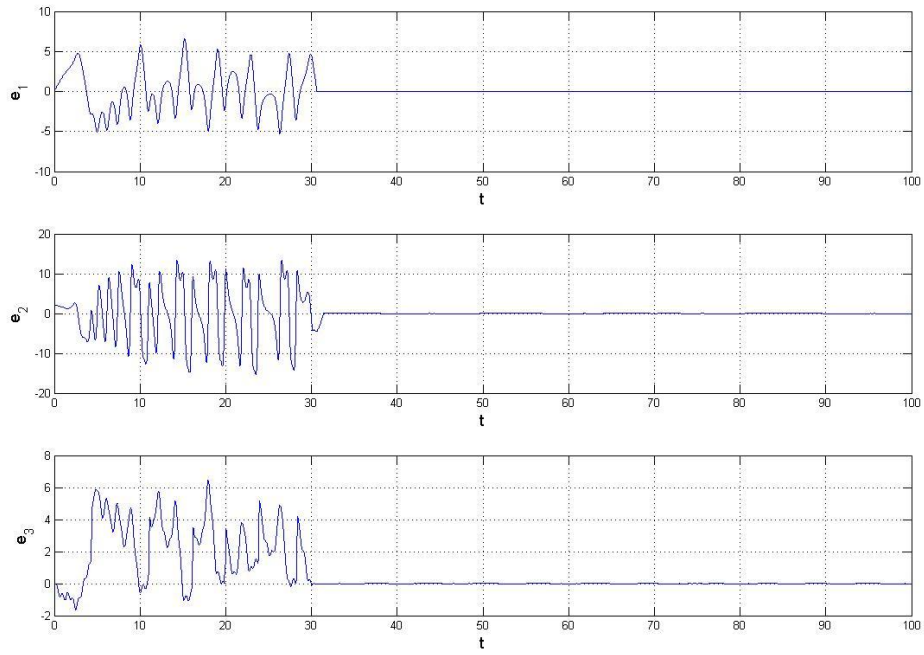


Fig. 5.7 Time histories of errors for Example 1 the FLCC is coming into after 30s.

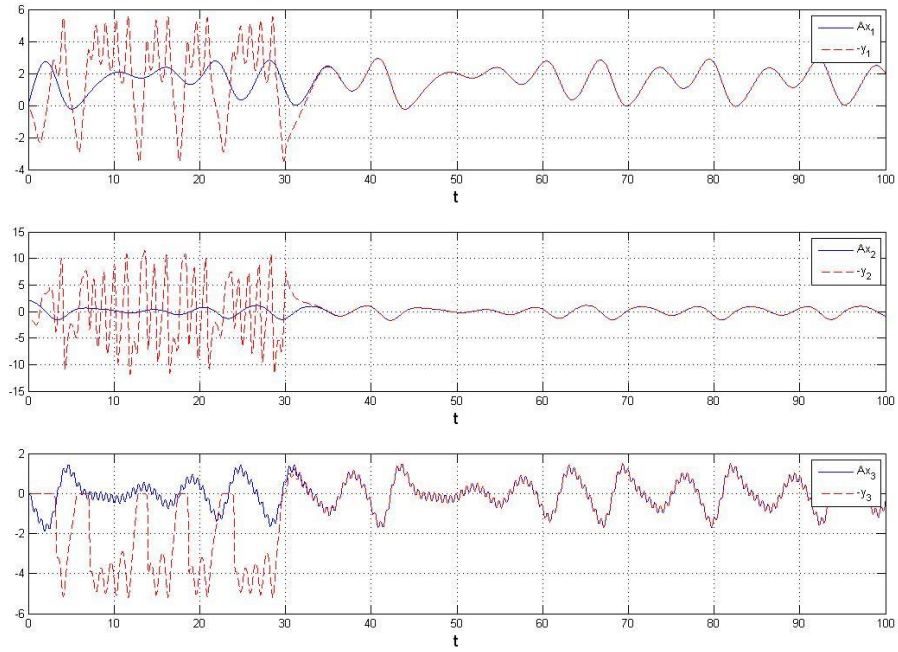


Fig. 5.8 Time histories of states for the traditional controller is coming into after 30s.

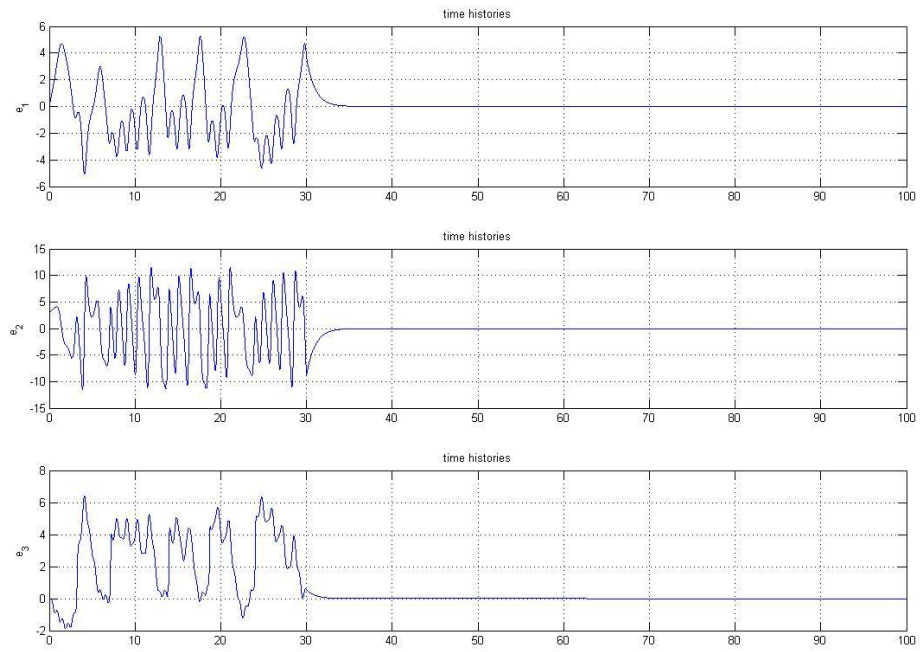


Fig. 5.9 Time histories of states for the traditional controller is coming into after 30s.

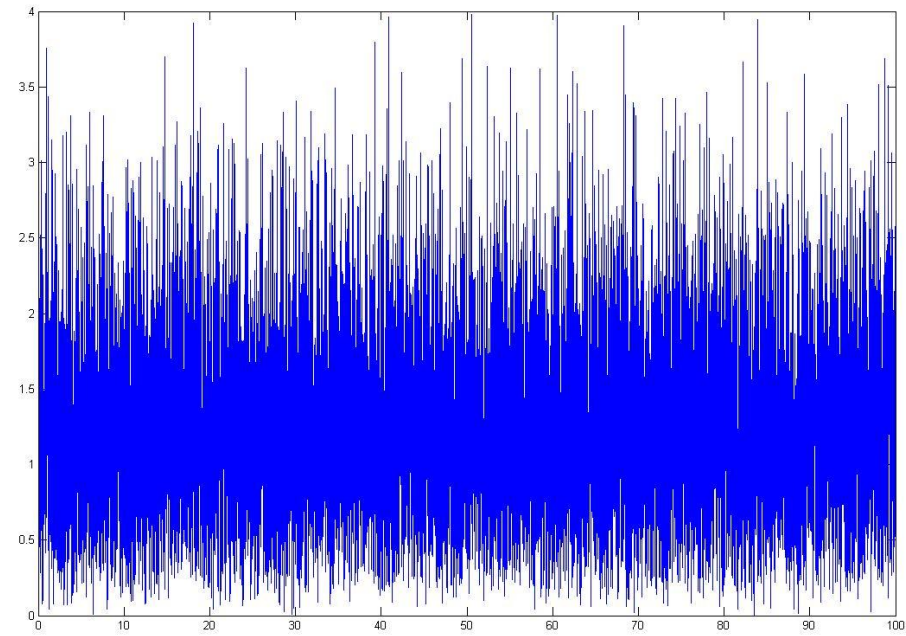


Fig. 5.10 The Rayleigh noise used.

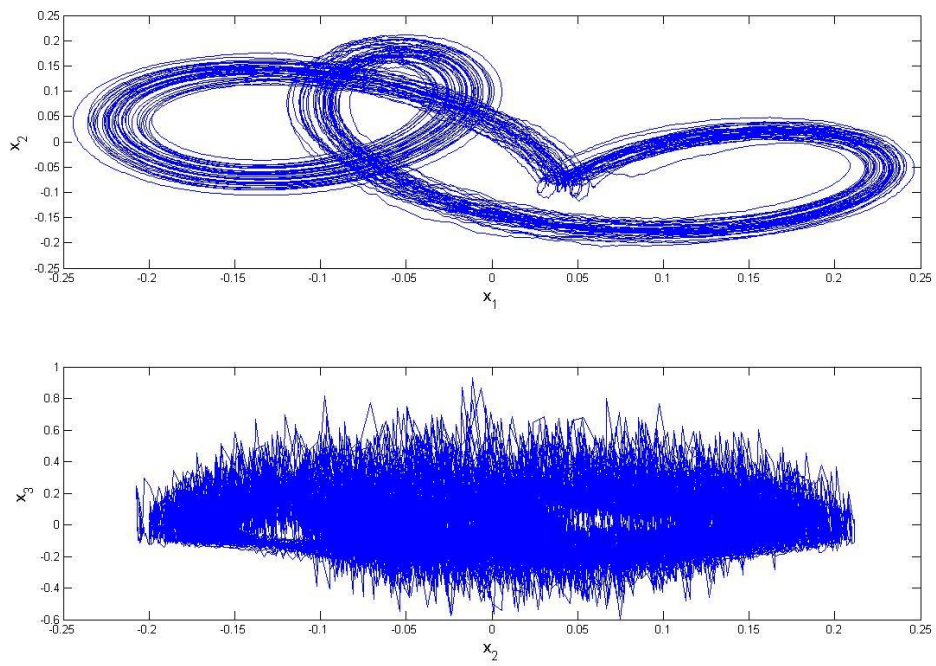


Fig. 5.11 Projection of phase portrait of Eq (5.28).

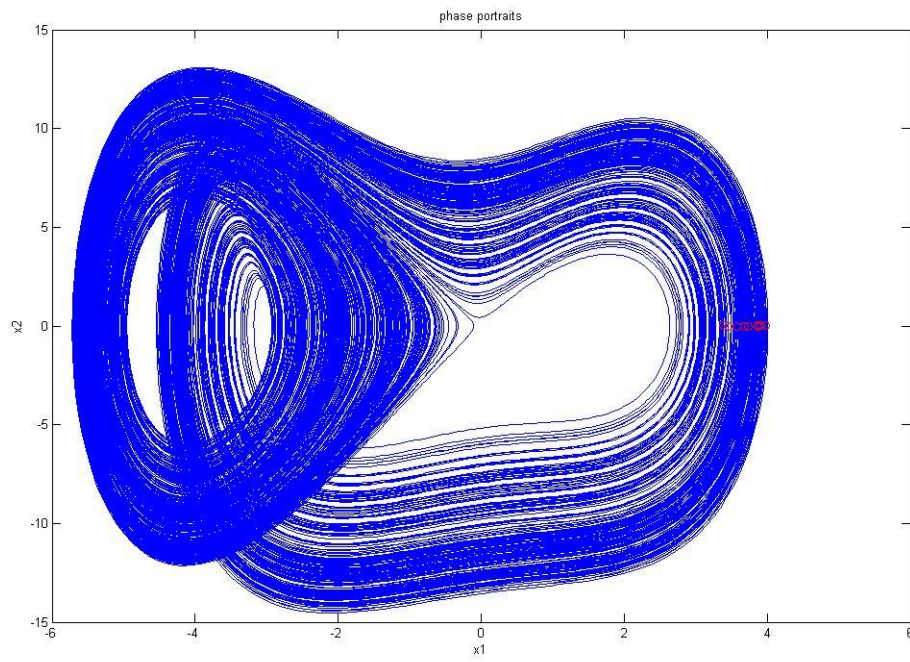


Fig. 5.12 Projections of phase portrait of chaotic DGK systems.

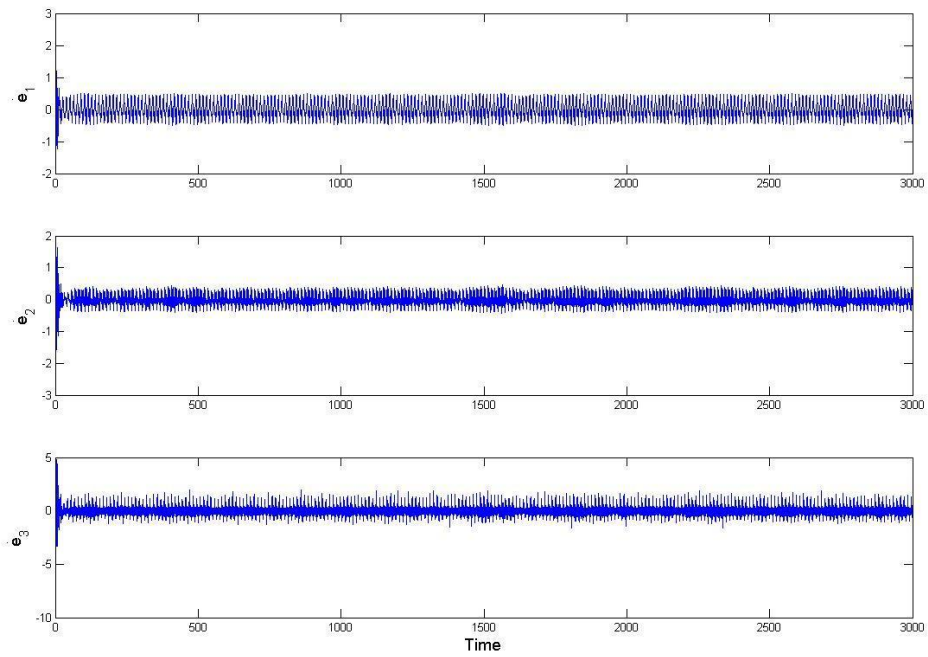


Fig. 5.13 Time histories of error derivatives for master and slave chaotic uncertain stochastic systems without controllers.

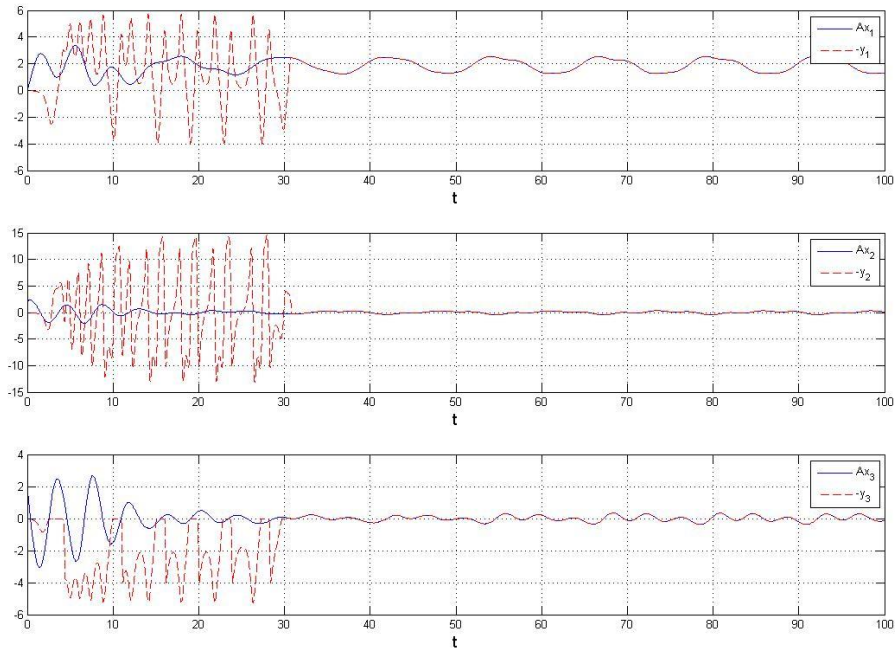


Fig. 5.14 Time histories of states for Example 2 the FLCC is coming into after 30s.

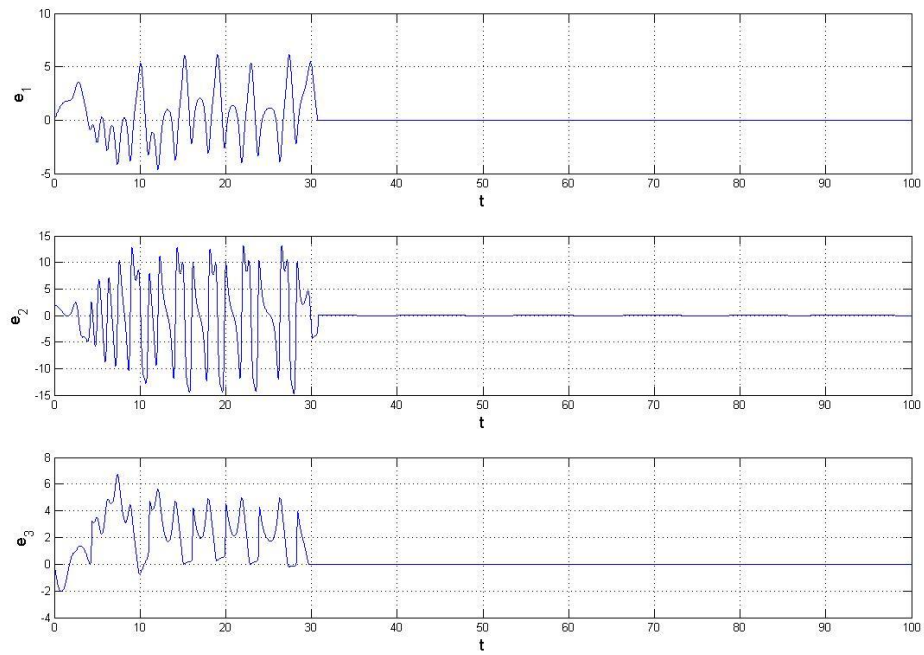


Fig. 5.15 Time histories of errors for Example 2 the FLCC is coming into after 30s.

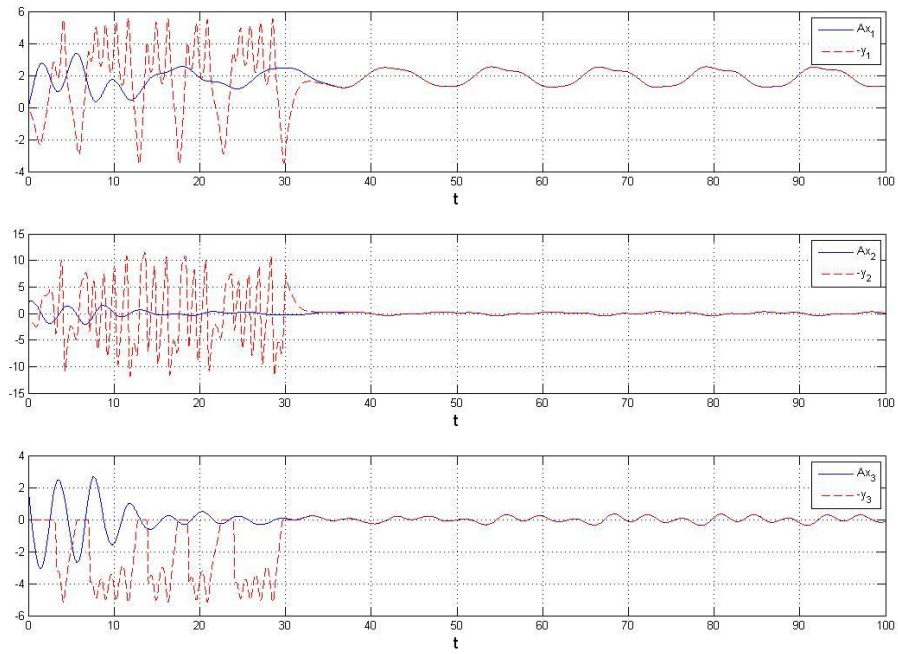


Fig. 5.16 Time histories of states for the traditional controller is coming into after 30s.



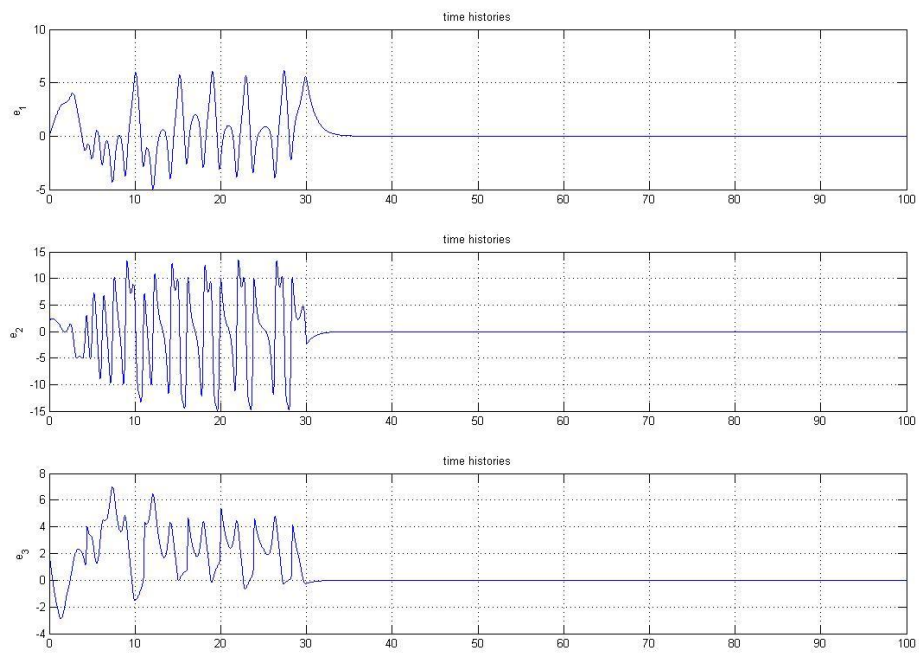


Fig. 5.17 Time histories of states for the traditional controller is coming into after 30s.



# Chapter 6

## Fuzzy Modeling and Synchronization of Chaotic Systems by a New Fuzzy Model

### 6.1 Preliminary

In this paper, a new fuzzy model [58] is used to simulate and synchronize two totally different chaotic systems, Sprott systems and Rössler system. Via the new fuzzy model, a complex nonlinear system is linearized to a simple form. Only two linear subsystems are needed and the numbers of fuzzy rules can be decreased from  $2^N$  to  $2 \times N$ . Sprott systems and Rössler system are used for examples in numerical simulation results to show the effectiveness and feasibility of our new model.

### 6.2 New Fuzzy Model Theory

In system analysis and design, it is important to select an appropriate model representing a real system. As an expression model of a real plant, the fuzzy implications and the fuzzy reasoning method suggested by Takagi and Sugeno are traditionally used. The new fuzzy model is also described by fuzzy IF-THEN rules. The core of the new fuzzy model is that we express each nonlinear equation into two linear sub-equations by fuzzy IF-THEN rules and take all the first linear sub-equations to form one linear subsystem and all the second linear sub-equations to form another linear subsystem. The overall fuzzy model of the system is achieved by fuzzy blending of this two linear subsystem models. Consider a continuous-time nonlinear dynamic system as follows:

Equation i:

rule 1:

IF  $z_i(t)$  is  $M_{i1}$

THEN  $\dot{x}_i(t) = A_{i1}x(t) + B_{i1}u(t)$ ,

rule 2:

IF  $z_i(t)$  is  $M_{i2}$

THEN  $\dot{x}_i(t) = A_{i2}x(t) + B_{i2}u(t)$ , (6.1)

where

$$x(t) = [x_1(t), x_2(t), \dots, x_n(t)]^T,$$

$$u(t) = [u_1(t), u_2(t), \dots, u_n(t)]^T,$$

$i=1,2,\dots,n$ , where  $n$  is the number of nonlinear terms.  $z_i(t)$  is nonlinear term,  $M_{i1}, M_{i2}$  are fuzzy sets,  $A_i, B_i$  are column vectors and  $\dot{x}_i(t) = A_{ij}x(t) + B_{ij}u(t)$ ,  $j=1,2$ , is the output from the first and the second IF-THEN rules.  $u(t)$  is vector controller. Given a pair of  $(x(t), u(t))$  and take all the first linear sub-equations to form one linear subsystem and all the second linear sub-equations to form another linear subsystem, the final output of the fuzzy system is inferred as follows:

$$\dot{x}(t) = M_1 \begin{bmatrix} A_{11}x(t) + B_{11}u(t) \\ A_{21}x(t) + B_{21}u(t) \\ \vdots \\ A_{i1}x(t) + B_{i1}u(t) \end{bmatrix} + M_2 \begin{bmatrix} A_{12}x(t) + B_{12}u(t) \\ A_{22}x(t) + B_{22}u(t) \\ \vdots \\ A_{i2}x(t) + B_{i2}u(t) \end{bmatrix} \quad (6.2)$$

where  $M_1$  and  $M_2$  are diagonal matrices as following:

$$\text{dia}(M_1) = [M_{11} \quad M_{21} \quad \dots \quad M_{i1}], \text{dia}(M_2) = [M_{12} \quad M_{22} \quad \dots \quad M_{i2}]$$

Note that for each equation  $i$ :

$$\sum_{j=1}^2 M_{ij}(z_i(t)) = 1,$$

$$M_{ij}(z_i(t)) \geq 0, i = 1, 2, \dots, n \text{ and } j=1,2.$$



Via the new fuzzy model, the final form of the fuzzy model becomes very simple. The new model provides a much more convenient approach for fuzzy model research and fuzzy application. The simulation results of chaotic systems are discussed in next Section.

### 6.3 New Fuzzy Model of Chaotic Systems

In this Section, the new fuzzy models of two different chaotic systems, Sprott 4 system [50] and Rössler system, are given for Model 1 and Model 2.

#### *Model 1: New fuzzy model of Sprott 4 system with uncertainty*

The Sprott 4 system with uncertainty is:

$$\begin{cases} \dot{x}_1 = x_2 + \Delta_1 \\ \dot{x}_2 = x_3 + \Delta_2 \\ \dot{x}_3 = -0.5x_3 - x_2 + x_1 - x_1^2 \end{cases} \quad (6.3)$$

with initial states (0.01, 1, 0.01). Uncertain terms are  $\Delta_1 = 0.1\sin(50t)$  and  $\Delta_2 = 0.01\cos(50t)$ . The chaotic attractor of the Sprott 4 system is shown in Fig. 6.1 and the chaotic attractor of Eq.(6.3) is shown in Fig. 6.2.

If T-S fuzzy model is used for representing local linear models of Sprott 4 system,  $N=3, 2^N=2^3=8$ , 8 fuzzy rules and 8 linear subsystems are need. The process of modeling is shown as follows:

*T-S fuzzy model:*

Assume that:

- (1)  $\Delta_1 \in [-Z_1, Z_1]$  and  $Z_1 > 0$
- (2)  $\Delta_2 \in [-Z_2, Z_2]$  and  $Z_2 > 0$
- (3)  $x_1 \in [-Z_3, Z_3]$  and  $Z_3 > 0$

Then we have the following T-S fuzzy rules:

Rule 1: IF  $\Delta_1$  is  $M_{11}$  ,  $\Delta_2$  is  $M_{21}$  and  $x_1$  is  $M_{31}$  THEN  $\dot{X} = A_1 X$  ,

Rule 2: IF  $\Delta_1$  is  $M_{11}$  ,  $\Delta_2$  is  $M_{21}$  and  $x_1$  is  $M_{32}$  THEN  $\dot{X} = A_2 X$  ,

Rule 3: IF  $\Delta_1$  is  $M_{11}$  ,  $\Delta_2$  is  $M_{22}$  and  $x_1$  is  $M_{31}$  THEN  $\dot{X} = A_3 X$  ,

Rule 4: IF  $\Delta_1$  is  $M_{11}$  ,  $\Delta_2$  is  $M_{22}$  and  $x_1$  is  $M_{32}$  THEN  $\dot{X} = A_4 X$  ,

Rule 5: IF  $\Delta_1$  is  $M_{12}$  ,  $\Delta_2$  is  $M_{21}$  and  $x_1$  is  $M_{31}$  THEN  $\dot{X} = A_5 X$  ,

Rule 6: IF  $\Delta_1$  is  $M_{12}$  ,  $\Delta_2$  is  $M_{21}$  and  $x_1$  is  $M_{32}$  THEN  $\dot{X} = A_6 X$  ,

Rule 7: IF  $\Delta_1$  is  $M_{12}$  ,  $\Delta_2$  is  $M_{22}$  and  $x_1$  is  $M_{31}$  THEN  $\dot{X} = A_7 X$  ,

Rule 8: IF  $\Delta_1$  is  $M_{12}$  ,  $\Delta_2$  is  $M_{22}$  and  $x_1$  is  $M_{32}$  THEN  $\dot{X} = A_8 X$  ,

Then the final output of the Sprott 4 system can be composed by fuzzy linear subsystems mentioned above. It is obviously an inefficient and complicated work.

*New fuzzy model:*

By using the new fuzzy model, Sprott 4 system can be linearized as simple linear equations. The steps of fuzzy modeling are shown as follows:

*Steps of fuzzy modeling:*

*Step 1:*

Assume that  $\Delta_1 \in [-Z_1, Z_1]$  and  $Z_1 > 0$  , then the first equation of (3-1) can be represented by new fuzzy model as following:

$$\text{Rule 1: IF } \Delta_1 \text{ is } M_{11} , \text{ THEN } \dot{x}_1 = x_2 + Z_1 , \quad (6.4)$$

$$\text{Rule 2: IF } \Delta_1 \text{ is } M_{12} , \text{ THEN } \dot{x}_1 = x_2 - Z_1 , \quad (6.5)$$

where

$$M_{11} = \frac{1}{2} \left( 1 + \frac{\Delta_1}{Z_1} \right), \quad M_{12} = \frac{1}{2} \left( 1 - \frac{\Delta_1}{Z_1} \right),$$

and  $Z_1 = 0.1$ .  $M_{11}$  and  $M_{12}$  are fuzzy sets of the first equation of (3-1) and  $M_{11} + M_{12} = 1$ .

*Step 2:*

Assume that  $\Delta_2 \in [-Z_2, Z_2]$  and  $Z_2 > 0$ , then the second equation of (3-1) can be exactly represented by new fuzzy model as following:

$$\text{Rule 1: IF } \Delta_2 \text{ is } M_{21}, \text{ THEN } \dot{x}_2 = x_3 + Z_2, \quad (6.6)$$

$$\text{Rule 2: IF } \Delta_2 \text{ is } M_{22}, \text{ THEN } \dot{x}_2 = x_3 - Z_2 \quad (6.7)$$

where

$$M_{21} = \frac{1}{2} \left(1 + \frac{\Delta_2}{Z_2}\right), \quad M_{22} = \frac{1}{2} \left(1 - \frac{\Delta_2}{Z_2}\right),$$

and  $Z_2 = 0.01$ .  $M_{21}$  and  $M_{22}$  are fuzzy sets of the second equation of (6.3) and  $M_{21} + M_{22} = 1$ .

*Step 3:*

Assume that  $x_1 \in [-Z_3, Z_3]$  and  $Z_3 > 0$ , then the third equation of (6.3) can be exactly represented by new fuzzy model as following:

$$\text{Rule 1: IF } x_1 \text{ is } M_{31}, \text{ THEN } \dot{x}_3 = -0.5x_3 - x_2 + x_1 - x_1 Z_3, \quad (6.8)$$

$$\text{Rule 2: IF } x_1 \text{ is } M_{32}, \text{ THEN } \dot{x}_3 = -0.5x_3 - x_2 + x_1 + x_1 Z_3 \quad (6.9)$$

where

$$M_{31} = \frac{1}{2} \left(1 + \frac{x_1}{Z_3}\right), \quad M_{32} = \frac{1}{2} \left(1 - \frac{x_1}{Z_3}\right),$$

and  $Z_3 = 1.5$ .  $M_{31}$  and  $M_{32}$  are fuzzy sets of the third equation of (6.3) and  $M_{31} + M_{32} = 1$ .

Here, we call Eqs.(6.4), (6.6) and (6.8) the first linear subsystem under the fuzzy rules, and Eqs.(6.5), (6.7) and (6.9) the second linear subsystem under the fuzzy rules.

The first linear subsystem is

$$\begin{cases} \dot{x}_1 = x_2 + Z_1 \\ \dot{x}_2 = x_3 + Z_2 \\ \dot{x}_3 = -0.5x_3 - x_2 + x_1 - x_1Z_3 \end{cases} \quad (6.10)$$

The second linear subsystem is

$$\begin{cases} \dot{x}_1 = x_2 - Z_1 \\ \dot{x}_2 = x_3 - Z_2 \\ \dot{x}_3 = -0.5x_3 - x_2 + x_1 + x_1Z_3 \end{cases} \quad (6.11)$$

The final output of the fuzzy Sprott 4 system is inferred as follows and the chaotic behavior of fuzzy system is shown in Fig. 6.3. Now we have:

$$\begin{aligned} \begin{bmatrix} \dot{x}_1 \\ \dot{x}_2 \\ \dot{x}_3 \end{bmatrix} &= \begin{bmatrix} M_{11} & 0 & 0 \\ 0 & M_{21} & 0 \\ 0 & 0 & M_{31} \end{bmatrix} \begin{bmatrix} x_2 + Z_1 \\ x_3 + Z_2 \\ -0.5x_3 - x_2 + x_1 - x_1Z_3 \end{bmatrix} \\ &+ \begin{bmatrix} M_{12} & 0 & 0 \\ 0 & M_{22} & 0 \\ 0 & 0 & M_{32} \end{bmatrix} \begin{bmatrix} x_2 - Z_1 \\ x_3 - Z_2 \\ -0.5x_3 - x_2 + x_1 + x_1Z_3 \end{bmatrix} \end{aligned} \quad (6.12)$$

Eq. (6.12) can be rewritten as a simple mathematical expression:

$$\dot{X}(t) = \sum_{i=1}^2 \Psi_i (A_i X(t) + \tilde{b}_i) \quad (6.13)$$

where  $\Psi_i$  are diagonal matrices as follows:

$$\text{dia}(\Psi_1) = [M_{11} \quad M_{21} \quad M_{31}], \quad \text{dia}(\Psi_2) = [M_{12} \quad M_{22} \quad M_{32}]$$

$$A_1 = \begin{bmatrix} 0 & 1 & 0 \\ 0 & 0 & 1 \\ 1-Z_3 & -1 & -0.5 \end{bmatrix}, \quad \tilde{b}_1 = \begin{bmatrix} Z_1 \\ Z_2 \\ 0 \end{bmatrix}$$

$$A_2 = \begin{bmatrix} 0 & 1 & 0 \\ 0 & 0 & 1 \\ 1+Z_3 & -1 & -0.5 \end{bmatrix}, \quad \tilde{b}_2 = \begin{bmatrix} -Z_1 \\ -Z_2 \\ 0 \end{bmatrix}$$

Via new fuzzy model, the number of fuzzy rules can be greatly reduced. Only two linear subsystems are enough to express such complex chaotic behaviors. The simulation results are similar the original chaotic behavior of the Sprott 4 system as

show in Fig. 6.3.

**Model 2: New fuzzy model of Rössler system with uncertainty**

The Rössler system with uncertainty is:

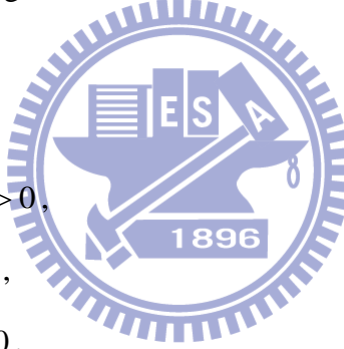
$$\begin{cases} \dot{y}_1 = -y_2 - y_3 + 0.1\Delta_3 \\ \dot{y}_2 = y_1 + 0.15y_2\Delta_4 \\ \dot{y}_3 = 0.2 + y_1y_3 - 9y_3 \end{cases} \quad (6.14)$$

where uncertainty terms  $\Delta_3$  is white noise (PSD=0.1),  $\Delta_4$  is Rayleigh noise and initial conditions are chosen as (2, 2.4, 5). The chaotic attractor of Rössler system is shown in Fig. 6.4, the chaotic attractor of Eq.(6.14) is shown in Fig. 6.5 and the Rayleigh noise is shown in Fig. 6.6.

*New fuzzy model:*

Assume that:

- (1)  $0.1\Delta_3 \in [-Z_4, Z_4]$  and  $Z_4 > 0$ ,
- (2)  $\Delta_4 \in [-Z_5, Z_5]$  and  $Z_5 > 0$ ,
- (3)  $y_3 \in [-Z_6, Z_6]$  and  $Z_6 > 0$ ,



then we have the following new fuzzy rules:

$$\text{Rule 1: IF } 0.1\Delta_3 \text{ is } N_{11}, \text{ THEN } \dot{y}_1 = -y_2 - y_3 + Z_4, \quad (6.15)$$

$$\text{Rule 2: IF } 0.1\Delta_3 \text{ is } N_{12}, \text{ THEN } \dot{y}_1 = -y_2 - y_3 - Z_4 \quad (6.16)$$

where

$$N_{11} = \frac{1}{2} \left( 1 + \frac{0.1\Delta_3}{Z_4} \right), \quad N_{12} = \frac{1}{2} \left( 1 - \frac{0.1\Delta_3}{Z_4} \right)$$

and

$$\text{Rule 1: IF } \Delta_4 \text{ is } N_{21}, \text{ THEN } \dot{y}_2 = y_1 + 0.15y_2Z_5, \quad (6.17)$$

$$\text{Rule 2: IF } \Delta_4 \text{ is } N_{22}, \text{ THEN } \dot{y}_2 = y_1 - 0.15y_2Z_5, \quad (6.18)$$

where

$$N_{21} = \frac{1}{2} \left(1 + \frac{\Delta_4}{Z_5}\right), \quad N_{22} = \frac{1}{2} \left(1 - \frac{\Delta_4}{Z_5}\right).$$

and

$$\text{Rule 1: IF } x_3 \text{ is } N_{31}, \text{ THEN } \dot{y}_3 = 0.2 + y_1 Z_6 - 9y_3, \quad (6.19)$$

$$\text{Rule 2: IF } x_3 \text{ is } N_{32}, \text{ THEN } \dot{y}_3 = 0.2 - y_1 Z_6 - 9y_3, \quad (6.20)$$

where

$$N_{31} = \frac{1}{2} \left(1 + \frac{x_3}{Z_6}\right), \quad N_{32} = \frac{1}{2} \left(1 - \frac{x_3}{Z_6}\right).$$

in Eqs. (6.15)~(6.20),  $Z_4 = 0.4$ ,  $Z_5 = 4$  and  $Z_6 = 150$ .  $N_{11}$ ,  $N_{12}$ ,  $N_{21}$ ,  $N_{22}$ ,  $N_{31}$  and

$N_{32}$  are fuzzy sets of Eq.(6.14) and  $N_{11} + N_{12} = 1$ ,  $N_{21} + N_{22} = 1$  and  $N_{31} + N_{32} = 1$

Here, we call (6.15) ,(6.17) and (6.19) the first liner subsystem under the fuzzy rules and (6.16) , (6.18) and (6.20) the second liner subsystem under the fuzzy rules.

The first linear subsystem is

$$\begin{cases} \dot{y}_1 = -y_2 - y_3 + Z_4 \\ \dot{y}_2 = y_1 + 0.15y_2 Z_5 \\ \dot{y}_3 = 0.2 + y_1 Z_6 - 9y_3 \end{cases} \quad (6.21)$$

The second linear subsystem is

$$\begin{cases} \dot{y}_1 = -y_2 - y_3 - Z_4 \\ \dot{y}_2 = y_1 - 0.15y_2 Z_5 \\ \dot{y}_3 = 0.2 - y_1 Z_6 - 9y_3 \end{cases} \quad (6.22)$$

The final output of the fuzzy Rössler system is inferred as follows and the chaotic behavior of fuzzy system is shown in Fig. 6.7.

$$\begin{aligned}
\begin{bmatrix} \dot{y}_1 \\ \dot{y}_2 \\ \dot{y}_3 \end{bmatrix} &= \begin{bmatrix} N_{11} & 0 & 0 \\ 0 & N_{21} & 0 \\ 0 & 0 & N_{31} \end{bmatrix}^T \begin{bmatrix} -y_2 - y_3 + Z_4 \\ y_1 + 0.15y_2Z_5 \\ 0.2 + y_1Z_6 - 9x_3 \end{bmatrix} \\
&+ \begin{bmatrix} N_{12} & 0 & 0 \\ 0 & N_{22} & 0 \\ 0 & 0 & N_{32} \end{bmatrix}^T \begin{bmatrix} -y_2 - y_3 - Z_4 \\ y_1 - 0.15y_2Z_5 \\ 0.2 - y_1Z_6 - 9x_3 \end{bmatrix}
\end{aligned} \tag{6.23}$$

Eq. (6.23) can be rewritten as a simple mathematical expression:

$$\dot{Y}(t) = \sum_{i=1}^2 \Gamma_i (C_i Y(t) + \tilde{c}_i) \tag{6.24}$$

where

$$dia(\Gamma_1) = [N_{11} \quad N_{21} \quad N_{31}], \quad dia(\Gamma_2) = [N_{12} \quad N_{22} \quad N_{32}]$$

$$C_1 = \begin{bmatrix} 0 & -1 & -1 \\ 1 & 0.15Z_5 & 0 \\ Z_6 & 0 & -9 \end{bmatrix}, \quad \tilde{c}_1 = \begin{bmatrix} Z_4 \\ 0 \\ 0.2 \end{bmatrix}$$

$$C_2 = \begin{bmatrix} 0 & -1 & -1 \\ 1 & -0.15Z_5 & 0 \\ -Z_6 & 0 & -9 \end{bmatrix}, \quad \tilde{c}_2 = \begin{bmatrix} -Z_4 \\ 0 \\ 0.2 \end{bmatrix}$$

Via new fuzzy model, two linear subsystems are enough to express such complex chaotic behaviors. The simulation results are similar the original chaotic behavior of the Rössler system.

## 6.4 Fuzzy Synchronization Scheme

In this Section, we derive the new fuzzy synchronization scheme based on our new fuzzy model to synchronize two totally different fuzzy chaotic systems. The following fuzzy systems as the master and slave systems are given:

master system:

$$\dot{X}(t) = \sum_{i=1}^2 \Psi_i (A_i X(t) + \tilde{b}_i) \tag{6.25}$$

slave system:

$$\dot{Y}(t) = \sum_{i=1}^2 \Gamma_i (C_i Y(t) + \tilde{c}_i) + BU(t) \quad (6.26)$$

Eq. (6.25) and Eq. (6.26) represent the two different chaotic systems, and in Eq. (6.26) there is control input  $U(t)$ . Define the error signal as  $e(t) = X(t) - Y(t)$ , we have:

$$\dot{e}(t) = \dot{X}(t) - \dot{Y}(t) = \sum_{i=1}^2 \Psi_i (A_i X(t) + \tilde{b}_i) - \sum_{i=1}^2 \Gamma_i (C_i Y(t) + \tilde{c}_i) - BU(t) \quad (6.27)$$

The fuzzy controllers are designed as follows:

$$U(t) = u_1(t) + u_2(t) \quad (6.28)$$

where

$$u_1(t) = \sum_{i=1}^2 \Psi_i F_i X(t) - \sum_{i=1}^2 \Gamma_i P_i Y(t),$$

$$u_2(t) = \sum_{i=1}^2 \Psi_i \tilde{b}_i - \sum_{i=1}^2 \Gamma_i \tilde{c}_i$$

such that  $\|e(t)\| \rightarrow 0$  as  $t \rightarrow \infty$ . Our design is to determine the feedback gains  $F_i$  and  $P_i$ .

By substituting  $U(t)$  into Eq.(6.27), we obtain:

$$\dot{e}(t) = \sum_{i=1}^2 \Psi_i \{(A_i - BF_i)X(t)\} - \sum_{i=1}^2 \Gamma_i \{(C_i - BP_i)Y(t)\} \quad (6.29)$$

**Theorem 1:** The error system in Eq. (6.29) is asymptotically stable and the slave system in Eq. (6.26) can synchronize the master system in Eq. (6.25) under the fuzzy controller in Eq. (6.28) if the following conditions below can be satisfied:

$$G = (A_1 - BF_1) = (A_2 - BF_2) = (C_1 - BP_1) = (C_2 - BP_2) < 0, \quad i=1 \sim 2. \quad (6.30)$$

*Proof:*

The errors in Eq. (6.29) can be exactly linearized via the fuzzy controllers in Eq. (6.28) if there exist the feedback gains  $F_i$  such that

$$(A_1 - BF_1) = (A_2 - BF_2) = (C_1 - BP_1) = (C_2 - BP_2) < 0. \quad (6.31)$$

Then the overall control system is linearized as

$$\dot{e}(t) = Ge(t), \quad (6.32)$$

where  $G = (A_1 - BF_1) = (A_2 - BF_2) = (C_1 - BP_1) = (C_2 - BP_2) < 0$ .

As a consequence, the zero solution of the error system (6.32) linearized via the



fuzzy controller (6.28) is asymptotically stable.

## 6.5 Simulation Results

There are two examples in this Section to investigate the effectiveness and feasibility of our new fuzzy model.

### *Example 1: Synchronization of Master and Slave Sprott 4 system*

The fuzzy Sprott 4 system in Eq. (6.13) is chosen as the master system and the fuzzy slave Sprott 4 system, with fuzzy controllers is as follows:

$$\dot{Y}(t) = \sum_{i=1}^2 \Gamma_i (C_i Y(t) + \tilde{c}_i) + BU(t) \quad (6.33)$$

where  $\Gamma_i$  are diagonal matrices

$$\text{dia}(\Gamma_1) = [N_{11} \quad N_{21} \quad N_{31}], \quad \text{dia}(\Gamma_2) = [N_{12} \quad N_{22} \quad N_{32}]$$

and

$$C_1 = \begin{bmatrix} 0 & 1 & 0 \\ 0 & 0 & 1 \\ 1-Z_3 & -1 & -0 \end{bmatrix}, \quad \tilde{c}_1 = \begin{bmatrix} Z_1 \\ Z_2 \\ 0 \end{bmatrix}$$

$$C_2 = \begin{bmatrix} 0 & 1 & 0 \\ 0 & 0 & 1 \\ 1+Z_3 & -1 & -0 \end{bmatrix}, \quad \tilde{c}_2 = \begin{bmatrix} -Z_1 \\ -Z_2 \\ 0 \end{bmatrix}.$$

Therefore, the error and error dynamics are:

$$\begin{bmatrix} e_1 \\ e_2 \\ e_3 \end{bmatrix} = \begin{bmatrix} x_1 - y_1 \\ x_2 - y_2 \\ x_3 - y_3 \end{bmatrix},$$

$$\begin{bmatrix} \dot{e}_1 \\ \dot{e}_2 \\ \dot{e}_3 \end{bmatrix} = \begin{bmatrix} \dot{x}_1 - \dot{y}_1 \\ \dot{x}_2 - \dot{y}_2 \\ \dot{x}_3 - \dot{y}_3 \end{bmatrix} = \sum_{i=1}^2 \Psi_i (A_i X(t) + \tilde{b}_i) - \dot{Y}(t) = \sum_{i=1}^2 \Gamma_i (C_i Y(t) + \tilde{c}_i) - BU(t) \quad (6.34)$$

B is chosen as an identity matrix and the fuzzy controllers in Eq. (6.28) are used:

$$\begin{aligned}
\begin{bmatrix} \dot{e}_1 \\ \dot{e}_2 \\ \dot{e}_3 \end{bmatrix} &= \Psi_1 [A_1 - BF_1]_{3 \times 3} \begin{bmatrix} x_1 \\ x_2 \\ x_3 \end{bmatrix} + \Psi_2 [A_2 - BF_2]_{3 \times 3} \begin{bmatrix} x_1 \\ x_2 \\ x_3 \end{bmatrix} \\
&\quad - \Gamma_1 [C_1 - BP_1]_{3 \times 3} \begin{bmatrix} y_1 \\ y_2 \\ y_3 \end{bmatrix} - \Gamma_2 [C_2 - BP_2]_{3 \times 3} \begin{bmatrix} y_1 \\ y_2 \\ y_3 \end{bmatrix}
\end{aligned} \tag{6.35}$$

According to Eq. (6.30), we have  $G = [A_1 - BF_1] = [A_2 - BF_2] = [C_1 - BP_1] = [C_2 - BP_2] < 0$ .  $G$  is chosen as:

$$G = \begin{bmatrix} -1 & 0 & 0 \\ 0 & -1 & 0 \\ 0 & 0 & -1 \end{bmatrix} \tag{6.36}$$

Thus, the feedback gains  $F_1$ ,  $F_2$ ,  $P_1$  and  $P_2$  can be determined by the following equations:

$$\begin{aligned}
F_1 = B^{-1} [A_1 - G] &= \begin{bmatrix} 1 & 1 & 0 \\ 0 & 1 & 1 \\ -1 & -1 & 0.5 \end{bmatrix} \\
F_2 = B^{-1} [A_2 - G] &= \begin{bmatrix} 1 & 1 & 0 \\ 0 & 1 & 1 \\ 3 & -1 & 0.5 \end{bmatrix} \\
P_1 = B^{-1} [C_1 - G] &= \begin{bmatrix} 1 & 1 & 0 \\ 0 & 1 & 1 \\ -1 & -1 & 0.5 \end{bmatrix} \\
P_2 = B^{-1} [C_2 - G] &= \begin{bmatrix} 1 & 1 & 0 \\ 0 & 1 & 1 \\ 3 & -1 & 0.5 \end{bmatrix}
\end{aligned} \tag{6.37}$$

The synchronization errors are shown in Fig. 6.8.

**Example 2: Synchronization of Sprott 4 system and Rössler system.**

The fuzzy Sprott 4 system in Eq. (6.13) is chosen as the master system and the fuzzy slave Rössler system, with fuzzy controllers is as follows:

$$\dot{Y}(t) = \sum_{i=1}^2 \Gamma_i (C_i Y(t) + \tilde{c}_i) + BU(t) \quad (6.38)$$

where  $\Gamma_i$  are diagonal matrices

$$\text{dia}(\Gamma_1) = [N_{11} \quad N_{21} \quad N_{31}], \quad \text{dia}(\Gamma_2) = [N_{12} \quad N_{22} \quad N_{32}]$$

and

$$C_1 = \begin{bmatrix} 0 & -1 & -1 \\ 1 & 0.15Z_5 & 0 \\ Z_6 & 0 & -9 \end{bmatrix}, \quad \tilde{c}_1 = \begin{bmatrix} Z_4 \\ 0 \\ 0.2 \end{bmatrix}$$

$$C_2 = \begin{bmatrix} 0 & -1 & -1 \\ 1 & -0.15Z_5 & 0 \\ -Z_6 & 0 & -9 \end{bmatrix}, \quad \tilde{c}_2 = \begin{bmatrix} -Z_4 \\ 0 \\ 0.2 \end{bmatrix}$$

Therefore, the error and error dynamics are:

$$\begin{bmatrix} e_1 \\ e_2 \\ e_3 \end{bmatrix} = \begin{bmatrix} x_1 - y_1 \\ x_2 - y_2 \\ x_3 - y_3 \end{bmatrix},$$

$$\begin{bmatrix} \dot{e}_1 \\ \dot{e}_2 \\ \dot{e}_3 \end{bmatrix} = \begin{bmatrix} \dot{x}_1 - \dot{y}_1 \\ \dot{x}_2 - \dot{y}_2 \\ \dot{x}_3 - \dot{y}_3 \end{bmatrix} = \sum_{i=1}^2 \Psi_i (A_i X(t) + \tilde{b}_i) - \dot{Y}(t) = \sum_{i=1}^2 \Gamma_i (C_i Y(t) + \tilde{c}_i) - BU(t) \quad (6.39)$$

B is chosen as an identity matrix and the fuzzy controllers in Eq. (6.28) are used:

$$\begin{bmatrix} \dot{e}_1 \\ \dot{e}_2 \\ \dot{e}_3 \end{bmatrix} = \Psi_1 [A_1 - BF_1]_{3 \times 3} \begin{bmatrix} x_1 \\ x_2 \\ x_3 \end{bmatrix} + \Psi_2 [A_2 - BF_2]_{3 \times 3} \begin{bmatrix} x_1 \\ x_2 \\ x_3 \end{bmatrix} - \Gamma_1 [C_1 - BP_1]_{3 \times 3} \begin{bmatrix} y_1 \\ y_2 \\ y_3 \end{bmatrix} - \Gamma_2 [C_2 - BP_2]_{3 \times 3} \begin{bmatrix} y_1 \\ y_2 \\ y_3 \end{bmatrix} \quad (6.40)$$

According to Eq. (6.30), we have  $G=[A_1-BF_1]=[A_2-BF_2]=[C_1-BP_1]$   
 $=[C_2-BP_2]<0$ .  $G$  is chosen as:

$$G = \begin{bmatrix} -1 & 0 & 0 \\ 0 & -1 & 0 \\ 0 & 0 & -1 \end{bmatrix} \quad (6.41)$$

Thus, the feedback gains  $F_1$ ,  $F_2$ ,  $P_1$  and  $P_2$  can be determined by the following equation:

$$\begin{aligned} F_1 &= B^{-1}[A_1 - G] = \begin{bmatrix} 1 & 1 & 0 \\ 0 & 1 & 1 \\ -1 & -1 & 0.5 \end{bmatrix} \\ F_2 &= B^{-1}[A_2 - G] = \begin{bmatrix} 1 & 1 & 0 \\ 0 & 1 & 1 \\ 3 & -1 & 0.5 \end{bmatrix} \\ P_1 &= B^{-1}[C_1 - G] = \begin{bmatrix} 1 & -1 & -1 \\ 1 & 1.75 & 0 \\ 260 & 0 & -8 \end{bmatrix} \\ P_2 &= B^{-1}[C_2 - G] = \begin{bmatrix} 1 & -1 & -1 \\ 1 & 0.25 & 0 \\ -260 & 0 & -8 \end{bmatrix} \end{aligned} \quad (6.42)$$

The synchronization errors are shown in Fig. 6.9.

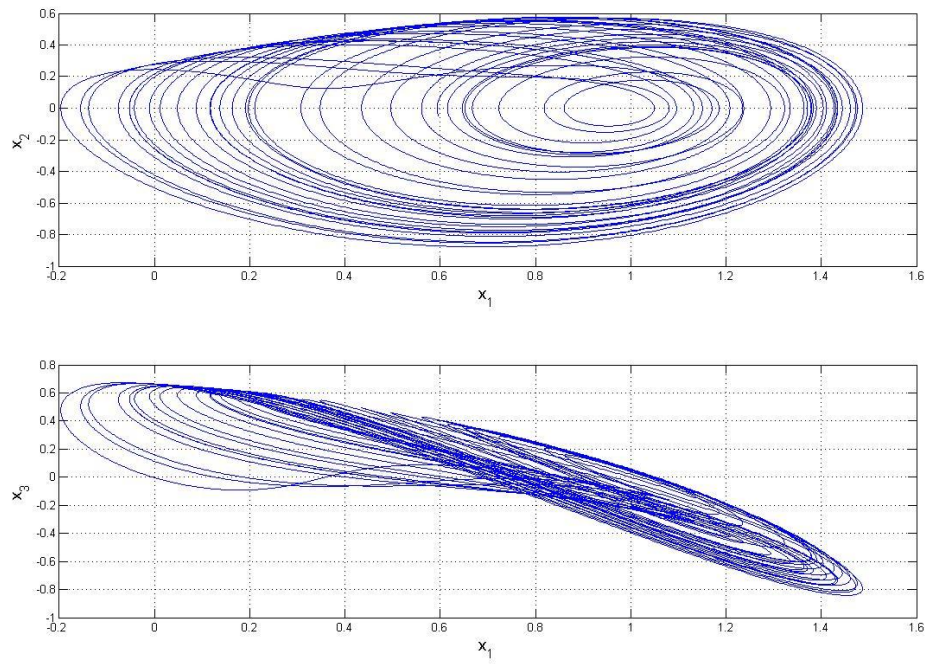


Fig. 6.1 Chaotic behavior of Sprott 4 system.

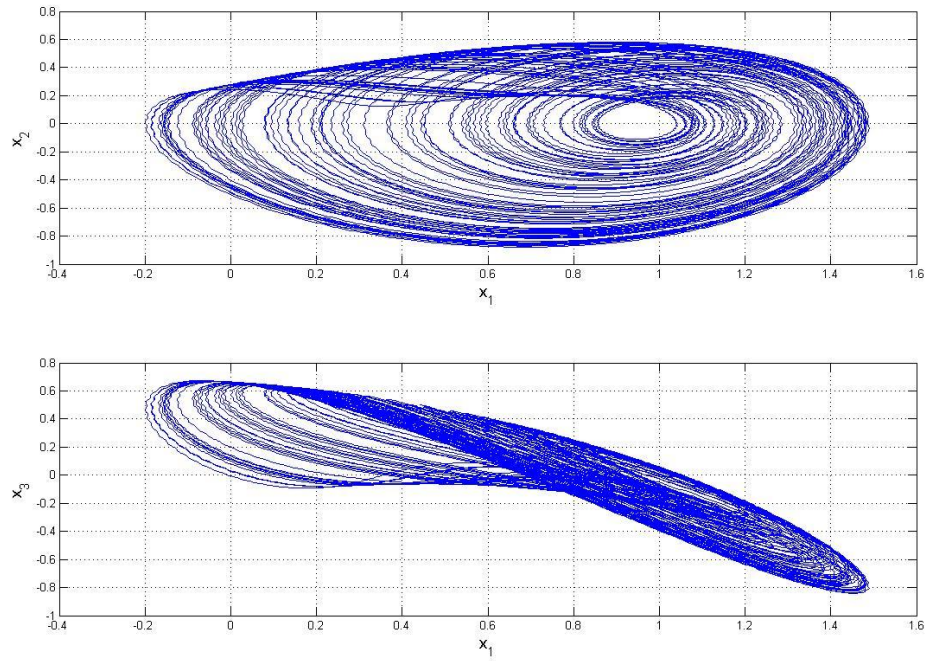


Fig. 6.2 Chaotic behavior of Sprott 4 system with uncertainty.

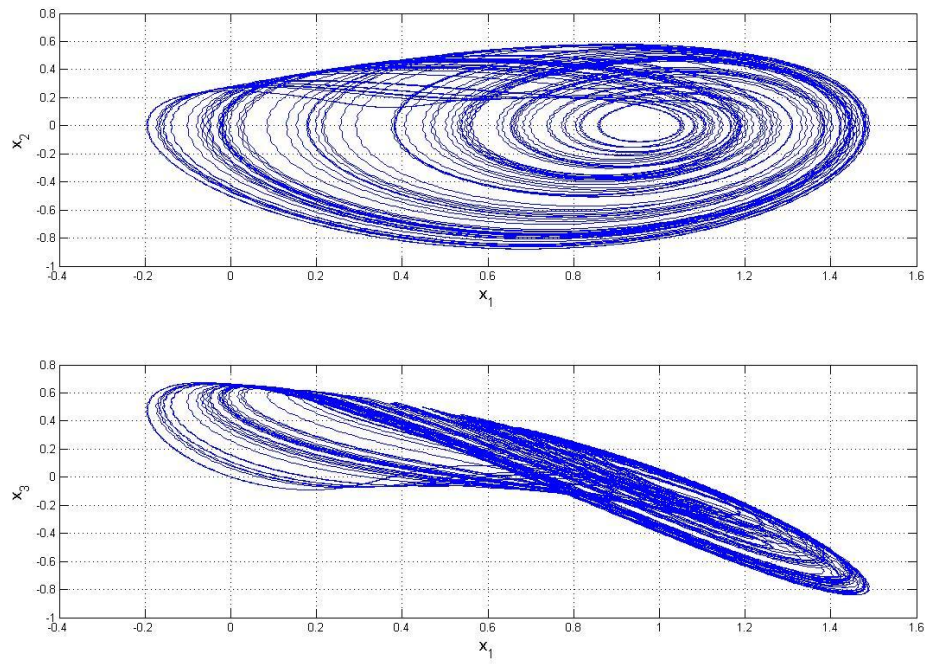


Fig. 6.3 Chaotic behavior of new fuzzy Sprott 4 system with uncertainty.

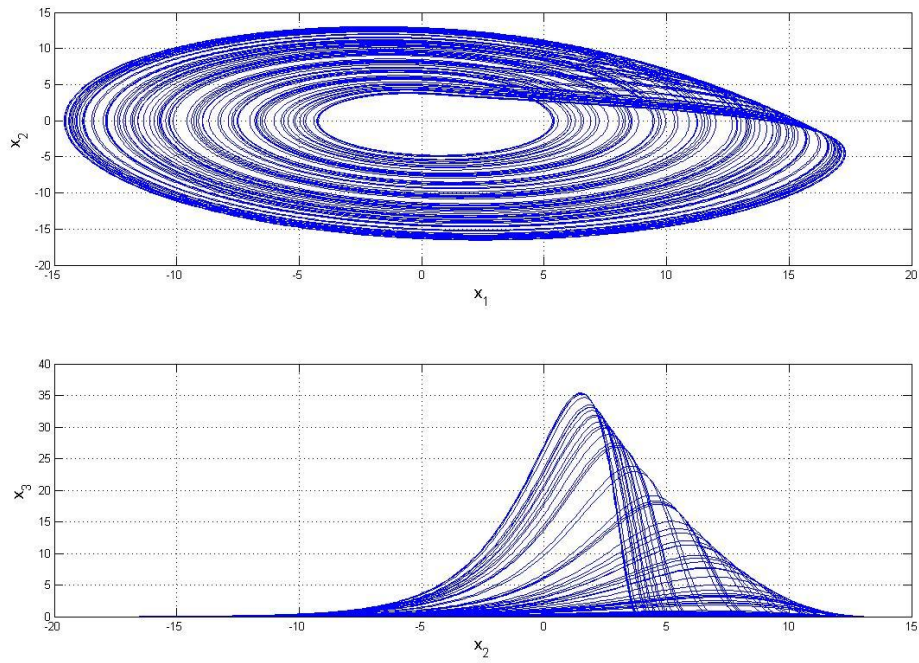


Fig. 6.4 Chaotic behavior of Rössler system.



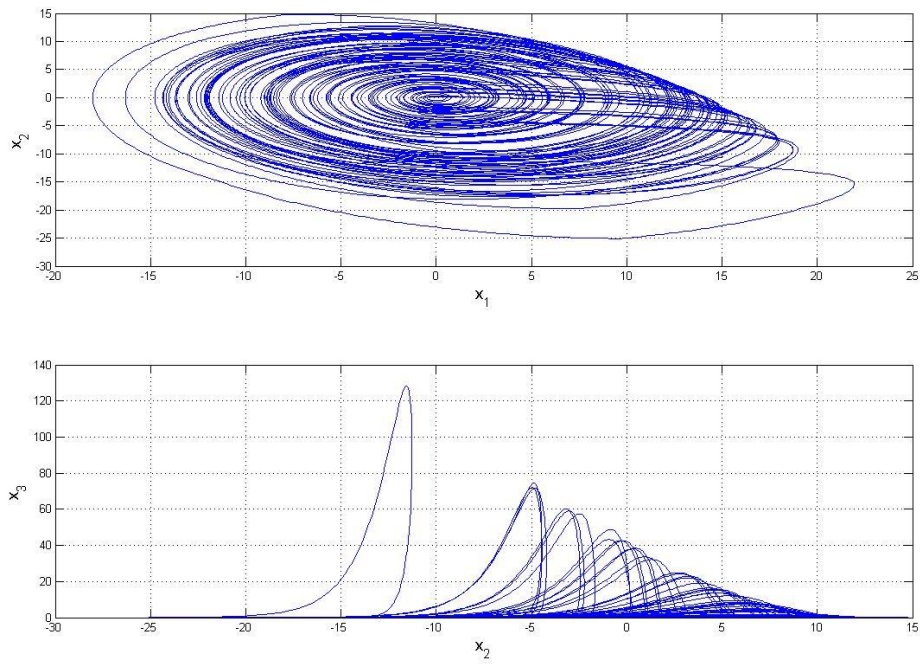


Fig. 6.5 Chaotic behavior of Rössler system with uncertainty.

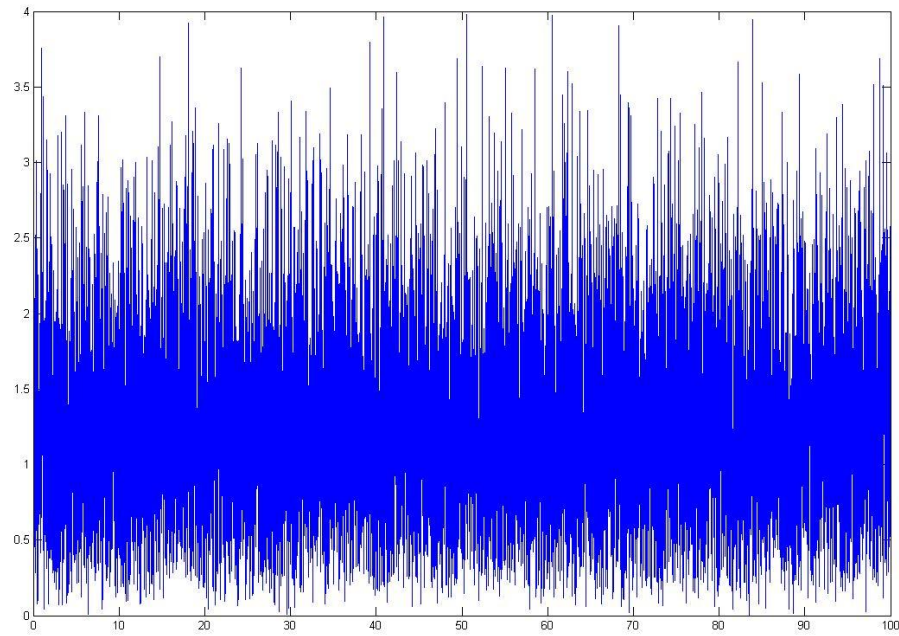


Fig. 6.6 The Rayleigh noise used.

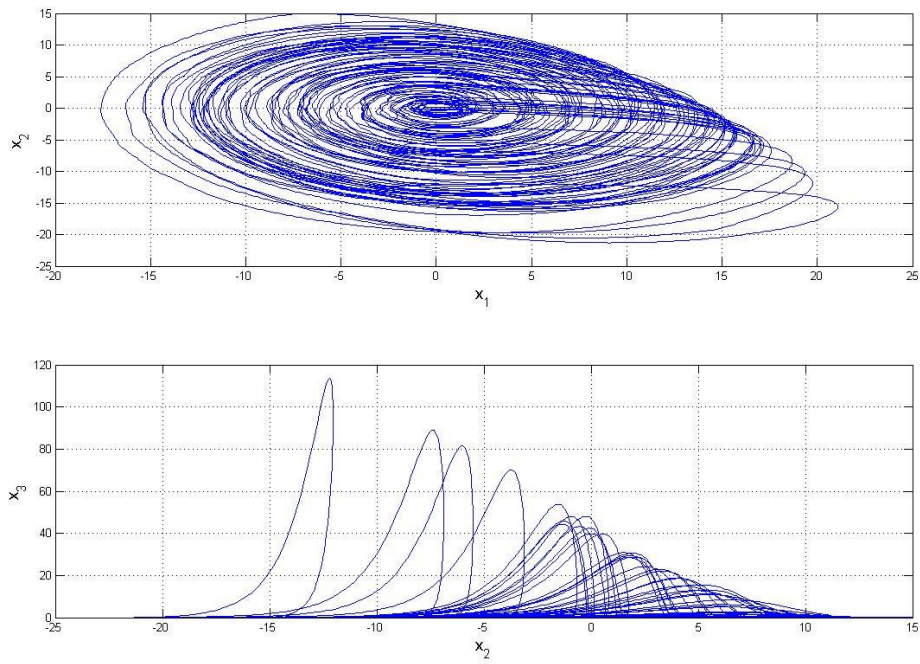


Fig. 6.7 Chaotic behavior of new fuzzy Rössler system with uncertainty.

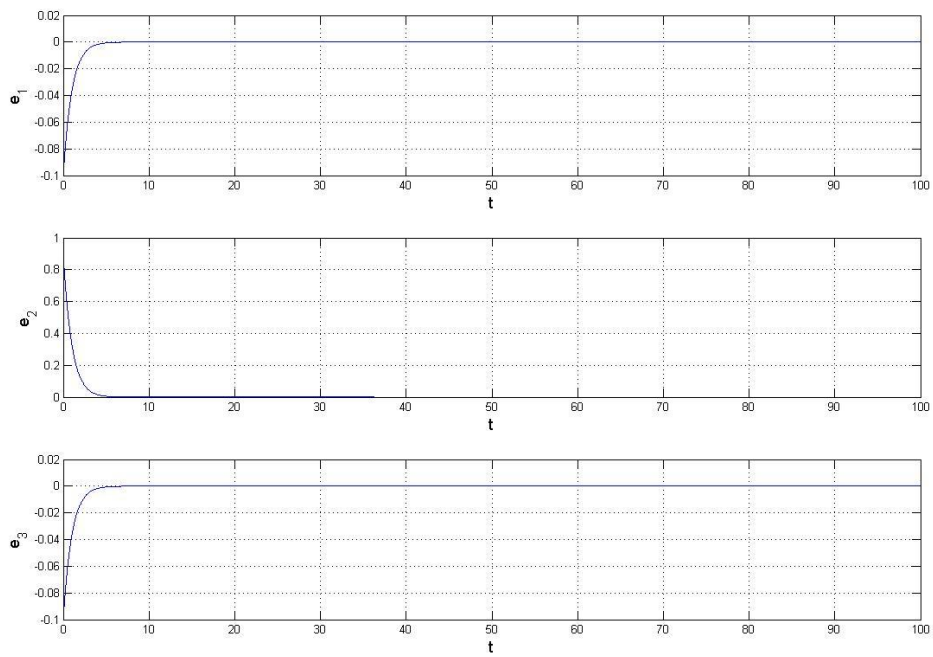


Fig. 6.8 Time histories of errors for Example 1.



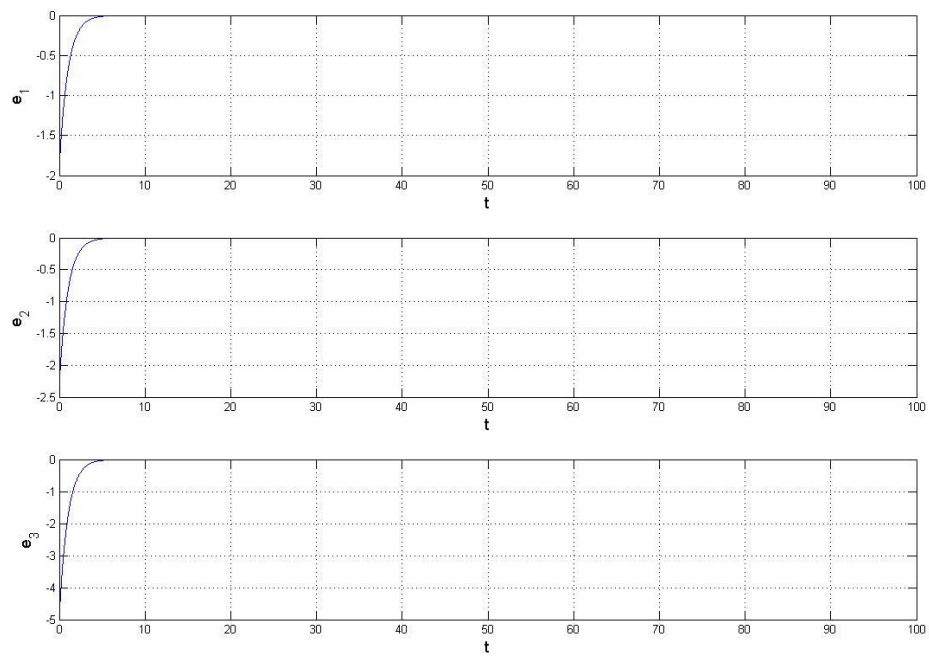
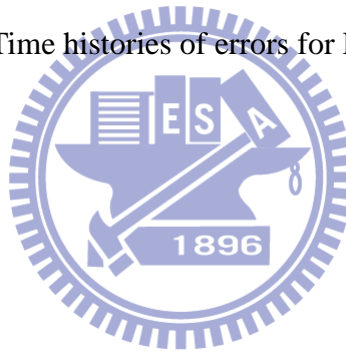


Fig. 6.9 Time histories of errors for Example 2.



# Chapter 7

## Conclusions

In this thesis, chaos and various chaos synchronizations of Double Ge-Ku system, Sprott 4 system and Rössler system are studied.

In Chapter 2, we propose the double symplectic synchronization. The double symplectic synchronization is a generalized case of generalized synchronization and symplectic synchronization. Because the synchronization form is more complex than generalized and symplectic synchronizations, so we usually use it on the purpose of secret communication. The simulation results show that the proposed scheme is feasible and effective for both autonomous and non-autonomous chaotic systems. When the double symplectic functions is extended to a more general form, multiple symplectic synchronization which is studied in Chapter 3.

In Chapter 4, a new strategy to achieve chaos synchronization by the different translation pragmatic synchronization using stability theory of partial region is studied. The pragmatical asymptotical stability theorem fills the vacancy between the actual asymptotical stability and mathematical asymptotical stability. The conditions of the Lyapunov function for pragmatical asymptotical stability are lower than that for traditional asymptotical stability. By using this theorem, with the same conditions for Lyapunov function as that in current scheme of adaptive synchronization, we not only obtain the synchronization of chaotic systems but also prove strictly that the estimated parameters approach the uncertain values. Furthermore the Lyapunov function used is a simple linear homogeneous function of states.

In Chapter 5, a simplest fuzzy controller (FLCC) is introduced to projective anti-synchronization of non-autonomous chaotic systems with uncertainty. Three main contributions can be concluded: (1) High performance of the convergence of error states in anti-synchronization; (2) Good robustness in anti-synchronization of the chaotic systems with uncertainty; (3) Simplest constant controller.

Further, due to the characters of FLCC, (1) the mathematical models of devoted chaotic systems can be unknown, all we have to do is capturing the output signals, (2) through the fuzzy logic rules, the strength of controller can be adjusted via the corresponding membership functions, the well robustness and high performance in anti-synchronization of this simplest controller (FLCC) can be applied to various kinds of fields with lots of perturbations, such as neuroscience, un-model bio-systems, complicated brain network and so on.

In Chapter 6, we successfully and efficiently simulate and synchronize systems by the new fuzzy model. Through the new fuzzy model, a complicated nonlinear system can be linearized to a simple form, linear coupling of only two linear subsystems and the numbers of fuzzy rules can be decreased from  $2^N$  to  $2 \times N$ . There are two examples in numerical simulation results to show the effectiveness and feasibility of our new model.

## Appendix A

### GYC Partial Region Stability Theory

#### A.1 Definition of the Stability on Partial Region

Consider the differential equations of disturbed motion of a non-autonomous system in the normal form

$$\frac{dx_s}{dt} = X_s(t, x_1, \dots, x_n), \quad (s = 1, \dots, n) \quad (\text{A.1})$$

where the function  $X_s$  is defined on the intersection of the partial region  $\Omega$  and

$$\sum_s x_s^2 \leq H \quad (\text{A.2})$$

and  $t > t_0$ , where  $t_0$  and  $H$  are certain positive constants.  $X_s$  which vanishes when the variables  $x_s$  are all zero, is a real valued function of  $t, x_1, \dots, x_n$ . It is assumed that  $X_s$  is smooth enough to ensure the existence, uniqueness of the solution of the initial value problem. When  $X_s$  does not contain  $t$  explicitly, the system is autonomous.

Obviously,  $x_s = 0$  ( $s = 1, \dots, n$ ) is a solution of Eq.(A.1). We are interested to the asymptotical stability of this zero solution on partial region  $\Omega$  (including the boundary) of the neighborhood of the origin which in general may consist of several subregions

#### Definition 1:

For any given number  $\varepsilon > 0$ , if there exists a  $\delta > 0$ , such that on the closed given partial region  $\Omega$  when

$$\sum_s x_{s0}^2 \leq \delta, \quad (s = 1, \dots, n) \quad (\text{A.3})$$

for all  $t \geq t_0$ , the inequality

$$\sum_s x_s^2 < \varepsilon, \quad (s=1, \dots, n) \quad (\text{A.4})$$

is satisfied for the solutions of Eq.(A.1) on  $\Omega$ , then the zero solution  $x_s = 0$  ( $s=1, \dots, n$ ) is stable on the partial region  $\Omega$ .

**Definition 2:**

If the undisturbed motion is stable on the partial region  $\Omega$ , and there exists a  $\delta' > 0$ , so that on the given partial region  $\Omega$  when

$$\sum_s x_{s0}^2 \leq \delta', \quad (s=1, \dots, n) \quad (\text{A.5})$$

The equality

$$\lim_{t \rightarrow \infty} \left( \sum_s x_s^2 \right) = 0 \quad (\text{A.6})$$

is satisfied for the solutions of Eq.(A.1) on  $\Omega$ , then the zero solution  $x_s = 0$  ( $s=1, \dots, n$ ) is asymptotically stable on the partial region  $\Omega$ .

The intersection of  $\Omega$  and region defined by Eq.(A.5) is called the region of attraction.

**Definition of Functions  $V(t, x_1, \dots, x_n)$ :**

Let us consider the functions  $V(t, x_1, \dots, x_n)$  given on the intersection  $\Omega_1$  of the partial region  $\Omega$  and the region

$$\sum_s x_s^2 \leq h, \quad (s=1, \dots, n) \quad (\text{A.7})$$

for  $t \geq t_0 > 0$ , where  $t_0$  and  $h$  are positive constants. We suppose that the functions are single-valued and have continuous partial derivatives and become zero when  $x_1 = \dots = x_n = 0$ .

**Definition 3:**

If there exists  $t_0 > 0$  and a sufficiently small  $h > 0$ , so that on partial region  $\Omega_1$  and  $t \geq t_0$ ,  $V \geq 0$  (or  $\leq 0$ ), then  $V$  is a positive (or negative) semidefinite, in

general semidefinite, function on the  $\Omega_1$  and  $t \geq t_0$ .

**Definition 4:**

If there exists a positive (negative) definitive function  $W(x_1 \dots x_n)$  on  $\Omega_1$ , so that on the partial region  $\Omega_1$  and  $t \geq t_0$

$$V - W \geq 0 \text{ (or } -V - W \geq 0), \quad (\text{A.8})$$

then  $V(t, x_1, \dots, x_n)$  is a positive definite function on the partial region  $\Omega_1$  and  $t \geq t_0$ .

**Definition 5:**

If  $V(t, x_1, \dots, x_n)$  is neither definite nor semidefinite on  $\Omega_1$  and  $t \geq t_0$ , then  $V(t, x_1, \dots, x_n)$  is an indefinite function on partial region  $\Omega_1$  and  $t \geq t_0$ . That is, for any small  $h > 0$  and any large  $t_0 > 0$ ,  $V(t, x_1, \dots, x_n)$  can take either positive or negative value on the partial region  $\Omega_1$  and  $t \geq t_0$ .

**Definition 6:** Bounded function  $V$

If there exist  $t_0 > 0$ ,  $h > 0$ , so that on the partial region  $\Omega_1$ , we have

$$|V(t, x_1, \dots, x_n)| < L$$

where  $L$  is a positive constant, then  $V$  is said to be bounded on  $\Omega_1$ .

**Definition 7:** Function with infinitesimal upper bound

If  $V$  is bounded, and for any  $\lambda > 0$ , there exists  $\mu > 0$ , so that on  $\Omega_1$  when

$$\sum_s x_s^2 \leq \mu, \text{ and } t \geq t_0, \text{ we have}$$

$$|V(t, x_1, \dots, x_n)| \leq \lambda$$

then  $V$  admits an infinitesimal upper bound on  $\Omega_1$ .

*A.2 GYC Theorem of Stability and of Asymptotical Stability on Partial Region*

**Theorem 1**

If there can be found a definite function  $V(t, x_1, \dots, x_n)$  on the partial region for

Eq. (A.1), and the derivative with respect to time based on these equations are:

$$\frac{dV}{dt} = \frac{\partial V}{\partial t} + \sum_{s=1}^n \frac{\partial V}{\partial x_s} X_s \quad (\text{A.9})$$

Then, it is a semidefinite function on the partial region whose sense is opposite to that of  $V$ , or if it becomes zero identically, then the undisturbed motion is stable on the partial region.

Proof:

Let us assume for the sake of definiteness that  $V$  is a positive definite function. Consequently, there exists a sufficiently large number  $t_0$  and a sufficiently small number  $h < H$ , such that on the intersection  $\Omega_1$  of partial region  $\Omega$  and

$$\sum_s x_s^2 \leq h, \quad (s=1, \dots, n)$$

and  $t \geq t_0$ , the following inequality is satisfied

$$V(t, x_1, \dots, x_n) \geq W(x_1, \dots, x_n),$$

where  $W$  is a certain positive definite function which does not depend on  $t$ . Besides that, Eq. (A.9) may assume only negative or zero value in this region.

Let  $\varepsilon$  be an arbitrarily small positive number. We shall suppose that in any case  $\varepsilon < h$ . Let us consider the aggregation of all possible values of the quantities  $x_1, \dots, x_n$ , which are on the intersection  $\omega_2$  of  $\Omega_1$  and

$$\sum_s x_s^2 = \varepsilon, \quad (\text{A.10})$$

and let us designate by  $l > 0$  the precise lower limit of the function  $W$  under this condition. By virtue of Eq. (A.8), we shall have

$$V(t, x_1, \dots, x_n) \geq l \quad \text{for } (x_1, \dots, x_n) \text{ on } \omega_2. \quad (\text{A.11})$$

We shall now consider the quantities  $x_s$  as functions of time which satisfy the differential equations of disturbed motion. We shall assume that the initial values  $x_{s0}$  of these functions for  $t = t_0$  lie on the intersection  $\Omega_2$  of  $\Omega_1$  and the region

$$\sum_s x_s^2 \leq \delta, \quad (\text{A.12})$$

where  $\delta$  is so small that

$$V(t_0, x_{10}, \dots, x_{n0}) < l \quad (\text{A.13})$$

By virtue of the fact that  $V(t_0, 0, \dots, 0) = 0$ , such a selection of the number  $\delta$  is obviously possible. We shall suppose that in any case the number  $\delta$  is smaller than  $\varepsilon$ . Then the inequality

$$\sum_s x_s^2 < \varepsilon, \quad (\text{A.14})$$

being satisfied at the initial instant will be satisfied, in the very least, for a sufficiently small  $t - t_0$ , since the functions  $x_s(t)$  vary continuously with time. We shall show that these inequalities will be satisfied for all values  $t > t_0$ . Indeed, if these inequalities were not satisfied at some time, there would have to exist such an instant  $t = T$  for which this inequality would become an equality. In other words, we would have

$$\sum_s x_s^2(T) = \varepsilon,$$

and consequently, on the basis of Eq. (A.11)

$$V(T, x_1(T), \dots, x_n(T)) \geq l \quad (\text{A.15})$$

On the other hand, since  $\varepsilon < h$ , the inequality (Eq.(A.7)) is satisfied in the entire interval of time  $[t_0, T]$ , and consequently, in this entire time interval  $\frac{dV}{dt} \leq 0$ . This yields

$$V(T, x_1(T), \dots, x_n(T)) \leq V(t_0, x_{10}, \dots, x_{n0}),$$

which contradicts Eq. (A.14) on the basis of Eq. (A.13). Thus, the inequality (Eq.(A.4)) must be satisfied for all values of  $t > t_0$ , hence follows that the motion is stable.

Finally, we must point out that from the view-point of mathematics, the stability on partial region in general does not be related logically to the stability on whole region. If an undisturbed solution is stable on a partial region, it may be either stable



or unstable on the whole region and vice versa. In specific practical problems, we do not study the solution starting within  $\Omega_2$  and running out of  $\Omega$ .

## Theorem 2

If in satisfying the conditions of Theorem 1, the derivative  $\frac{dV}{dt}$  is a definite function on the partial region with opposite sign to that of  $V$  and the function  $V$  itself permits an infinitesimal upper limit, then the undisturbed motion is asymptotically stable on the partial region.

Proof:

Let us suppose that  $V$  is a positive definite function on the partial region and that consequently,  $\frac{dV}{dt}$  is negative definite. Thus on the intersection  $\Omega_1$  of  $\Omega$  and the region defined by Eq. (A.7) and  $t \geq t_0$  there will be satisfied not only the inequality (Eq.(A.8)), but the following inequality as well:

$$\frac{dV}{dt} \leq -W_1(x_1, \dots, x_n), \quad (A.16)$$

where  $W_1$  is a positive definite function on the partial region independent of  $t$ .

Let us consider the quantities  $x_s$  as functions of time which satisfy the differential equations of disturbed motion assuming that the initial values  $x_{s0} = x_s(t_0)$  of these quantities satisfy the inequalities (Eq. (A.12)). Since the undisturbed motion is stable in any case, the magnitude  $\delta$  may be selected so small that for all values of  $t \geq t_0$  the quantities  $x_s$  remain within  $\Omega_1$ . Then, on the basis of Eq. (A.16) the derivative of function  $V(t, x_1(t), \dots, x_n(t))$  will be negative at all times and, consequently, this function will approach a certain limit, as  $t$  increases without limit, remaining larger than this limit at all times. We shall show that this limit is equal to some positive quantity different from zero. Then for all values of  $t \geq t_0$  the following inequality will be satisfied:

$$V(t, x_1(t), \dots, x_n(t)) > \alpha \quad (\text{A.17})$$

where  $\alpha > 0$ .

Since  $V$  permits an infinitesimal upper limit, it follows from this inequality that

$$\sum_s x_s^2(t) \geq \lambda, \quad (s = 1, \dots, n), \quad (\text{A.18})$$

where  $\lambda$  is a certain sufficiently small positive number. Indeed, if such a number  $\lambda$  did not exist, that is, if the quantity  $\sum_s x_s(t)$  were smaller than any preassigned number no matter how small, then the magnitude  $V(t, x_1(t), \dots, x_n(t))$ , as follows from the definition of an infinitesimal upper limit, would also be arbitrarily small, which contradicts Eq. (A.17).

If for all values of  $t \geq t_0$  the inequality (Eq. (A.18)) is satisfied, then Eq. (A.16) shows that the following inequality will be satisfied at all times:

$$\frac{dV}{dt} \leq -l_1,$$

where  $l_1$  is positive number different from zero which constitutes the precise lower limit of the function  $W_1(t, x_1(t), \dots, x_n(t))$  under condition (Eq. (A.18)). Consequently, for all values of  $t \geq t_0$  we shall have:

$$V(t, x_1(t), \dots, x_n(t)) = V(t_0, x_{10}, \dots, x_{n0}) + \int_{t_0}^t \frac{dV}{dt} dt \leq V(t_0, x_{10}, \dots, x_{n0}) - l_1(t - t_0),$$

which is, obviously, in contradiction with Eq.(A.17). The contradiction thus obtained shows that the function  $V(t, x_1(t), \dots, x_n(t))$  approached zero as  $t$  increase without limit. Consequently, the same will be true for the function  $W(x_1(t), \dots, x_n(t))$  as well, from which it follows directly that

$$\lim_{t \rightarrow \infty} x_s(t) = 0, \quad (s = 1, \dots, n),$$

which proves the theorem.

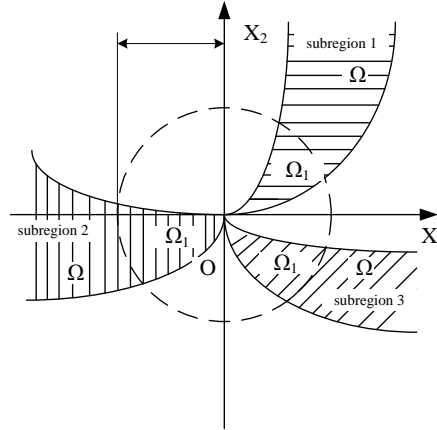


Fig. A.1 Partial regions  $\Omega$  and  $\Omega_1$ .

## Appendix B

### Pragmatical Asymptotical Stability Theory

The stability for many problems in real dynamical systems is actual asymptotical stability, although may not be mathematical asymptotical stability. The mathematical asymptotical stability demands that trajectories from all initial states in the neighborhood of zero solution must approach the origin as  $t \rightarrow \infty$ . If there are only a small part or even a few of the initial states from which the trajectories do not approach the origin as  $t \rightarrow \infty$ , the zero solution is not mathematically asymptotically stable. However, when the probability of occurrence of an event is zero, it means the event does not occur actually. If the probability of occurrence of the event that the trajectories from the initial states are that they do not approach zero when  $t \rightarrow \infty$ , is zero, the stability of zero solution is actual asymptotical stability though it is not mathematical asymptotical stability. In order to analyze the asymptotical stability of the equilibrium point of such systems, the pragmatical asymptotical stability theorem is used.

Let  $X$  and  $Y$  be two manifolds of dimensions  $m$  and  $n$  ( $m < n$ ), respectively, and  $\varphi$  be a differentiable map from  $X$  to  $Y$ , then  $\varphi(X)$  is subset of Lebesgue measure 0 of  $Y$  [59]. For an autonomous system

$$\frac{dx}{dt} = f(x_1, \dots, x_n) \quad (\text{B-1})$$

where  $x = [x_1, \dots, x_n]^T$  is a state vector, the function  $f = [f_1, \dots, f_n]^T$  is defined on  $D \subset R^n$  and  $\|x\| \leq H > 0$ . Let  $x=0$  be an equilibrium point for the system (B-1).

Then

$$f(0) = 0 \quad (\text{B-2})$$

For a non-autonomous systems,

$$\dot{x} = f(x_1, \dots, x_{n+1}) \quad (\text{B-3})$$

where  $x = [x_1, \dots, x_{n+1}]^T$ , the function  $f = [f_1, \dots, f_n]^T$  is define on  $D \subset R^n \times R_+$ , here  $t = x_{n+1} \in R_+$ . The equilibrium point is

$$f(0, x_{n+1}) \ni 0. \quad (\text{B-4})$$

**Definition** The equilibrium point for the system (B-1) is pragmatically asymptotically stable provided that with initial points on  $C$  which is a subset of Lebesgue measure 0 of  $D$ , the behaviors of the corresponding trajectories cannot be determined, while with initial points on  $D - C$ , the corresponding trajectories behave as that agree with traditional asymptotical stability [60,61].

**Theorem** Let  $V = [x_1, \dots, x_n]^T : D \rightarrow R_+$  be positive definite and analytic on  $D$ , where  $x_1, x_2, \dots, x_n$  are all space coordinates such that the derivative of  $V$  through Eq. (A-1) or (A-3),  $\dot{V}$ , is negative semi-definite of  $[x_1, x_2, \dots, x_n]^T$ .

For autonomous system, Let  $X$  be the  $m$ -manifold consisted of point set for which  $\forall x \neq 0, \dot{V}(x) = 0$  and  $D$  is a  $n$ -manifold. If  $m+1 < n$ , then the equilibrium

point of the system is pragmatically asymptotically stable.

For non-autonomous system, let  $X$  be the  $m+1$ -manifold consisting of point set of which  $\forall x \neq 0, \dot{V}(x_1, x_2, \dots, x_n) = 0$  and  $D$  is  $n+1$ -manifold. If  $m+1+1 < n+1$ , i.e.  $m+1 < n$  then the equilibrium point of the system is pragmatically asymptotically stable. Therefore, for both autonomous and non-autonomous system the formula  $m+1 < n$  is universal. So the following proof is only for autonomous system. The proof for non-autonomous system is similar.

**Proof** Since every point of  $X$  can be passed by a trajectory of Eq. (B-1), which is one-dimensional, the collection of these trajectories,  $A$ , is a  $(m+1)$ -manifold [60, 61].

If  $m+1 < n$ , then the collection  $C$  is a subset of Lebesgue measure 0 of  $D$ . By the above definition, the equilibrium point of the system is pragmatically asymptotically stable.

If an initial point is ergodically chosen in  $D$ , the probability of that the initial point falls on the collection  $C$  is zero. Here, equal probability is assumed for every point chosen as an initial point in the neighborhood of the equilibrium point. Hence, the event that the initial point is chosen from collection  $C$  does not occur actually. Therefore, under the equal probability assumption, pragmatical asymptotical stability becomes actual asymptotical stability. When the initial point falls on  $D-C$ ,  $\dot{V}(x) < 0$ , the corresponding trajectories behave as that agree with traditional asymptotical stability because by the existence and uniqueness of the solution of initial-value problem, these trajectories never meet  $C$ .

In Eq. (5-8)  $V$  is a positive definite function of  $n$  variables, i.e.  $p$  error state variables and  $n-p=m$  differences between unknown and estimated parameters, while  $\dot{V} = e^T C e$  is a negative semi-definite function of  $n$  variables. Since the number of

error state variables is always more than one,  $p > 1$ ,  $m+1 < n$  is always satisfied, by pragmatistical asymptotical stability theorem we have

$$\lim_{t \rightarrow \infty} e = 0 \quad (\text{B-5})$$

and the estimated parameters approach the uncertain parameters. The pragmatistical adaptive control theorem is obtained. Therefore, the equilibrium point of the system is *pragmatically asymptotically stable. Under the equal probability assumption, it is actually asymptotically stable for both error state variables and parameter variables.*

## References

- [1] Pecora, L.M., Carroll, T.L., "Synchronization in chaotic systems", Phys. Rev. Lett. 64 (1990) 821
- [2] Han, S. K., Kerr, C., and Kuramoto, Y., "Dephasing and bursting in coupled neural oscillators", Phys. Rev. Lett. 75 (1995) 3190.
- [3] Blasius, B., Huppert, A. and Stone, L., "Complex dynamics and phase synchronization in spatially extended ecological systems", Nature 399 (1999) 354.
- [4] Cuomo, K. M. and Oppenheim, V., "Circuit implementation of synchronized chaos with application to communication", Phys. Rev. Lett. 71 (1993) 65.
- [5] Kocarev, L. and Parlitz, U., "General approach for chaotic synchronization with application to communication", Phys. Rev. Lett. 74 (1995) 5028.
- [6] Wang, C. and Ge, S. S., "Adaptive synchronization of uncertain chaotic systems via backstepping design", Chaos, Solitons and Fractals, 12 (2001) 119-120.
- [7] Femat, R., Ramirze, J. A. and Anaya, G. F., "Adaptive synchronization of high-order chaotic systems: A feedback with low-order parameterization", Physica D, 139 (2000) 231-246.
- [8] Sun, M. T. L. and Jiang, S. X. J., "Feedback control and adaptive control of the energy resource chaotic system", Chaos, Solitons and Fractals, (2007) 1725-2834,.
- [9] Femat, R. and Perales, G. S., "On the chaotic synchronization phenomenon", Phys. Lett. A, 262 (1999) 50-60,.
- [10] Abarbanel, H. D. I., Rulkov, N. F. and Sushchik, M. M., "Generalized synchronization of chaos: The auxiliary systems", Phys. Rev. E, 53 (1996) 4528-4535.
- [11] Yang, S. S. and Duan, C. K., "Generalized synchronization in chaotic systems", Chaos, Solitons and Fractals, 9 (1998) 1703-1707.
- [12] Yang, X. S., "Concepts of synchronization in dynamic systems", Phys. Lett. A, 260 (1999) 340-344.
- [13] Rosenblum, M. G., Pikovsky, A. S. and Kurths, J., "Phase synchronization of chaotic oscillators", Phys. Rev. Lett. 76 (1996) 1805.
- [14] Rosenblum, M. G., Pikovsky, A. S. and Kurths, J., "From phase to lag synchronization in coupled chaotic oscillators", Phys. Rev. Lett. 78 (1997) 4193.
- [15] Rulkov, N. F., Sushchik, M. M., Tsimring, L. S. and Abarbanel, H. D. I.,

- “Generalized synchronization of chaos in directionally coupled chaotic systems”, *Phys. Rev. E*, 51 (1995) 980.
- [16] Ge, Z. M., Yang, C. H. “Pragmatical generalized synchronization of chaotic systems with uncertain parameters by adaptive control”, *Physica D: Nonlinear Phenomena*, 231 (2007) 87–94.
- [17] Yang, S. S., Duan, C. K., “Generalized synchronization in chaotic systems”, *Chaos, Solitons & Fractals*, 9 (1998) 1703–7.
- [18] Krawiecki, A., Sukiennicki, A., “Generalizations of the concept of marginal synchronization of chaos”, *Chaos, Solitons & Fractals*, 11(9) (2000) 1445–58.
- [19] Ge, Z. M., Yang, C. H., Chen, H. H., Lee, S. C., “Non-linear dynamics and chaos control of a physical pendulum with vibrating and rotation support”, *J Sound Vib*, 242(2) (2001) 247–64.
- [20] Chen, M. Y., Han, Z. Z., Shang, Y., “General synchronization of Genesio–Tesi system”, *Int J Bifurcat Chaos*, 14(1) (2004) 347–54.
- [21] Tanaka, K., Ikeda, T., Wang, H. O., “A unified approach to controlling chaos via LMI-based fuzzy control system design”, *IEEE Trans. on Circuits and Systems I*, 45 (1998) 1021–1040.
- [22] Zadeh, L. A., “Fuzzy sets”, *Information and Control*, 8 (1965) 338–353.
- [23] Kuo, C.L., Li, T. H., Guo, N., “Design of a novel fuzzy sliding-mode control for magnetic ball levitation system”, *Journal of Intelligent and Robotic Systems*, 42 (2005) 295–316.
- [24] Feng, G., Chen, G., “Adaptive control of discrete-time chaotic systems: a fuzzy control approach”, *Chaos Solitons & Fractals*, 23 (2005) 459–467.
- [25] Xue, Y. J., Yang, S. Y., “Synchronization of generalized Henon map by using adaptive fuzzy controller”, *Chaos Solitons & Fractals*, 17 (2003) 717–722.
- [26] Xia, Y. et al., “Damage identification of structures with uncertain frequency and mode shape data”, *Earthquake Engineering and Structural Dynamics*, 31 (5) (2002) 1053–1066.
- [27] Collins, J. D., Hart, G. C., Hasselman, T. K., Kennedt, K., “System identification of structures”, *American Institute of Aeronautics and Astronautics Journal*, 12 (2) (1974) 185–190.
- [28] Shahraz, A., Bozorbmehty Boozarjomehry, R., “A fuzzy sliding mode control approach for nonlinear chemical processes”, *Control Engineering Practice*, 17 (2009) 541-550.
- [29] Chen, C. Y., Li, T. H. S., Yeh, Y. C., “EP-based kinematic control and adaptive fuzzy sliding-mode dynamic control for wheeled mobile robots”, *Information Science*, 179 (2009) 180-195.
- [30] Wang Y. W., Guan Z. H. and Wang H. O., “LMI-based fuzzy stability and synchronization of Chen’s system”, *Phy. Lett. A*, 320 (2003) 154-159.

- [31] Li, G., Khajepour, A., "Robust control of a hydraulically driven flexible arm using backstepping technique", *Journal of Sound and Vibration*, 280 (2005) 759-779.
- [32] Li, T. H. S., Kuo, C. L. and Guo, N. R., "Design of an EP-based fuzzy sliding-mode control for a magnetic ball suspension system", *Chaos, Solitons & Fractals*, 33 (2007) 1523-1531.
- [33] Yau, H. T. and Shieh, C. S., "Chaos synchronization using fuzzy logic controller", *Nonlinear Analysis: Real World Applications*, 9 (2008) 1800-1810.
- [34] Zadeh, L. A., "Fuzzy logic", *IEEE Comput*, 21 (1988) 83-93.
- [35] Takagi, T. and Sugeno, M., "Fuzzy identification of systems and its applications to modelling and control", *IEEE Trans. Syst., Man., Cybern.*, 15(1) (1985) 116-132.
- [36] Luoh, L., "New stability analysis of T-S fuzzy system with robust approach", *Math Comput Simul*, 59(4) (2002) 335-340.
- [37] Wu, X. j., Zhu, X. j., Cao, G. y. and Tu, H. y., "Dynamic modeling of SOFC based on a T-S fuzzy model", *Simul Model Prac Theory*, 16(5) (2008) 494-504.
- [38] Liu, X. and Zhong, S., "T-S fuzzy model-based impulsive control of chaotic systems with exponential decay rate", *Phys. Lett. A*, 370(3-4) (2007) 260-264.
- [39] Kim, J. H., Park, C. W., Kim, E. and Park, M., "Adaptive synchronization of T-S fuzzy chaotic systems with unknown parameters", *Chaos Solitons & Fractals*, 24(5) (2005) 1353-1361.
- [40] Chiu, C. S. and Chiang, T. S., "Robust output regulation of T-S fuzzy systems with multiple time-varying state and input delays", *IEEE Trans. Fuzzy Syst.*, 17(4) (2009) 962 – 975.
- [41] Wang, J., Xiong, X., Zhao, M. and Zhang, Y., "Fuzzy stability and Synchronization of hyperchaos systems", *Chaos Solitons & Fractals*, 35(5) (2008) 922-930.
- [42] Wang, Y. W., Guan, Z. H. and Wang, H. O., "LMI-based fuzzy stability and synchronization of Chen's system", *Phys Lett A*, 320(2-3) (2003) 154-159.
- [43] Zhang, H., Liao, X. and Yu, J., "Fuzzy modeling and synchronization of hyperchaotic systems", *Chaos Solitons & Fractals*, 26(3) (2005) 835-843.
- [44] Kau, S. W., Lee, H. J., Yang, C. M., Lee, C. H., Hong, L. and Fang, C. H., "Robust  $H_\infty$  fuzzy static output feedback control of T-S fuzzy systems with parametric uncertainties", *Fuzzy Sets Syste*, 158(2) (2007) 135-146.
- [45] Ge, Z. M. and Ku, F. N., "Stability, bifurcation and chaos of a pendulum on a rotating arm", *Jpn. J. Appl. Phys.*, 36 Part 1 (1997) 7052-7060.
- [46] Khalil, H. K., "*Nonlinear Systems*", 3rd edition, Prentice Hall, New Jersey, 2002.



- [47] Ge, Z. M., Yao, C. W., Chen, H. K., "Stability on partial region in dynamics", Journal of Chinese Society of Mechanical Engineer, 115 (1994) 140-151.
- [48] Ge, Z. M., Chen, H. K., "Three asymptotical stability theorems on partial region with application", Japanese Journal of Applied Physics, 37 (1998) 2762-2773.
- [49] Ge, Z. M., "Necessary and sufficient conditions for the stability of a sleeping top described by three forms of dynamic equations", Phy. Rev. E, 77 (2008) 046606.
- [50] Sprott, J. C., "Simple chaotic systems and circuits", Am. J. Phys., 68(8) 2000 758-763.
- [51] Park, J. H., "Adaptive synchronization of hyperchaotic chen system with uncertain parameters", Chaos Solitons Fractals, 26 (2005) 959.
- [52] Park, J. H., "Adaptive synchronization of rossler system with uncertain parameters", Chaos Solitons Fractals, 25 (2005) 333.
- [53] Elabbasy, E. M., Agiza, H. N., El-Desoky, M.M., "Adaptive synchronization of a hyperchaotic system with uncertain parameter", Chaos Solitons Fractals, 30 (2006) 1133.
- [54] Wu, X., Guan, Z. H., Wu, Z., Li, T., "Chaos synchronization between Chen system and Genesio system", Phys. Lett. A, 364 (2007) 315.
- [55] Xu, M. Z., Zhang, R., Hu, A., "Adaptive full state hybrid projective synchronization of chaotic systems with the same and different order", Phys. Lett. A, 365 (2007) 315-27.
- [56] Ge, Z. M., Tsai, S. E., "Double symplectic synchronization for Ge-Ku-van der Pol System", Nonlinear Analysis : Theory, Methods & Applications (2009).
- [57] Mainieri, R. and Rehacek, J., "Projective synchronization in three-dimensional chaotic systmes", Phys. Rev. Lett., 82 (1999) 3042.
- [58] Ge, Z. M. and Li, S. Y., "Fuzzy modeling and synchronization of chaotic two-cells quantum cellular neural networks nano system via a novel fuzzy model", accepted by Journal of Computational and Theoretical Nanoscience 2009.
- [59] Matsushima, Y., *Differentiable Manifolds*, Marcel Dekker, City, 1972.
- [60] Ge, Z. M., Yu, J. K. and Chen, Y. T., "Pragmatical asymptotical stability theorem with application to satellite system", Jpn. J. Appl. Phys., 38 (1999) 6178.
- [61] Ge, Z. M. and Yu, J. K., "Pragmatical asymptotical stability theorem partial region and for partial variable with applications to gyroscopic systems", the Chinese Journa of Mechanics, 16 (2000) 179.